Characterization of four functionally distinct human B-cell subsets that are defined by the expression of CD21 and CD86

Inaugural-Dissertation zur

Erlangung des Doktorgrades

der Mathematisch-Naturwissenschaftlichen Fakultät

der Universität zu Köln

vorgelegt von

María Alejandra García Márquez

aus Maracay, Venezuela

Köln

2015

Berichterstatter: PD. Dr. Thomas Wunderlich

Prof. Dr. Björn Schumacher

Tag der mündlichen Prüfung: 19 June, 2015

Para mis padres Luis y Pilar

DANKSAGUNG

I would like to thank everyone who has supported me and has contributed to the success of this work.

My thanks go to Prof. Hallek, for providing helpful advice, comments, or suggestions through the years. Many thanks to my thesis committee members Dr. Thomas Wunderlich, Prof. Björn Schumacher, Prof. Ines Neundorf and Dr. Isabell Witt for their kind willingness to support this work.

I would like to make a special recognition to my advisor Prof. Michael von Bergwelt-Baildon who gave me the opportunity to research in his group and provided me his guidance throughout my graduate studies. I am grateful for all his support, encouragement and enthusiastic discussions sustained through the years. It is also important to mention and express my gratitude to Dr. Alexander Shimabukuro-Vornhagen for his helpful advice, critiques and insightful comments as well as his expert and technical assistance. I will continue to learn and grow as I pursue my career with the foundation that Michael and Alex helped to build. Thanks also to Rieke Fischer for trusting me to continue with her research project.

I cannot forget Kerstin and Juliane, who created a supportive and fun working environment over the years. They have been not only my colleges but also my friends and they have always being there for me, lending me their assistance and advice in every possible way. You will forever have a place in my heart. Thanks Kerstin for your comments, suggestions, and proofreading of my thesis.

I would like to further thank Michael, Kerstin, Juliane, Martin, Sabrina, Anne, Hans S., Hans B., Sebastian, Alex, Sacha, Geothy, Rieke, Steffi and Claudia, for the great time spent in the laboratory, the entertaining lunch breaks, dinners and lab excursions. Those good memories and the time we spent together will remain with me forever.

Quiero agradecer a Helmut, Luz Angela, Helmut papá, Erich, Dani, Ricardo, Max, Zivile, Adrian, Kati, Marina, José Daniel, Ingrid, Felipe, Andy y Santi por darme una familia en Alemania y por hacerme sentir en casa.

Helmut, tú me has acompañado desde el principio en este camino, gracias por tu apoyo incondicional, por tu paciencia en esos días en los que no estuve tan segura de si conseguiría esta meta. Por hacerme reír cuando estaba triste, por saber escucharme y saber cómo aligerar mis cargas, gracias. Por ser mi “fiel chofer” y llevarme a todos lados, y por acompañarme en las madrugadas y fines de semanas en los que tuve que estar en el lab. Infinitas gracias.

Por último pero no menos importante, quiero agradecer a mi familia. A mis papas Luis y Pilar por siempre apoyarme, por estar orgullosos de mi, por acompañarme desde la distancia. Gracias a ustedes es que soy quien soy, este título es de ustedes. Ustedes son mi fuerza y aunque no los pueda ver todos los días siempre los llevo en mi corazón. A mis hermanos Luijo e Isa, por apoyarme y ayudarme siempre que los necesito. Los amo con todo mi corazón. A mis abuelitas Margoth y Teresa por las conversaciones de los fines de semana que siempre me alegran el día y a mis abuelitos Luis y Darío que desde el cielo siempre me acompañan.

ZUSAMMENFASSUNG

Inzwischen ist bekannt, dass B-Lymphozyten phänotypisch und funktional heterogen sind. Zusätzlich zu ihrer wesentlichen Funktion als Antikörper-produzierende B-Zellen, dienen sie als Antigen-präsentierende Zellen und regulieren Immunreaktionen, unter anderem durch die Sekretion von Cytokinen und Chemokinen. Obwohl bereits mehrere Subpopulationen identifiziert worden sind, ist ein tieferes Verständnis für die Rolle der B-Zellen in der Pathophysiologie bei menschlichen Erkrankungen durch einen Mangel an exakt definierten B-Zell-Subpopulationen behindert worden. In der vorliegenden Arbeit wurden vier B-Zell-Subpopulationen mit sehr verschiedenen phänotypischen und funktionellen Eigenschaften durch eine umfassende phänotypische und funktionierende Charakterisierung mittels Expression von CD21 und CD86 definiert. Die $CD21^{pos}$ $CD86^{low}$ B-Zell-Untergruppe zeigte einen naiven, IgD^{+} IgM^{+} Phänotyp, der durch die fehlende Expression von Costimulatorischen- und Gedächtnis-Markern charakterisiert war. Zusätzlich wies sie ein niedriges Calcium- und Phosphorilierungs-Niveau sowie eine starke Reaktion nach Stimulierung des B-Zellrezeptors auf. Darüber hinaus induzierte diese B-Zell-Untergruppe nur eine sehr langsame Aktivierung in autologen T-Zellen nach Cokultivierung. Die $CD21^{pos}$ $CD86^{pos}$ B-Zellen-Untergruppe zeigte einen aktivierten, IgD^{+} IgM^{+} $CD27^{+}$ Gedächtnis-Phänotyp und eine moderate Fähigkeit zur Induktion einer T-Zellreaktion. Die $CD21^{low}$ Population, die in andere Untersuchungen in verschiedenen Erkrankungen als „ermüdet“ und wenig immunstimulatorisch beschrieben worden ist, konnte durch die unterschiedliche Expression von CD86 in zwei Untergruppen aufgeteilt werden. Die $CD21^{low}$ $CD86^{pos}$ B-Zell-Untergruppe zeigte einen aktivierten, IgD^{-} IgM^{-} $CD27^{+}$ Gedächtnis-Phänotyp, eine starke immunangregende Fähigkeit und eine beeinträchtigte Reaktion des B-

Zellrezeptors. Diese konnte jedoch durch die synergistische Stimulierung mit dem CD40-Liganden wieder hergestellt werden. Im Gegensatz dazu war die $CD21^{low}$ $CD86^{neg}$ B-Zellen-Untergruppe funktionell beeinträchtigt und wies Merkmale auf, die zu einem anergischen oder „ermüdeten" Zustand passten.

In der vorliegenden Arbeit wurden bemerkenswerte Unterschiede in der Frequenz dieser B-Zell-Subpopulation in verschiedenen Erkankungen fest gestellt. Dies lässt darauf schließen, dass die homöostatische Balance zwischen diesen Subpopulationen den funktionellen Zustand des gesamten B-Zell-Kompartiments definieren könnte. So hatten Patienten mit traumatischen Verletzungen beispielsweise einen erhöhten Prozentsatz an $CD21^{pos}$ $CD86^{pos}$ B-Zellen im Vergleich zu gesunden Spendern und Patienten mit rheumatischer Arthritis wiesen eine höhere Frequenz an $CD21^{pos}$ $CD86^{pos}$ und $CD21^{low}$ $CD86^{pos}$ B-Zellen auf. In Patienten mit Darmkrebs waren $CD21^{low}$ $CD86^{pos}$ B-Zellen im Tumorgewebe angereichert im Vergleich zu peripherem Blut von Darmkrebspatienten und gesunden Spendern. Zusammenfassend lässt sich fest halten, dass die verschiedenen B-Zell-Untergruppen unterschiedliche funktionelle Eigenschaften aufweisen, und dass sie eine Rolle in Autoimmun- und Krebserkankungen zu spielen scheinen. Dies legt den Schluss nahe, dass eine stärkere Fokussierung auf die spezifischen B-Zellen-Untergruppen eine viel versprechende therapeutische Strategie repräsentieren könnte.

ABSTRACT

It is now recognized that B lymphocytes are phenotypically and functionally heterogeneous. In addition to their essential role as antibody producing B cells, they serve as antigen-presenting cells, contribute to immunoregulation and represent an important source of cytokines and chemokines. Although several subpopulations have been identified, a deeper understanding of the role of B cells in the pathophysiology of human diseases has been hampered by the lack of well-defined functional B-cell subsets. In this study, a comprehensive phenotypic and functional characterization of B cells defined by expression of CD21 and CD86, revealed four B-cell subpopulations with very distinct phenotypical and functional properties. $CD21^{pos}$ $CD86^{low}$ B-cell subset had a naïve, non-switched phenotype characterized by the absence of expression of costimulatory and memory markers. Additionally, it was characterized by low basal calcium and phosphorylation levels and robust response after B-cell receptor stimulation. Furthermore, when cultivated with autologous T cells they induced very low stimulation. The $CD21^{pos}$ $CD86^{pos}$ B-cell subset had an activated, non-switched-memory phenotype and moderated immunostimulatory capacity. The $CD21^{low}$ "exhausted" population described by others in several diseases could be partitioned in two subsets based on the expression of CD86. $CD21^{low}$ $CD86^{pos}$ B-cell subset had an activated, class-switched-memory phenotype, potent immunostimulatory capacity and impaired B-cell receptor signaling that was restored by synergistic stimulation with CD40 ligand. On the other hand, $CD21^{low}$ $CD86^{neg}$ B-cell subset was composed of functionally impaired B cells with features consistent of an anergic or exhausted state.

Since striking differences were detected in the frequency of these subsets in several medical conditions, it appears that the homeostatic balance between these

subpopulations could describe the functional state of the B-cell compartment. For instance, patients with traumatic fractures contained an increased percentage of $CD21^{pos}$ $CD86^{pos}$ B cells compared to healthy donors. Patients with active rheumatoid arthritis had a higher frequency of $CD21^{pos}$ $CD86^{pos}$ and $CD21^{low}$ $CD86^{pos}$ B cells. Patients with colorectal cancer revealed that $CD21^{low}$ $CD86^{pos}$ B cells were enriched within the tumor tissue compared to the peripheral blood of colorectal cancer patients and healthy controls. Taken together, the observation that the different B-cell subsets display distinct functional features and that the different subsets are associated with immune-related diseases suggests that a more specific targeting of B-cell subsets could represent a promising therapeutic strategy.

ABBREVIATIONS

Acronym	Expansion
AM	Acetoxymethyl esters
APCs	Antigen-presenting cells
ATP	Adenosine triphosphate
B10 cells	IL-10 producing regulatory B cells
BAFF	B cell-activating factor
B_{APC}	antigen-presenting $CD21^{low}$ $CD86^{pos}$ B cells
B_{conv}	conventional $CD21^{pos}$ $CD86^{neg}$ B cells
BCR	B cell receptor
B_{inact}	Inactivated $CD21^{low}$ $CD86^{neg}$ B cells
Bm	B mature
B_{react}	Recently activate $CD21^{pos}$ $CD86^{pos}$ B cells
BSA	Bovine serum albumin
°C	Degrees Celsius
Ca^{2+}	Calcium ions
$CaCl_2$	Calcium chloride
CD40B cell	CD40-activated B cell
CD40L	CD40 Ligand
CFSE	5-(and-6)-carboxyfluoresceindiacetate, succinimidyl ester
CLP	Common lymphoid progenitor
CO_2	Carbon dioxide

CR	Complement receptor
CRC	Colorectal cancer
CSR	Class switch recombination
CVID	Common variable immunodeficiency
D	Diversity gene
DC	Dendritic cell
DMSO	Dimethyl sulfoxide
DNA	Deoxyribonucleic acid
EBV	Epstein-Barr virus
EDTA	Ethylenediaminetetraacetic acid
ER	Endoplasmic reticulum
ERK	Extracellular signal regulated kinase
FACS	Fluorescence activated cell sorting
FBS	Fetal bovine serum
$FoxP_3$	Forkhead box P3
FS	Forward scatter
FSS	Forward scatter signal
G	Gravity
GC	Germinal center
Gy	Gray
H_2O_2	Hydrogen Peroxide
HCV	Hepatitis C virus
HIV	Human immunodeficiency virus
HSCs	hematopoietic stem cells

Ig	Immunoglobulin
IgLC	Immunoglobulin light chain
IκBα	Inhibitor of κ B α
IKK	IκB kinase
IL-	Interleukin
IFN	Interferon
IP3	Inositol-1,4,5-trisphosphate
ITAM	Immunoreceptor tyrosine-based activation motif
ITIM	Immunoreceptor tyrosine-based inhibitory motif
J	Joining gene
JAK	Janus kinase
Jnk	c-Jun N-terminal kinase
L	Liter
LFA-1	leukocyte function antigen-1
M	Molar
mAbs	Monoclonal antibodies
MALT	Mucosa-associated lymphoid tissue
MAPKs	Mitogen activated protein kinases
MFI	Mean fluorescence intensity
Mg	Milligram
MHC	Major histocompatibility complex
mIg	Membrane-bound immunoglobulin
mL	Mililiter
MLR	Mixed lymphocyte reaction

mM	Milimolar
Mm	Millimeter
µHC	Immunoglobulin heavy chain
µL	Microliter
µm	Micrometer
µM	Micromolar
µSM	µ-suppressed mice
NF	Nuclear factor
NIK	Nuclear ƙ B inducing kinase
NK	Natural killer
PBMCs	Peripheral blood mononuclear cells
PBS	Phosphate-buffered saline
PCs	plasma cells
PFA	Paraformaldehyde
Pg	Picogram
PhosphoFlow	Multiplexed phospho-specific flow cytometric profiling
PI3K	Phosphoinositol 3 kinase
PIP_2	Phosphatidylinositol 4,5-bisphosphate
PLCγ2	phospholipase Cγ2
pro-B cells	Progenitor B cells
PTPs	Protein tyrosine phosphatases
RAG	Recombination-activating gene
rCD40L	Recombinant CD40 ligand
rh	human recombinant

RNA	Ribonucleic acid
RT	Room temperature
sCD40L	Soluble CD40 ligand
SD	Standard deviation
SEM	Standard error of the mean
SHM	Somatic hyper mutation
SLC	Surrogate light chain
SLE	Systemic lupus erythematosus
SPADE	Spanning-tree progression analysis of density-normalized
SS	Side scatter
STAT	Signal transducer and activator of transcription
TCR	T cell antigen receptor
TGF	Transforming growth factor
T_h	T helper cell
TLR	Toll-like receptors
TNF	Tumor necrosis factor
TOF	Time of flight
TRAF	TNF receptor associated factor
Treg	Regulatory T cell
U	Units
V	Variable gene
w/w	Weight of solute over weight of solution

TABLE OF FIGURES

Figure 1. B cell development and differentiation subsets 8

Figure 2. B cell functions 18

Figure 3. Interaction between B and T lymphocytes 21

Figure 4. CD40 signaling 26

Figure 5. CD21 down-regulation and CD86 up-regulation as features of long-term activated B cells 31

Figure 6. CD21 and CD86 defined four B-cell subsets in peripheral blood from healthy donors. 33

Figure 7. Gating strategy for flow cytometry analysis 52

Figure 8. Ligation of B cells by CD40L induced activation and homotypic cluster formation 61

Figure 9. B cell proliferation in response to CD40 ligation 63

Figure 10. CD40 activated B cells induced strong proliferation of allogeneic T cells 64

Figure 11. Frequency of B-cell subsets in human peripheral blood, bone marrow and lymphoid tissue. 66

Figure 12. Individual variation in the frequency of B-cell subsets 68

Figure 13. $CD21^{low}$ $CD86^{pos}$ B cells were larger than B cells from the other three cell subsets 70

Figure 14. $CD21^{low}$ $CD86^{pos}$ B-cell subset had a higher proportion of proliferating cells 72

Figure 15. CD21^{low} CD86^{pos} subset consisted primarily of IgM^{neg} IgD^{neg} class-switched B cells....73

Figure 16. B-cell subsets differed in terms of expression of several cell surface molecules....75

Figure 17. CD21^{low} CD86^{pos} B cells expressed lower levels of the inhibitory receptors CD22, and CD32....76

Figure 18. Expression of molecules involved in cell trafficking....78

Figure 19. The majority of CD21^{low} CD86^{pos} and CD21^{pos} CD86^{pos} B cells expressed CD43 on their surface....80

Figure 20. Isolation on B-cell subsets via FACS....81

Figure 21. Mixed lymphocyte reaction with purified B-cell subpopulations and autologous T cells....83

Figure 22. Baseline cytosolic calcium levels and response to BCR stimulation in the four B-cell subsets....86

Figure 23. BCR-triggering induced calcium flux on CD40B cells....87

Figure 24. CD40L stimulation induced no calcium flux in B-cell subsets....89

Figure 25. Addition of extracellular calcium induced signaling after CD40 ligation on B cells....90

Figure 26. Addition of extracellular calcium induced signaling after CD40 ligation on B-cell subsets....91

Figure 27. CD40B cells were unresponsive to brief CD40L stimulation....93

Figure 28. BCR induced signaling....95

Figure 29. Elevated basal levels of phospho-proteins in $CD21^{pos}$ $CD86^{pos}$ B-cell subset 96

Figure 30. BCR induced signaling was impaired in all but $CD21^{pos}$ $CD86^{neg}$ B-cell subset 98

Figure 31. Impaired BCR-induced signaling in $CD86^{pos}$ subsets was not restored by inhibition of H_2O_2 - sensitive phosphatases 100

Figure 32. Pervanadate was required for pZAP/SYK phosphorylation in $CD21^{low}$ $CD86^{pos}$ subset 101

Figure 33. Baseline phosphorylation of NF-kB-p65 102

Figure 34. Impaired phosphorylation of pERK and NF-kB-p65 after CD40L stimulation in $CD21^{low}$ B-cell subsets 104

Figure 35. Combination of BCR and CD40 ligation restored signaling on $CD21^{low}$ $CD86^{pos}$ B cells 106

Figure 36. Hypothetical model for the function-based categorization of B-cell subsets divided by the expression of CD21 and CD86 108

Figure 37. B_{APC} were increased following vaccination 109

Figure 38. B_{APC} were increased in patients with EBV reactivation following allogeneic stem cell transplantation 112

Figure 39. B_{react} were increased in patients with acute traumatic fractures 113

Figure 40. B_{react} and B_{APC} were increased in patients with rheumatoid arthritis 114

Figure 41. B_{react}, B_{APC} and B_{inact} were increased in tumors specimens of CRC patients 116

LIST OF TABLES

Table 1: Chemicals 36

Table 2: Reagents 36

Table 3: Buffers and solutions 37

Table 4: NIH3T3 Standard medium 38

Table 5: Human CD40B wash medium 39

Table 6: Human CD40B culture medium 39

Table 7: Calcium flux medium 39

Table 8: Kits 40

Table 9: Tools and instrumentation 40

Table 10: Consumables 41

Table 11: Software 42

Table 12: Anti-Human antibodies 50

Table 13: Dyes used for the detection of free intracellular Ca^{2+} by flow cytometry 54

TABLE OF CONTENTS

Danksagung I

Zusammenfassung III

Abstract V

Abbreviations VII

Table of Figures XII

List of Tables XV

Table of Contents XVI

1 Introduction 2

1.1 Immune system 2

1.2 Innate and adaptive responses 3

1.3 T lymphocytes 4

1.3.1 $CD8^+$ cytotoxic T Cells 4

1.3.2 $CD4^+$ helper T Cells 5

1.4 B lymphocytes 6

1.4.1 B cell origin and development 6

1.4.2Circulating peripheral blood B-cell subsets 10

1.4.3 B cells in health and disease 13

1.4.4 Molecular architecture of B cells 14

1.4.4.1 The complement receptor (CR) 2: CD21 15

1.4.5 B cell functions 17

1.4.5.1 How B cells capture, process and present antigens? 20

1.4.5.1.1 BCR internalization and signaling 21

1.4.5.2 CD40-CD40L interaction 23

1.4.5.2.1 Signaling through CD40L 24

1.4.6 Generation of CD40-activated B cells in vitro 27

1.4.6.1 DCs vs. CD40B cells as antigen presenting cells 29

1.5 $CD21^{low}$ $CD86^{pos}$ cells: an in vivo counterpart to in vitro generated CD40B cells? 30

1.6 Aim of the study 34

2 Materials and Methods 36

2.1 Materials 36

2.1.1 Chemicals 36

2.1.2 Reagents 36

2.1.3 Buffers and solutions 37

2.1.4 Cell culture media 38

2.1.5 Kits 40

2.1.6 Cell lines 40

2.2 Methods 42

2.2.1 Blood samples 42

2.2.2 Cell subset enrichment 43

2.2.2.1 B cell purification 43

2.2.2.2 ..... B-cell subset isolation by fluorescence activated cell sorting (FACS) 44

2.2.2.3 $CD3^+$ T cell isolation 44

2.2.2.4 Cell isolation from human tumor tissue 45

2.2.3 Cell culture 45

2.2.3.1 Counting of cells – Trypan Blue exclusion test 46

2.2.3.2 Cryopreservation and thawing of cells 46

2.2.3.3 Trypsinization of adherent cells 46

2.2.3.4 Culture of NIH3T3/tCD40L cell line 47

2.2.3.5 .....Generation of CD40-activated B cells with NIH3T3/tCD40L cell line 47

2.2.3.6 Generation of CD40-activated B cells with soluble CD40L 48

2.2.3.7 Assessment of cell morphology by microscopy 48

2.2.4 Phenotype analysis of single cells by FACS 49

2.2.5 Surface staining with monoclonal antibodies 49

2.2.6 Human monoclonal antibodies used for frequency and conventional phenotype analysis 50

2.2.7 Gating strategy for flow cytometry analysis 51

2.2.8 Autologous and allogeneic MLR for T cell proliferation analysis 53

2.2.9 Analysis of Ca^{2+} mobilization.....54

2.2.10 Multiplexed phospho-specific flow cytometric profiling (PhosphoFlow) 55

2.2.10.1 Stimulants used in PhosphoFlow experiments 55

2.2.10.2 Cell stimulation 55

2.2.10.3 Staining and fluorescent-cell barcoding.....56

2.2.11 Statistics 56

3 Results 59

3.1 Generation of highly proliferative antigen presenting B cells was achieved by activation via soluble as well as membrane bound CD40L 59

3.2 Similar distribution of B-cell subsets was found in human peripheral blood, as well as in primary and secondary lymphoid organs 65

3.3 Phenotypic characterization of the four B-cell subsets.....69

3.3.1 $CD21^{low}$ $CD86^{pos}$ B cells were significantly larger than the other subsets 69

3.3.2 $CD21^{pos}$ $CD86^{pos}$ and $CD21^{low}$ $CD86^{pos}$ B-cell subsets were actively proliferating 70

3.3.3 $CD21^{low}$ $CD86^{pos}$ B-cell subset contained mostly antigen experienced IgM^{neg} IgD^{neg} class-switched B cells 72

3.3.4 Expression of cell surface molecules among B-cell subsets.....73

3.3.5 Expression of molecules involved in cell trafficking among B-cell subsets 77

3.4 Isolation of B-cell subsets via fluorescence activated cell sorting (FACS) 79

3.5 $CD21^{pos}$ $CD86^{pos}$ and $CD21^{low}$ $CD86^{pos}$ B cells were potent antigen-presenting cells....81

3.6 Triggering of BCR poorly induced calcium flux in $CD21^{low}$ B-cell subsets....84

3.7 $CD21^{pos}$ $CD86^{pos}$ subsets exhibited increased constitutive SYK, BTK and ERK phosphorylation and decreased response to BCR mediated stimulation....94

3.8 Impaired CD40 signaling in $CD21^{low}$ B-cell subsets....102

3.9 Combined CD40 engagement and BCR stimulation restored signaling in $CD21^{low}$ $CD86^{pos}$ subset....105

3.10 CD21 and CD86 delineated four functionally distinct peripheral blood B-cell subsets....107

3.11 B_{APC} were increased following vaccination....109

3.12 EBV-infected human B-lymphocytes gain a $CD21^{low}$ $CD86^{pos}$ phenotype in vivo....110

3.13 The balance of $CD21^{low}$ B cells was altered in patients with inflammatory diseases....112

4 Discussion....118

4.1 Soluble rCD40L system to generate antigen-presenting B cells....118

4.2 The $CD21^{low}$ population....120

4.3 Functional and phenotypic characterization of B cells classified by the expression of CD21 and CD86 revealed striking differences among subsets 121

4.3.1 $CD21^{pos}$ $CD86^{neg}$ B_{conv} subset....121

4.3.2 $CD21^{pos}$ $CD86^{pos}$ B_{react} subset....121

4.3.3 CD21^{low} CD86^{pos} B_{APC} subset 123

4.3.4 CD21^{low} CD86^{neg} B_{inact} subset 128

4.4 Calcium flux signaling in B cells after CD40L stimulation 131

4.5 B-cell subset homeostasis is disturbed in some diseases 132

4.6 Conclusion 136

References 139

5 Attachments 181

5.1 Erklärung § 4 Abs. 1 Nr. 9 181

5.2 Teilpublikationen 181

5.3 Lebenslauf 182

5.4 Publikationen 184

Introduction

1 INTRODUCTION

In addition to their recognized role in humoral immune response, B cells have several other functions less well understood. This research project seeks to contribute to a deeper understanding of the role that B cells play in antibody-independent human responses. In order to get a better understanding of the alterations in B cell homeostasis and composition in physiologic as well as in the context of immune-related diseases, a detailed analysis of the B-cell compartments of healthy and patient samples was performed.

1.1 Immune system

Humans and other higher-order animals are constantly exposed to a broad range of microorganisms that might threaten their survival. As a result, the immune system has evolved in a complex array of protective mechanisms, which recognize, control and eradicate such threats and preserve the homeostasis and normal function of the host. Using an interactive network of physical and chemical barriers, lymphoid organs, immune cells and secreted factors, the immune system is able to fight and discriminate whether these microbes are pathogenic or beneficial commensal organisms. More importantly, it can distinguish self from non-self. These functions become more obvious when the immune system is not functioning properly. As a consequence, immunocompromised patients are prone to development of severe infections and tumors while failure of tolerance mechanisms leads to allergic reactions and autoimmunity.

1.2 Innate and adaptive responses

The immune system is composed of two main branches referred to as innate and adaptive immunity. Although determined by the speed and specificity of the response, they are not mutually exclusive and act together (Parkin and Cohen 2001). The innate response is the first line of host defense while the adaptive response is more prominent after a few days when B and T lymphocytes have undergone clonal expansion. Innate immunity includes common physical and chemical barriers to prevent the entry of harmful organisms. Moreover, cells such as neutrophils, monocytes and macrophages equipped with highly conserved recognition molecules identify the majority of pathogens, thereby ensuring a rapid and unspecific host reaction (Chaplin 2010).

It is not surprising that in order to defend the host against the overwhelming amount of microorganisms that are constantly changing and evolving, the immune system needs to evolve as well. The adaptive immune response is the answer to this challenge. The hallmark of adaptive immunity is that it relies mainly on the recognition of specific antigens by receptors expressed on B and T lymphocytes. Hence, adaptive immune responses are highly specific. In contrast to the germline-encoded recognition receptors found on cells of the innate immune response, B and T lymphocytes express antigen-specific receptors, whose genes are assembled by somatic recombination of germline gene segments. The rearrangement of these elements results in a vast variety of intact T or B-cell receptor genes, each with a potentially unique specificity for a different antigen. This process ensures that at least few naïve B and T cells will have a high-affinity receptor to bind virtually any pathogenic antigen. Thus, the encounter with the specific antigen will lead to clonal expansion and generation of immunological memory for a rapid response in case of re-exposure (Bonilla and Oettgen 2010).

1.3 T lymphocytes

T cells develop from progenitor cells in the bone marrow that migrate to the thymus at early stage of their development. Naïve T lymphocytes that have not yet encountered their antigen traffic to secondary lymphoid tissues (lymph nodes, tonsils, mucosa-associated lymphoid tissue -MALT- and spleen). These areas provide the appropriate microenvironment in which lymphocytes and cells of the innate immune response, such as antigen-presenting cells (APCs) interact. Trafficking of lymphocytes through lymphoid organs is regulated by an array of adhesion molecules and chemokines, which brings cells in contact and increases the chances to recognize their specific antigen. Binding of antigen by the specific T cell in the context of costimulation by activated APCs leads to cell priming, activation and differentiation (Parkin and Cohen 2001).

T lymphocytes bind antigen through the T cell antigen receptor (TCR). This type of receptor recognizes antigenic peptides that have been processed and presented in the context of major histocompatibility complex (MHC) molecules on the cell surface of APCs. After antigen recognition, T cells proliferate, migrate to antigenic sites and perform effector functions such as direct killing of antigen-expressing cells ($CD8^+$ cytotoxic T cells) or release of cytokines to modulate the immune response ($CD4^+$ helper T cells) (Broere et al. 2011).

1.3.1 $CD8^+$ cytotoxic T Cells

$CD8^+$ cytotoxic T cells recognize 8-10 amino acid long peptides presented on the surface of their target cells in combination with self-MHC class I molecules (Klein and Sato 2000). Among their effector functions are the secretion of interferon (IFN)-γ and apoptosis-inducing molecules, such as perforin and granzyme B, and the up-

regulation of Fas ligand. Moreover, specific antigen binding induces differentiation of memory T cells, which are faster and more efficient responders upon antigen re-exposure (Weninger et al. 2002).

1.3.2 $CD4^+$ helper T Cells

$CD4^+$ T helper cells recognize 10-34 amino acid long peptides from exogenous proteins presented in combination with MHC class II molecules by APCs (Klein and Sato 2000). $CD4^+$ T cells can differentiate into several functionally distinct subsets depending on the context of antigen encounter. According to the cytokine profile secreted, helper T cells can be divided broadly into type 1 (T_h1), type 2 (T_h2), T_h17 and regulatory T cells (Tregs). The cytokine environment plays a critical role in this lineage commitment process, for example interleukin-12 (IL-12) promotes T_h1 differentiation, whereas IL-4 promotes T_h2 differentiation (O'Garra 1998). T_h1 cells produce the proinflamatory cytokine IFN-γ and are responsible for regulating cellular immunity (Cohen et al. 2011). On the other hand, T_h2 secrete IL-4, IL-5 and IL-13 which favors humoral immune responses by B cells, while inhibiting T_h1 cellular immune responses (Chang et al. 2009).

A novel family of $CD4^+$ helper T cells was identified during the last years, which is essentially characterized by the production of IL-17 and was therefore named "T_h17" (Cua et al. 2003, Harrington et al. 2005). T_h17 cells exist both in mice and humans, but their phenotypic and functional characteristics, as well as the mechanisms responsible for their development in the two species, appear to be different (Romagnani 2008). In humans they have been found after polyclonal stimulation in peripheral blood and in gut from healthy individuals or patients with Crohn's disease (Acosta-Rodriguez et al. 2007, Annunziato et al. 2007).

Finally, Tregs are characterized by the constitutive expression of CD25 and the transcription factor forkhead box P3 ($FoxP_3$) (Wing and Sakaguchi 2010). Tregs are key controllers of peripheral tolerance to self-antigens and alloantigens (Sakaguchi et al. 1995).

1.4 B lymphocytes

B lymphocytes are cells of the acquired immune response. They develop from progenitor cells in the bone marrow and remain there through their development. B cells recognize intact antigens through the B-cell receptor (BCR) that consists of an immunoglobulin (Ig) bound to the cell membrane (mIg). Activation of B cells is triggered by the binding of antigen to the BCR, thus initiating a cascade of signaling events that lead to antigen processing and presentation to T cells (Treanor 2012).

1.4.1 B cell origin and development

During early fetal development, Pre-B cells can be found in several tissues such as fetal liver (Gathings et al. 1977) and fetal omentum (Solvason and Kearney 1992). However, after this stage and throughout life, B lymphopoiesis occurs only in the bone marrow (Figure 1).

B lineage cells develop from hematopoietic stem cells (HSCs) in fetal liver or adult bone marrow. Once HSCs undergo an asymmetrical division to generate one stem cell and one differentiating cell, it gives rise to progenitor cells that undertake lineage commitment to originate lymphoid or myeloid/erythroid progenitors. The common lymphoid progenitor (CLP) has the capacity to develop into T, B or natural killer (NK) cells but low or no capacity to generate cells of myeloid/erythroid lineage.

The model proposes that CLP can differentiate into two types of intermediate lymphoid progenitors: early-B cells or T/NK/dendritic cell (DC) tri-lineage cell (LeBien 2000). Early-B cells that have not yet started BCR rearrangement are named progenitor B cells (pro-B cells) (Figure 1). During differentiation from CLP to pro-B cells recombination enzymes such as recombination-activating gene (RAG)-1, RAG-2 and deoxynucleotidyl transferasa are activated to promote the ordered rearrangement of variable (V), diversity (D) and joining (J) gene segments to form the BCR (Ichii et al. 2014).

Pre-B cells arise from pro-B cells with the expression of the so-called pre-BCR. The pre-BCR consists of the immunoglobulin heavy chain (µHC) pair with the surrogate light chain (SLC) components (VpreB and λ5) and the transmembrane proteins Igα and Igβ (also known as CD79a and CD79b) (Brouns et al. 1995). Pre-BCR expression is a pre-requisite for B cell development and also a signal for its own internalization and degradation (Burrows et al. 2002) as well as for inactivation of genes encoding the SLC components. Therefore, as cells proliferate, less pre-BCR complex can be formed on the surface. If a cell fails to generate a viable immunoglobulin light chain (IgLC) to associate to its µHC, it undergoes cell arrest and eventually death (Lam et al. 1997). Moreover, pre-BCR signaling induces rearrangements of the V and J light genes and allelic excision at µHC (Ichii et al. 2014). At this stage IgLC assembles with the µHC resulting in an immunoglobulin of the IgM class, which is transported to the cell surface. Although BCR rearrangement is complete, cells at this stage are called immature B cells since they only express IgM and their ability to bind self-antigens is still to be tested (Figure 1).

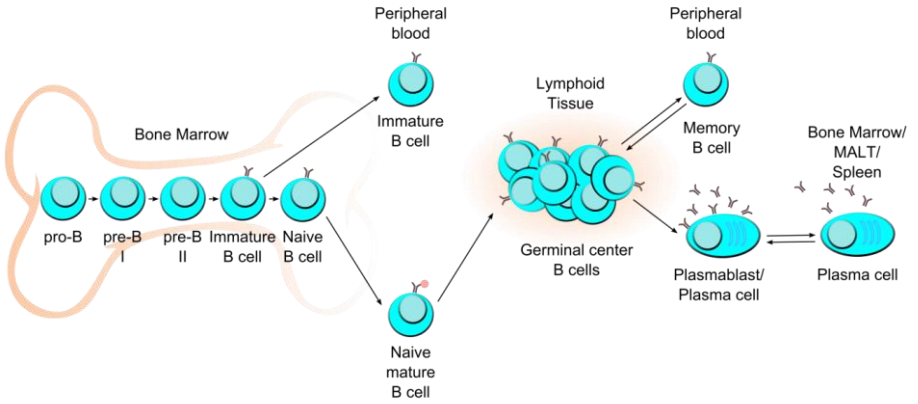

Figure 1. B cell development and differentiation subsets

Human B cell development in the bone marrow, differentiation subsets in peripheral blood and secondary lymphoid tissues: spleen and mucosa-associated lymphoid tissues (MALT). Modified from (Perez-Andres et al. 2010).

Immature B cells are particularly sensitive to tolerogenic signals, a feature that is lost after maturation and differentiation into B-cell subtypes with unique functions (Allman and Northrup 2007). In this respect, immature B cells undergo a receptor-mediated negative selection. During the process, only 20% of the cells survive and can emigrate from the bone marrow. Self-reactive B cells undergo negative selection through three known mechanisms: deletion, anergy and receptor editing in which auto-reactive cells undergo a further gene rearrangement to modify their receptors (Wang and Clark 2003). The fate of self-reactive immature B cells depends on several factors, including receptor affinity, IgM expression, stage of maturation and site of ligand encounter. It has been shown that binding of high-avidity ligands leads to deletion (Erikson et al. 1991, Chen et al. 1994) while immature B cells that bind lower-avidity ligands become anergic (Goodnow et al.

2009). Level of IgM expression has also been related to how B cells respond to antigen. In vitro experiments done by Melamed et al, demonstrated that IgM^{low} immature B cells undergo receptor editing after BCR stimulation. In contrast, BCR ligation on IgM^{hi} B cells induces apoptosis (Melamed et al. 1998). The microenvironment surrounding the place where immature B cells find the antigen is also affecting the outcome; while binding in the bone marrow induces receptor editing, ligation in the spleen induces deletion (Wang and Clark 2003). These mechanisms of tolerance diminish to a minimum the risk of reaction of B cells to tissues of the host organism.

As soon as the small proportion of cells that escape negative selection leave the bone marrow or fetal liver to populate peripheral blood and lymphoid tissues, B cells start to diversify the constant region of the membrane bound immunoglobulin (Figure 1). Via the process known as class switch recombination (CSR), maturing B cells start to express on the surface a second isotype with the same specificity, IgD. Isotype switching takes place through a mechanism of alternative splicing of a large primary messenger ribonucleic acid transcript containing both μ and δ constant region genes. After splicing, the recombined VDJ gene contains the exon coding δ heavy chain segment to produce mIg of the IgD isotype (Geisberger et al. 2006). At this stage naïve B lymphocytes are characterized by their short-life span, their dominance during early phases of reconstitution of the peripheral B-cell pool and their susceptibility to undergo apoptosis rather than to proliferate in response to BCR ligation (Allman et al. 2001).

Naïve B cells recirculate through peripheral blood and enter lymph nodes, spleen and MALT (Figure 1). If they do not encounter antigen, they will continue recirculating until they die after a couple of days due to failed positive selection.

Those naïve B cells that bind their cognate antigen in the secondary lymphoid tissue will be primed and start the germinal center (GC) reaction in cooperation with $CD4^+$ and $CD8^+$ antigen-specific T cells (Figure 1) (Allen et al. 2007). In the GC, B cells are constantly migrating between the dark zone (centroblasts) and the light zone (centrocytes). In the dark zone, B cells undergo clonal expansion, CSR and somatic hypermutation (SHM) of variable heavy-chain region genes. By the SHM process, non-templated point mutations are introduced in the variable region of rearranged immunoglobulin heavy and light chain genes. Then, in the light zone, they re-encounter the antigen and undertake affinity maturation of the BCR (Allen et al. 2007, LeBien and Tedder 2008). This results in the preferential outgrowth of B cells expressing an immunoglobulin that has high affinity for its cognate antigen (Odegard and Schatz 2006).

GC-B cells are characterized by up-regulation of CD10, CD38, CD95 and HLA-DR and decreased expression of CD44 and bcl2 and heterogeneous expression of CD27 which differentiated them from naïve, memory B cells and plasmablasts (Allen et al. 2004, Allen et al. 2007). After undertaking several rounds of proliferation and affinity maturation, these cells become memory and pre-effector (plasmablasts) B cells (Allen et al. 2007). Quiescent memory B cells remain recirculating in peripheral blood or through tissues, where they can find antigen, while plasmablasts migrate to bone marrow or MALT to complete the differentiation and become antibody-producing B cells (plasma cells -PCs-) (Figure 1) (Perez-Andres et al. 2010).

1.4.2 Circulating peripheral blood B-cell subsets

B lymphocytes are phenotypically and functionally heterogeneous. During the past years, several subpopulations of B cells have been discovered. The use of

monoclonal antibodies (mAbs) and multicolor flow cytometry combined with functional assays has facilitated this work. The first attempt to classify human B cells was the introduction of the B mature (Bm) system (Liu and Arpin 1997). Tonsillar B cells were classified according to the surface expression of IgD and CD38. Five major subsets were reported: naïve B cells (IgD^{pos} $CD38^{neg)}$ that can be further subdivided in Bm1 ($CD23^{neg}$) and Bm2 ($CD23^{pos}$) subsets, GC-B cells (IgD^{neg} $CD38^{pos}$), which were separated by CD77 into centrocytes and centroblasts (Bm3 and Bm4) and the double negatives (IgD^{neg} $CD38^{neg}$), which were described to be memory B cells (Bm5). This was the first classification of B cells. Although extremely useful, it is now clear that binary classification is not enough to discriminate between phenotypically different subpopulations that share the same surface profile.

In this way, IgM and/or CD27 are included nowadays to further categorize the populations (Weller et al. 2004). Therefore, new subgroups have been identified within the above subsets, i.e. Bm5 cells can be subdivided into memory B cells, which express CD27, and PCs, which do not (Youinou 2007). Moreover, later work demonstrated that CD77 does not discriminate centrocytes and centroblasts (Hogerkorp and Borrebaeck 2006).

Human naïve B cells comprise most of the peripheral blood B cells; they co-express IgM and IgD and have unmutated Ig variable regions. On the other hand, memory B cells consist of about 20 to 30% of all peripheral blood B cells and have undergone SHM, affinity maturation and about half also underwent CSR (Klein et al. 1998, Tangye et al. 1998). Naïve and memory B cells also differ in terms of in vitro responsiveness to stimulation, mimicking the primary and secondary response in vivo. Therefore, memory B cells rapidly enter the cell cycle and undertake more rounds of division. A higher proportion of them become antibody-secreting PCs

(Fecteau and Neron 2003, Good et al. 2009). Both naïve and memory B cells recirculate in peripheral blood and lymphoid tissues. However, many of the memory B cells inhabit places of antigen draining such as the marginal zone of the spleen and the mucosa epithelium of the tonsils (Klein et al. 1998, Tangye and Tarlinton 2009).

Plasmablasts and PCs can be found in low frequencies in peripheral blood from healthy donors (Caraux et al. 2010). They are responsible for high affinity antibody secretion and humoral memory, providing a high quality defense when reencountering antigen. They represent 1-3% of total peripheral blood B cells and might be newly generated plasmablasts that are migrating from secondary lymphoid tissues to a niche in bone marrow or inflamed tissues (Brandtzaeg and Johansen 2005). Higher frequency of PCs in peripheral blood has been associated with bacterial infection and systemic lupus erythematosus (SLE) (Ten Boekel et al. 2007).

Another minor subset of circulating immature B cells has been described in peripheral blood from healthy donors. In addition to expression of the B cell-specific marker CD19, this transitional B-cell subset can be identified using expression of the developmentally regulated markers CD24 and CD38. Transitional B cells make up around 2% of B cells, express high levels of both CD24 and CD38 ($CD24^{bright}$ $CD38^{bright}$), and co-express IgM and IgD and lack CD27 (Carsetti et al. 2004).

Additionally, recently multiple regulatory B-cell subsets that suppresses cellular immune responses through the production of immunomodulatory cytokines have been identified. IL-10-producing B cells (B10 cells) are the most widely studied regulatory B cells (Yanaba et al. 2008, DiLillo et al. 2010, Mauri and Bosma 2012). These rare cells are named B10 cells to highlight that their regulatory function is mediated solely by its IL-10-dependent regulatory properties, and to distinguish

them from other B-cell subsets that regulate immune responses through different mechanisms (Ray et al. 2012).

In recent years, the development of multi-parameter flow cytometry coupled with improvements in the ability to purify minor cellular subsets using cell sorting has enabled the identification and characterization of novel B-cell subsets that can only be identified using a complex set of surface markers.

1.4.3 B cells in health and disease

Immunity is coordinated by a complex network of cells that are continuously changing in response to the signals they receive. Therefore, there is a high degree of interdependency among the components, and any disruption in the tightly regulated process might result in a failure of the protective mechanisms of the immune system. The introduction of B cell-depleting agents has helped to uncovered the role of B cells in the pathogenesis of several immune-related diseases (Edwards et al. 2004, Looney et al. 2004, Sanz et al. 2007). Interestingly, depletion of B cells not only improved symptoms in diseases typically considered of B cell origin (such as SLE, idiopathic autoimmune thrombocytopenia, dermatomyositis and autoimmune blistering diseases) but also diseases in which B cells where not thought to play a major role (rheumatoid arthritis, multiple sclerosis and type 1 diabetes) (Edwards et al. 2004, Looney et al. 2004, Hauser et al. 2008, Xiu et al. 2008, Mei et al. 2012, Fuertes et al. 2013). Studies done in mice might explain the phenomenon, since they showed that mAb Rituximab (anti-CD20) therapy leads to B cell depletion by monocyte-mediated antibody-dependent cellular cytotoxicity (Uchida et al. 2004) and that amelioration of symptoms might be due to regulation of $CD4^+$ T cell expansion, thus delaying and controlling the acute inflammatory phase that leads to

tissue damage (Bouaziz et al. 2007). Moreover, it might be that the therapeutic effect seen by this intervention is to a large extent related to the disturbance of the functional balance of B-cell subsets (Sanz and Lee 2010).

Malfunction in B-cell compartment influences development of immunodeficiencies, autoimmunity or hematologic malignancies. For instance, a typical immunodeficiency generated by disturbances in later stages of B cell development is common variable immunodeficiency (CVID). It is a disease that can be manifested at any time of life and is probably influenced by genetic or environmental factors. Patients exhibiting this disease have low serum immunoglobulin and are more susceptible to infections. Additionally, they have low levels of B cell memory, CSR and B cell activation (LeBien and Tedder 2008). It is important to stress that disruption in tolerance checkpoints in this disease results in a loosening of tightly-controlled screening process for reactivity to self-antigens and predisposes to autoantibody production and autoimmunity. However, the role of B cells in the pathogenesis of autoimmune diseases is not restricted to autoantibody production but also contributes to autoantigen presentation to T cells and through proinflamatory cytokine production (Shlomchik 2008). In the case of B cell-related cancer, disruption of differentiation at any stage of development (Figure 1) can lead to the expansion of a malignant counterpart of dominant subclones that ultimately derive in leukemia and lymphoma.

1.4.4 Molecular architecture of B cells

It was not until 1980, with the use of mAbs that the molecular constitution of the B cell surface started to be identified. B cell molecules that have been characterized so far are associated with BCR signaling, development, function,

adhesion and communication with the extracellular environment (LeBien and Tedder 2008).

B lymphocytes express on their surface several molecules that are shared with many other leukocyte types. For instance, B cells proliferate in response to bacterial deoxyribonucleic acid (DNA) due to signaling through Toll-like receptors (TLR), which are also known to be expressed by multiple leukocyte lineages (LeBien and Tedder 2008). As discussed earlier, CD38 and CD27 molecules are essential to define B-cell subsets although they are not B-cell lineage restricted (Jackson et al. 2008).

On the other hand, several molecules are preferentially expressed by B cells. Among them are CD19, which can be found in virtually all B-lineage cells, CD20 that functions as a calcium (Ca^{2+}) channel embedded in the membrane, CD21 (also known as complement receptor 2), CD22 and CD72 that negatively regulate BCR signaling, CD23 a low-affinity receptor for IgD, CD24 – a molecule with unknown function - and CD40 that serves as a survival factor for GC-B cells when binding to its ligand on T cells (CD40 Ligand -CD40L- also known as CD154) (LeBien and Tedder 2008).

1.4.4.1 The complement receptor (CR) 2: CD21

It is well known that in order to generate an appropriate immune response, B cells require not only BCR cross-linking but also additional signals through coreceptors such as CR1, CR2 and Fcɣ (FcɣRI, FcɣRII and FcɣRIII) receptors (Erdei et al. 2009).

CR2, also known as CD21, is a glycoprotein receptor expressed by B cells, T cells and follicular DCs. On B cells it appears at the mature stage and disappears after PC differentiation. In humans, it is composed of 15 to 16 short consensus repeats, a

transmembrane domain and a short cytoplasmic tail and is generated from the CD21 gene which encodes a single RNA transcript (Erdei et al. 2009). The interaction of CD21 with its ligands is known to require the first 2 consensus repeats (Lowell et al. 1989, Szakonyi et al. 2001). CD21 binds C3 degradation products C3d, iC3b and C3b (Boackle et al. 1997). In addition it also binds CD23 (Aubry et al. 1992) and IFN-α (Asokan et al. 2006) and serves as entry receptor for Epstein-Barr virus (EBV) by binding pg350/220 glycoprotein on EBV (Nemerow et al. 1987). CD21, as a receptor of complement fragments facilitates the cross-talk between the innate and adaptive branches of the immune response.

CD21 is expressed on the surface of B cells either as part of a trimolecular complex of CD21, CD19 and CD81 or associated with CR1 (CD35); very few reside alone (Tuveson et al. 1991, Grattone et al. 1999). As part of the B-cell coreceptor complex, cross-linking of CD21 and BCR by antigen-complex augments and potentiates activation through recruitment of CD19 and CD81, and helps to initiate downstream stimulatory events (Rickert 2005). In fact, C3d fragments deposit on antigen increases the immunogenicity by recruiting both proteins and inducing phosphorylation not only in CD19 but also in CD21 cytoplasmic tail (Dempsey et al. 1996, Barrault and Knight 2004). In summary, there is substantial evidence that supports the in vivo significance of CD21 providing an important link between the innate and adaptive immune responses (Dempsey et al. 1996, Fearon and Carroll 2000).

Most of circulating B lymphocytes expresses high levels of CD21. However, there is a small fraction of naïve and memory B cells with low levels of CD21 expression. Although to date little information is known about the role of $CD21^{low}$ B cells, in diseases such as CVID and human immunodeficiency virus (HIV) infection, the

frequency of this subset is increased (Moir et al. 2008, Rakhmanov et al. 2009).

1.4.5 B cell functions

During the past years, the old concept that B cells are exclusively committed to produce antibodies has been reconsidered. Nowadays, it is apparent that in addition to their essential role in humoral immunity, B cells accomplish many other tasks crucial for immune homeostasis (Figure 2). Of great importance is the requirement of B cells to initiate T cell immune responses. The first in vivo evidence for this assumption came from studies done by Ron et al., in which mice were depleted of B cells by administration of anti-μ antibodies from birth (μ-suppressed mice (μSM)) (Ron et al. 1981, Ron et al. 1983). After antigen inoculation with complete Freund's adjuvant, μSM had a severe impairment in $CD4^+$ T cell activation. In addition, these mice were also more susceptible to bacterial and viral infection (Cerny et al. 1988, Cerny et al. 1988), had a reduced delayed-type hypersensitivity reaction to soluble antigens (Herrmann et al. 1988) and were resistant to diabetes by abrogating completely the development of insulitis and sialitis (done with μSM-Nonobese diabetic mice) (Noorchashm et al. 1997). When mice were injected with B cells prior to antigenic challenge, the observed defects in μSM were largely overcome (Janeway et al. 1987, Ron and Sprent 1987, Noorchashm et al. 1997). All this evidence suggests that $CD4^+$ T cell could not be efficiently primed in the absence of B cells and that B cells play a direct role as APCs.

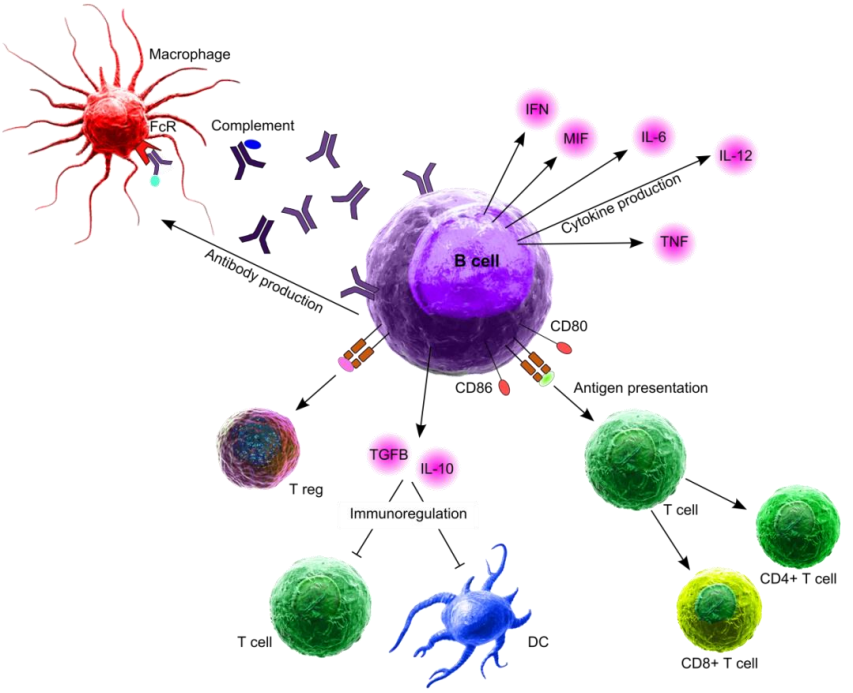

Figure 2. B cell functions

Selected examples of the multifunctional attributions of B cells and how they regulate immune homeostasis. Most of the functions of B cells are independent from antibody production. Modified from (LeBien and Tedder 2008).

APC function by B cells became controversial with the introduction of B-cell deficient mice generated by gene targeting either of the µ-chain or Ig heavy chain genes (Kitamura et al. 1991, Chen et al. 1993). Experiments done by independent groups with these B-cell deficient mice range from complete deficiency to almost normal T cell response (Epstein et al. 1995, Liu et al. 1995, Phillips et al. 1996, Macaulay et al. 1998). A more recent study using several B-cell deficient mice strains

generated by the same gene targeting technique demonstrated that in all but one strain (C57BL/6 background; which were used for most of the previous studies) T cell responses were impaired (Rivera et al. 2001). They showed that T cell priming of B-cell deficient mice of C57BL/6 background were much more variable, explaining the controversial results.

In addition, by breeding chimeras it was possible to show that the congenital absence of B cells also plays a role during immune system development, which is evidenced by a diminished amount and diversity of thymocytes, defects within DC and T cell compartments, Peyer patch organogenesis and impaired chemokine expression by macrophages (LeBien and Tedder 2008).

Moreover, B cells are also important for regulation and maintenance of the immune system by cytokine secretion. Cytokine-producing B cells can be divided into regulatory B cells, which secrete IL-10 (B10 cells) or transforming growth factor (TGF)β-1 and effector B cells that produce IL-2, IL-4, tumor necrosis factor (TNF)α, IL-6 or INFγ, IL-12 and TNFα (Lund 2008). By releasing cytokines, B cells can influence T cells, DCs, APC functions, regulate lymphoid tissue organogenesis and wound healing, modulate transplant rejection, tumor development and tumor immunity (LeBien and Tedder 2008). Moreover, the profile of cytokine released by effector B cells can influence the polarization of the T cell response (Harris et al. 2000). Additionally, cytokine production and antigen presentation by B cells have been associated to influence a range of diseases such as atherosclerosis, insulin resistance, HIV, graft-versus-host disease, and allograft rejection (Moir and Fauci 2009, Shimabukuro-Vornhagen et al. 2009, Ait-Oufella et al. 2010, Winer et al. 2011).

1.4.5.1 How B cells capture, process and present antigens?

In order to confer effective protection against the huge variety of pathogenic antigens that can face the immune system throughout the body, the response must be tightly harmonized. Therefore, antigenic interaction occurs mostly in defined sites (secondary lymphoid organs) such as lymph nodes and spleen. The lymphoid tissue possesses a highly compartmentalized microarchitecture that is essential for cellular interactions and initiation of optimal immune responses. In order to get activated and to exert APC function, B cells require two main signals. First, B cells recognize and capture the specific antigen by their BCR, which induces growth, proliferation, survival and expression of the costimulatory molecule CD86 on the B cells (Lenschow et al. 1994). Then, the antigen is degraded into peptide fragments that are loaded onto MHC class II molecules that are next presented on the cell surface to specific $CD4^+$ T cells. Interaction with $CD4^+$ T cells provides the second stimulatory signal mediated by CD40-CD40L binding and secretion of IL-4 by T cells (Figure 3) (Ranheim and Kipps 1993, Evans et al. 2000). T and B cell cooperation is required for proper B cell activation, GC formation, differentiation into high-affinity antibody-producing PC, generation of memory B cells (Yuseff et al. 2013) and proper APC function by up-regulation of the expression of MHC class I and II and costimulatory molecules CD80 and CD86 (Kennedy et al. 1994, Faassen et al. 1995).

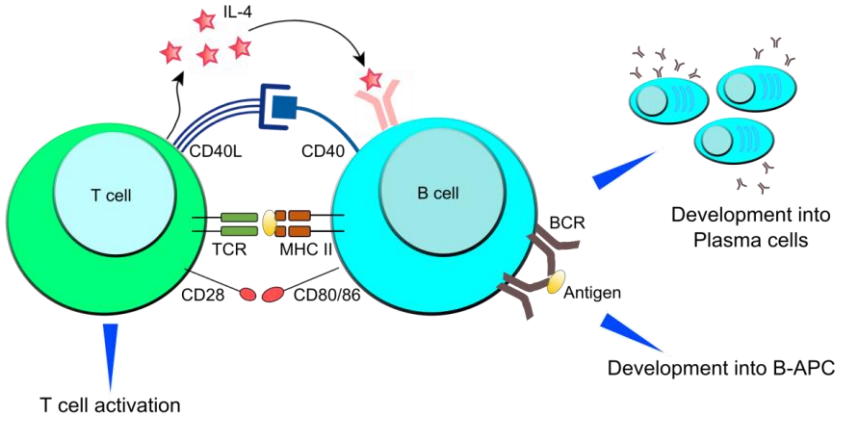

Figure 3. Interaction between B and T lymphocytes

Model for interaction between $CD4^+$ helper T cell and B cell after antigen encounter. The antigen bound to the B-cell receptor (BCR) of the specific B cell is processed and the peptides of the processed antigen are presented in the context of MHC class II (MHC II) molecules to the helper $CD4^+$ T cells via the T cell receptor (TCR). Optimal T-cell activation takes place when the costimulatory molecules CD80 and CD86 interact with CD28, providing the necessary costimulation. The activated $CD4^+$ helper T cells upregulate CD40L and secrete IL-4, which results in contact-dependent B-cell activation through CD40 and through IL-4 signaling. The functional end point after antigen encounter is differentiation of effector T and B cells. Modified from (Guttormsen et al. 1999).

1.4.5.1.1 BCR internalization and signaling

Receptor endocytosis and initiation of signaling events required for B cell activation are induced by both soluble and membrane-bound antigens binding to BCR. Signaling through BCR and coreceptor starts with the recruitment and activation of tyrosine kinases. Critical for signaling is the transmembrane heterodimer Igα/β, which is associated noncovalently with the BCR coreceptor complex (Campbell et al.

1991). Upon antigen binding, mIg and Igα/β heterodimer, which contain highly conserved phosphorylation motifs (immunoreceptor tyrosine-based activation motif or ITAMs) are phosphorylated. Upon phosphorylation the BCR complex translocates to the glycolipid and cholesterol-rich membrane microdomains where proteins of the non-receptor protein tyrosine kinase Src family including Lyn, Fyn and Blk are constitutively present to initiate the down-stream cascade of activation signaling (Rickert 2005). Once phosphorylated, Igα/β ITAMs recruit and activate the tyrosine kinase SYK (Kurosaki et al. 1995). Subsequently, SYK and Src family kinases initiate separate but inter-related signaling pathways. While Src family kinases serve to phosphorylate nuclear factor (NF)-kB (Saijo et al. 2003), CD22 (Fujimoto et al. 1999) and BAM32 (Niiro et al. 2002), SYK phosphorylates BLNK (Fu et al. 1998), which in turns coordinates the assembly and activation of a receptor-retained signalosome containing phospholipase Cγ2 (PLCγ2), Vav, BTK, Nck, and Grb2 (Chiu et al. 2002).

Concurrent with signal initiation, the majority of BCR-antigen complexes are rapidly cleared from the cellular membrane. In fact, BCR-antigen engagement induces maturation of late endosomal and lysosomal compartments, into which BCR complexes are internalized and antigen is depredated by the acidification of the vesicles (Siemasko et al. 1998). Initial activation events in response to membrane-bound antigen induce a biphasic spreading and contraction reaction on B cells. First, in the rapid spreading phase B cells extend lamellipodia across the follicular DC loaded with antigen increasing the amount of BCR-antigen interactions depending on the reorganization of the actin cytoskeleton. This dynamic structure, in addition to integrins such as leukocyte function antigen-1 (LFA-1), promotes the adhesion of B cells to APCs lowering the threshold for activation (Carrasco et al. 2004). Subsequently and more slowly, the B cell contracts cumulating antigen into a central cluster that acts as a platform for antigen internalization (Fleire et al. 2006).

Collectively the spreading and contraction responses determine how much antigen is acquired and presented by the B cell, and therefore determine the outcome of B cell activation (Depoil et al. 2008).

In addition, secretion of molecules of both endocytic and exocytic processes takes place in the immunological synapse. It is believed that proteases and hydrolases released in the vesicles are required to free the membrane-bound antigens from APCs and to start antigen degradation at the extracellular space (Yuseff et al. 2011). Some antigenic peptides released are directly loaded onto MHC class II molecules in the extracellular space probably at the same time that occurs in the main intracellular pathway. On the other hand, B cells also extract tethered antigen by trogocytosis, which involves the exchange of membrane fragments between cells (Aucher et al. 2008).

Synthesis of MHC class II and the costimulatorymolecules CD80 and CD86 are also enhanced by BCR signaling (Reth and Wienands 1997, Zimmermann et al. 1999). Internalization of the BCR is regulated by clathrin (Stoddart et al. 2002) and depends on the ubiquitylation of BCR-antigen complexes that occur downstream of SYK-dependent signaling (Katkere et al. 2012) providing evidence for the relationship between signaling and endocytic trafficking. Propagation of the signal continues within endocytic compartments, with further kinase phosphorylation that ultimately leads to transcription of genes required for B cell activation (Chaturvedi et al. 2011).

1.4.5.2 CD40-CD40L interaction

CD40 is a type 1 transmembrane protein member of the TNF-receptor family. It was first described in 1985 as a molecule constitutively expressed on B cells throughout development and differentiation (van Kooten and Banchereau 2000).

Furthermore, it is expressed by a variety of immune and non-immune cells including APCs such as macrophages, DCs and endothelial cells (Schonbeck et al. 2000). Its natural ligand, CD40L, is expressed mainly on activated $CD4^+$ T cells (van Kooten and Banchereau 2000). It is a type 2 transmembrane protein of the TNF family of ligands and forms homotrimers on the cell membrane (Schonbeck et al. 2000). Moreover, CD40L is also released in a soluble form (sCD40L) retaining its function and the trimeric structure of the membrane-bound protein (Mazzei et al. 1995). As described in section 1.4.5.1, interaction between CD40 and CD40L results in proliferation, differentiation and increased expression of surrogate molecules of APC function, which enhance efficacy of their antigen presentation capacity (Banchereau et al. 1994, Yellin et al. 1994, von Bergwelt-Baildon et al. 2002). Antigen presentation in the context of MHC class II on the surface of APCs together with costimulation through receptors and ligand pairs, such as CD40-CD40L, enhances T cell activation and differentiation modulating the immune response (Figure 3) (Bretscher 1999).

1.4.5.2.1 Signaling through CD40L

Ligation of CD40 by its ligand induces the activation of several signaling pathways (Figure 4). The cytoplasmic signaling domain of CD40 lacks intrinsic catalytic activity, therefore upon activation relies on several proteins of the TNF receptor associated factor (TRAF) family that interact with different recognition motif in the cytoplasmic domains (Harnett 2004). Association of TRAF with CD40 leads to activation of MAPKs (mitogen activated protein kinases) ERK (extracellular signal regulated kinase), Jnk (c-Jun N-terminal kinase) and p38 and the canonical and noncanonical NF-ĸB pathways. ERK, p38 and Jnk are activated by a cascade of MAP kinases and result in the activation of transcription factors, among them Elk-1, ATF1 and AP-1 (Fos/Jun), respectively (van Kooten and Banchereau 2000). Binding of

CD40L also induces phosphorylation of Janus Kinase 3 (JAK3) which produces a subsequent phosphorylation of STAT3 (signal transducer and activator of transcription) and STAT6 (Hanissian and Geha 1997, Karras et al. 1997). The JAK3 pathway is relevant for activation of monocytes and DCs but seems to be of little importance for CD40-mediated B cell activation (Jabara et al. 1998, Revy et al. 1999, Saemann et al. 2002). In some systems, pathways such as PI3K (phosphoinositol 3 kinase) and PLCγ2 have been shown to be induced upon CD40 signaling (Hanissian and Geha 1997, Harnett 2004). Additionally, there is some evidence that CD40 stimulation activates protein Tyr kinases, such as Lyn, Fyn and SYK (Faris et al. 1994).

Downstream events of CD40 signaling include activation of canonical and noncanonical NF-ƙB and NF-ƙB-like transcription factors (Figure 4) (van Kooten and Banchereau 2000). The activation of the NF-ƙB pathway is mediated by the targeting of inhibitory proteins in a proteasome-dependent manner. In the case of the canonical NF-ƙB pathway, IƙBα is the inhibitor of p50/p65 and p50/c-Rel heterodimers, which retains them in the cytoplasm. Upon activation of the canonical NF-ƙB pathway, phosphorylation of IƙBα leads to its ubiquitination and subsequent degradation by the proteasome, which allows NF-ƙB translocation to the nucleus. On the other hand, in the noncanonical pathway, a protein called p100 is associated with RelB in the cytoplasm preventing the dimer's translocation to the nucleus. Activation leads to phosphorylation and ubiquitin-proteasomal processing of p100 that then remains associated with as a p52- RelB dimer that can enter the nucleus and act as a transcription factor. CD40 triggering thus leads to the transcriptional activation of a variety of genes, including anti-apoptotic as well as cell cycle promoting genes (Figure 4) (van Kooten and Banchereau 2000, Harnett 2004).

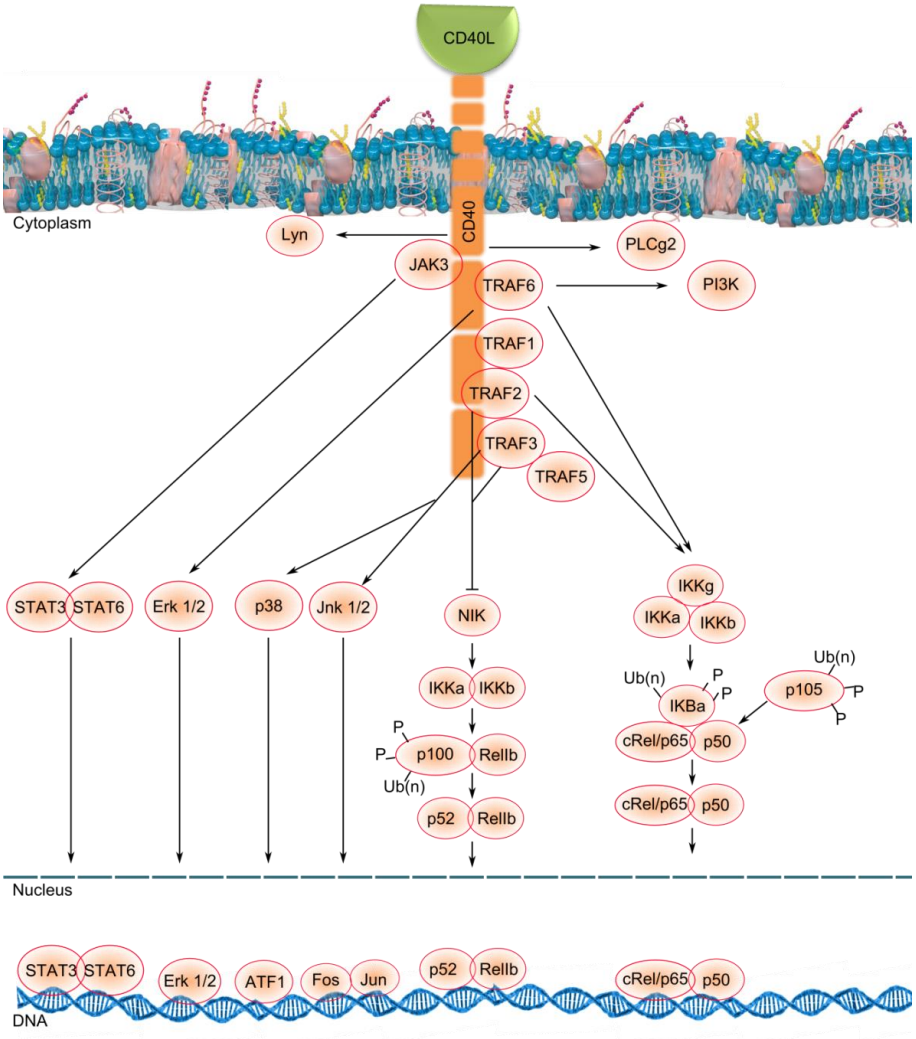

Figure 4. CD40 signaling

Upon CD40L binding and trimerization, CD40 associates with TRAF1, 2, 3, 5, 6 and JAK3 which leads to the activation of the MAPKs ERK, Jnk and p38, the canonical (p50/p65, p50/c-Rel) and the noncanonical (p52/RelB) NF-kB pathway, the PI3K and the PLCγ2 lipid-metabolizing enzymes and the JAK-STAT pathway. ERK, Jnk and p38

activate transcription factors in the nucleus that bind to DNA to activate gene transcription. Specific kinases (NIK and IKKs) activate the canonical and noncanonical NF-κB pathways by phosphorylation of inhibitors of NF-κB (p100, IκB) marking them for processing and degradation, respectively, by the ubiquitin-proteasomal pathway. P105 is processed constitutively to p50 by the proteasome. NF-κB heterodimers then translocate to the nucleus and act as transcription factors for specific genes. CD40 also mediates phosphorylation of Lyn by unknown mechanisms. TRAF (TNF receptor associated factor), JAK (Janus kinase), NIK (nuclear κ B inducing kinase), IKK (IκB kinase), IκBα (Inhibitor of κ B α), Ub (Ubiquitin), P (phosphorylation), PI3K (Phosphoinositol 3 kinase), PLCγ2 (Phospholipase Cγ2), STAT (signal transducer and activator of transcription), Jnk (c-Jun N-terminal kinase), ERK (extracellular signal regulated kinase). Modified from (van Kooten and Banchereau 2000, Harnett 2004).

1.4.6 Generation of CD40-activated B cells in vitro

Since antigen presentation by B cells has been shown to be essential for optimal induction of T cell immunity (section 1.4.5) a system for generation of B cells with antigen-presenting capacities was urgently needed. Banchereau et al. were the first to report in 1991 the “CD40-system”. They established a protocol to generate long term human B cell lines by continuous stimulation with CD40L and IL-4 (Banchereau et al. 1991, Banchereau and Rousset 1991). BCR stimulation combined with CD40-mediated signaling is the most potent activation stimulus for B lymphocytes. After CD40-activation B cells up-regulate the expression of key molecules involved in antigen presentation such as MHC class II or the costimulatory molecules CD80 and CD86. Schultze et al., described CD40-activated B cells (CD40B cells) to be an alternative source of extremely efficient APCs (Schultze et al. 1997). Since then, several ex vivo strategies based on interaction between CD40 and its ligand have been developed to generate highly potent APCs either by soluble or membrane-bound CD40L-expressing cell line (Wennhold et al. 2013). CD40B cells can be loaded to generate antigen-specific APCs by peptide, protein or tumor lysates

pulsing, by transfection with DNA or RNA or by transduction with viral vectors (Kondo et al. 2002, von Bergwelt-Baildon et al. 2002, Lapointe et al. 2003, Coughlin et al. 2004, Ahmadi et al. 2008).

Phenotypically CD40B cells are characterized by high and stable expression during long-term culture of MHC class I and II molecules, costimulatory molecules such as CD80 and CD86 and adhesion molecules CD58 and CD54. More importantly, CD40B cells are able to induce antigen-specific T cell responses in vitro and in vivo by either priming naïve or expanding antigen-experienced memory T cells. In addition, expression levels of molecules and APC function of CD40B cells are comparable to CD40L-stimulated mature monocyte-derived DCs (Schultze et al. 1997, von Bergwelt-Baildon et al. 2002). Phenotypically and based on their pattern of gene expression they resemble germinal center B cells (Kondo et al. 2002, Wennhold et al. 2013).

As described in section 1.4.5, in order to initiate an immune response, APCs need to encounter T cells, a process regulated by chemokine gradients in the T cell areas of secondary lymphoid organs (von Andrian and Mempel 2003). CD40B cells induce chemotaxis of T cells by expression of chemokines CCL17 (TARC), CCL5 (RANTES), CCL22 (MDC) and CXCL10 (IP-10) as evidenced by increasing migration of both $CD4^+$ and $CD8^+$ T cells in transwell experiments with CD40B supernatant. In addition, CD40B home to secondary lymphoid organs as confirmed by the expression of CD62L, CCR7/CXCR4 and LFA-1 (Klein-González et al. 2010).

Although, the activity of CD40B cells as APC and their capacity to induce immunity in vivo is still being investigated, it is clear that they are potent APCs.

1.4.6.1 DCs vs. CD40B cells as antigen presenting cells

Since DCs are highly specialized in antigen capture, processing, presentation and activation of T cells, they are frequently used in cellular immunotherapy as source of APCs (Cella et al. 1997). Moreover, they have been used in several antitumor vaccine clinical trials (Lapteva et al. 2007). Nevertheless, despite the encouraging results and their significant immunostimulatory capacity, several challenges have been identified in the context of clinical application. On the one hand, they are very rare in peripheral blood and their expansion ex vivo is expensive and laborious (Ardeshna et al. 2000). On the other hand, with the use of standard protocols the generation of homogeneous population of DCs is very difficult. This procedure usually gives rise to subpopulations that may act tolerogenic (Hackstein et al. 2001) or DCs that lack L-selectine, an important molecule for homing to the lymph nodes (Barratt-Boyes et al. 2000). Furthermore, reports from our group and others have shown that DC purity in clinical trials rarely exceeds 50% of the vaccine preparation (Draube et al. 2011).

An alternative source of highly efficient APCs are B cells activated through CD40 and IL-4 signaling. Their use in clinical settings and research can overcome the difficulties found in generation and cultivation of DCs. CD40B cells become highly proliferative upon activation, they can be easily expanded from small amounts of peripheral blood B cells and its possible to obtain highly pure preparations of CD40B cells with potent antigen presentation capacity in vitro (Schultze et al. 1997, von Bergwelt-Baildon et al. 2002, Garcia-Marquez et al. 2014).

1.5 $CD21^{low}$ $CD86^{pos}$ cells: an in vivo counterpart to in vitro generated CD40B cells?

There is a lack of phenotypically well-defined B-cell subset with antigen-presenting capacity that helps to elucidate the exact role that B cells play in these processes in humans. Recently a B-cell subset with phenotypic characteristics resembling CD40B cells was identified (Shimabukuro-Vornhagen et al. in review).

It was demonstrated using a transcriptomic approach that after in vitro CD40 activation several genes involved in B cell differentiation and activation were down-regulated. Specially, immunoreceptors such as complement and Fc receptors, which are known to participate in BCR signaling and antigen uptake (Figure 5A). Additionally, long-term activation with CD40L was accompanied by the up-regulation of the costimulatory molecule CD86 but more importantly the down-regulation of the complement receptor 2, CD21 (Figure 5B). Therefore, a feature of long-term CD40 activated B cells (after 21 days of culture) was the down-regulation of CD21 and up-regulation of CD86 (Figure 5C). The long-term CD40B cells were shown to induce strong proliferation of allogeneic T cells compared to non-activated B cells (Figure 5D and E). These data were kindly provided by Rieke Fischer.

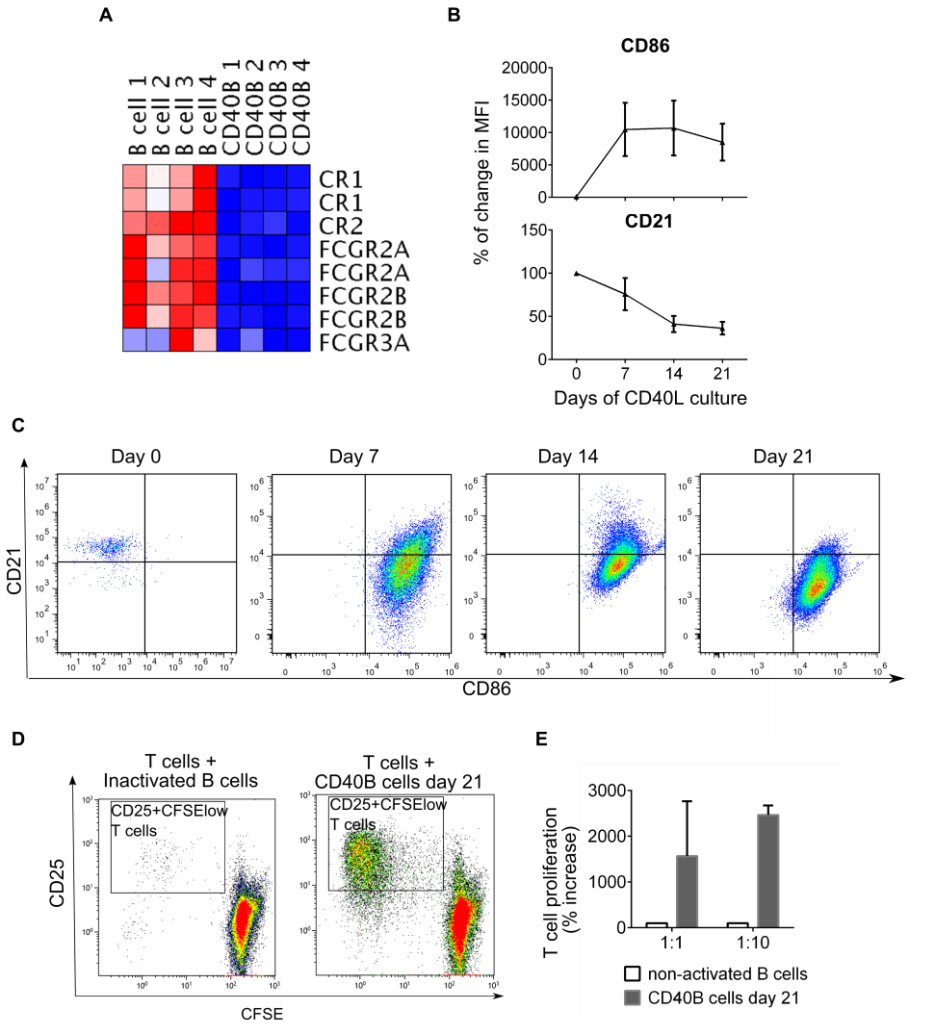

Figure 5. CD21 down-regulation and CD86 up-regulation as features of long-term activated B cells

Purified Human B cells were activated by culture in the presence of CD40L-expressing NIH3T3 fibroblast and pro-inflamatory cytokine IL-4. (A) Heat map visualizing expression of immunoreceptors involved in antigen uptake in resting B cells (B cells)

and CD40-activated B cells (CD40B). Only genes differentially expressed are depicted. Relative expression values are normalized across each row and color coded. Genes with high levels of expression are shown in red, those with low or no expression in blue (n=4). (B) Up-regulation of the costimulatorymolecule CD86 as well as down-regulation of CD21 are the result of prolonged B cell activation. Data are represented as the percentage of change in mean fluorescence intensity to day 0 of culture of the indicated molecule over time, with standard deviation bars (MF ± SD) gated on the $CD19^{+}$ $CD20^{+}$ B-cell population (n=14). (C) Change in CD21 and CD86 expression during the course of the CD40 culture. Shown are representative plots from one donor. (D,E) T cell proliferation in response to a mixed lymphocyte reaction (MLR) with either 21-days CD40-activated or non-activated B cells. (D) FACS plots from one representative donor. T cells that proliferate in response to B cell activation were identified as $CD25^{+}$ $CFSE^{Low}$ T cells. (E) The decrease in CD21 expression was associated with an increase in immunostimulatory capacity of CD40B cells as shown by increase proliferation of allogeneic CFSE-labeled T cells cultured with CD40B cells at day 21. Bar charts represent the mean ± SD of 2 independent experiments with samples from different donors.

Since reduced expression of CD21 and increased expression of CD86 turned out to be a characteristic phenotype for long term-activated CD40B cells with strong immunostimulatory capacity, these markers were used to search for a similar phenotype in humans. Based on the expression of the markers CD21 and CD86, human peripheral blood B cells were divided into four B-cell subsets (Figure 6A). The majority of B cells were $CD21^{pos}$ $CD86^{neg}$. The $CD21^{low}$ B cells could also be further separated into a $CD86^{neg}$ and $CD86^{pos}$ subpopulations (Figure 6B). Interestingly, a spanning-tree progression analysis of density-normalized events (SPADE), which allows the visualization of multidimensional flow cytometric data without prior knowledge, also identified the presence of the distinct B-cell subsets (Figure 6C). Importantly, flow cytometric analysis of peripheral blood of a patient with CVID revealed that expanded $CD21^{low}$ B subset in patients with CVID corresponded to

CD21^{low} CD86^{neg} B-cell subsets (Figure 6D) (Shimabukuro-Vornhagen et al. in review). These data were kindly provided by Rieke Fischer.

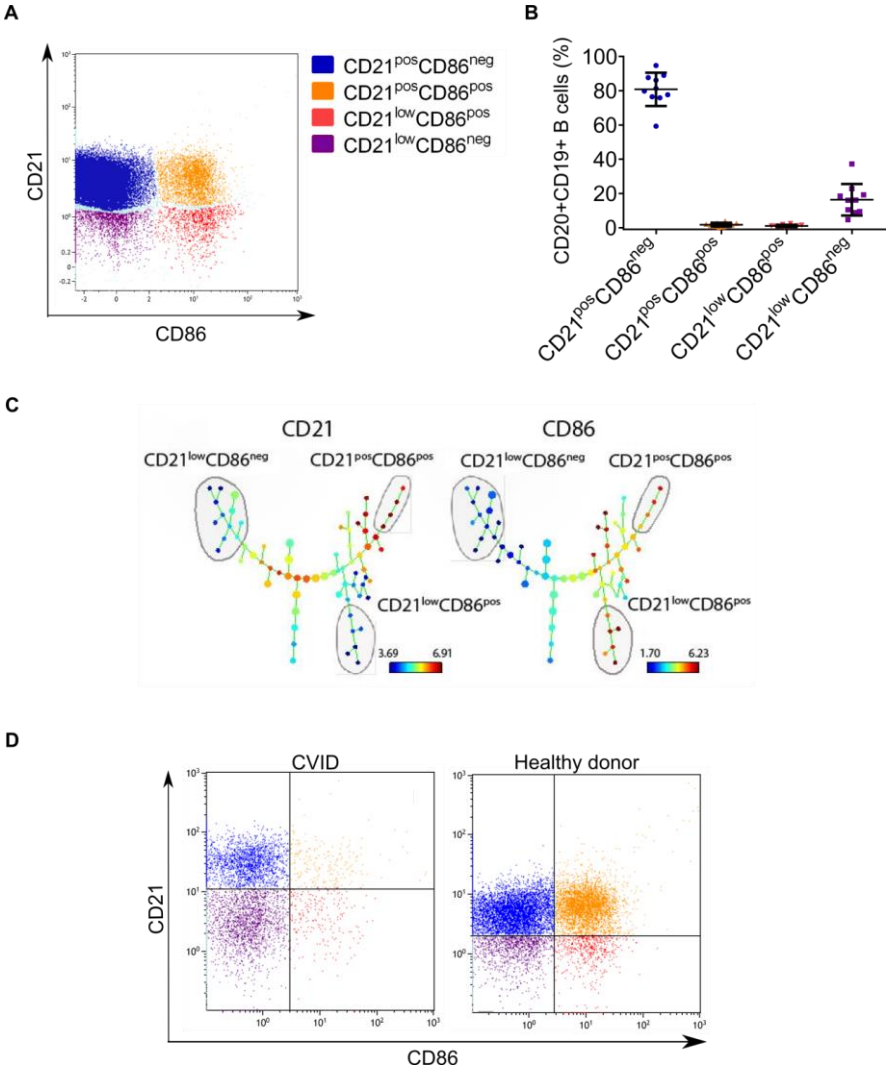

Figure 6. CD21 and CD86 defined four B-cell subsets in peripheral blood from healthy donors.

(A) Flow cytometric analysis of human peripheral blood B cells. Shown is a representative dot plot from a healthy donor showing the distribution of four B-cell subsets according to the expression of CD21 and CD86. Populations are color-coded ($CD21^{pos}$ $CD86^{low}$ in blue, $CD21^{pos}$ $CD86^{pos}$ in orange, $CD21^{low}$ $CD86^{pos}$ in red and $CD21^{low}$ $CD86^{neg}$ in violet). This color-code for the populations will be use throughout the rest of the document. (B) Scatter plot showing the frequency of the four B cells subsets in healthy human individuals (n=10). Bars denote the mean ± SD. (C) SPADE tree colored by the two markers CD21 and CD86. The size of each circle in the tree indicates the relative frequency of cells that fall within boundaries of surface marker expression that define each node. Node color is scaled to the median intensity of expression of the indicated markers. (D) FACS plot from peripheral blood of a CVID patient compared to a healthy control.

1.6 Aim of the study

Since four B-cell subsets were identified according to the expression of the markers CD21 and CD86, this study aimed to extensively characterize phenotypically and functionally these human B-cell populations. Based on the fact that CD40B cells are potent antigen-presenting cells and that $CD21^{low}$ $CD86^{pos}$ B-cell subset resembled CD40B cells in terms of CD21 and CD86 expression, it was hypothesized that they could have an immunostimulatory phenotype and function. In order to test this hypothesis, a novel cell-free CD40L system was established to produce potent antigen-presenting B cells in vitro. Activated B cells generated with this system were used to compare the phenotype and the function to $CD21^{low}$ $CD86^{pos}$ B cells to study whether they represent the physiologic counterpart to in vitro generated CD40B cells in humans. Finally, B-cell subsets were analyzed in several clinically relevant human diseases to determine whether and how the four B-cell subsets were disturbed.

Materials and Methods

2 MATERIALS AND METHODS

2.1 Materials

2.1.1 Chemicals

For preparation of buffers and solutions, chemicals of analytical purity were used exclusively.

Table 1: Chemicals

Name	Manufacturer
2-Propanol	Roth
Bovine Serum Albumin (BSA)	Sigma Adrich
Calcium chloride ($CaCl_2$)	Merck
CFSE: 5-(and-6)-carboxyfluoresceindiacetate, succinimidyl ester	Invitrogen
Ethanol 70 %	Roth
Ethylenediaminetetraacetic acid (EDTA)	Sigma Aldrich
Hygromycin B	PanreacAppliChem
Trypsin-EDTA	Life Technologies

2.1.2 Reagents

Table 2: Reagents

Name	Composition/Manufacturer
10 x Phosphate buffered saline (PBS)	Life Technologies

AB-Human serum	Life technologies
AIM-V medium	Life Technologies
CpG-ODN 2006 human TLR-9 ligand	Miltenyi Biotech
DMEM medium	Life Technologies
Fetal Bovine Serum (FBS)	Lonza
Fluo-3 acetoxymethyl esters	Molecular Probes
Fura-Red acetoxymethyl esters	Molecular Probes
G418	Biochrom
Goat F(ab´)2 anti-human IgM (µ chain specific)	Southern Biotech
IMDM medium	Life Technologies
LEAF Purified anti-human CD3 clone OKT3	BioLegend
Pacific blue succinimidyl ester	Molecular Probes
Pacific orange succinimidyl ester	Molecular Probes
Pancoll human, density 1.077 g/mL	PAN-Biotech
Sodium Orthovanadate	Sigma Aldrich
Trypan Blue Stain 0.4 %	Life technology
Tumor Dissociation Enzyme	DCS-Innovative

2.1.3 Buffers and solutions

Table 3: **Buffers and solutions**

Name	**Composition/Manufacturer**
Cell fix (1 x)	BD Biosciences

Cell wash	BD Biosciences
Cell staining buffer	1 x PBS
PBS (1 x)	1 L 10 x PBS
EasySep Purification Buffer	1 x PBS
MACs Separation Buffer	1 x PBS
HEPES Buffer (1 M)	Biochrom
FACS sheath fluid	BD Biosciences
Freezing medium	FBS
Perm Buffer III	BD Bioscience
PhosphoFlow wash buffer	1 x PBS
Pervanadate Solution (10	20 µL 100 mM Sodium Orthovanadate solution
Pervanadate Solution (500	Dilution 1:20 Pervanadate solution (10 mM) in RPMI +

2.1.4 Cell culture media

Table 4: NIH3T3 Standard medium

Medium	Supplementation (Final Concentration)
DMEM-Ham´s / F12	
	L-Glutamine 365 µg/mL
	FBS 10 %
	HEPES 10 mM
	Penicillin/Streptomycin 10 %

Table 5: Human CD40B wash medium

Medium	Supplementation (Final Concentration)
IMDM	
	L-Glutamine 584 µg/mL
	HEPES 25 mM
	Penicillin/Streptomycin 10 %

Table 6: Human CD40B culture medium

Medium	Supplementation (Final Concentration)
IMDM	
	L-Glutamine 584 µg/mL
	HEPES 25 mM
	AB-Human serum 10 %
	rh Transferrin 50 µg/mL
	rh Insulin 5 µg/mL
	Penicillin/Streptomycin 10 %

Table 7: Calcium flux medium

Medium	Supplementation (Final Concentration)
RPMI without Red Phenol	
	FBS 2.5 %
	Penicillin/Streptomycin 10 %

2.1.5 Kits

Table 8: Kits

Name	Manufacturer
CD19 MicroBeads®, human	Miltenyi Biotec
CD20 microbeads®, human	Miltenyi Biotec
EasySep Human T cell enrichment kit	Stemcell Technologies
Human CD40-Ligand multimer kit	Miltenyi Biotec
LEGENDScreen™ Human Cell Screening (PE) Kit	BioLegend

2.1.6 Cell lines

The adherent CD40L-transfected NIH3T3 fibroblasts were used. These feeder cells were kindly provided by Dr. Gordon Freeman (DFCI, Boston, USA).

Table 9: Tools and instrumentation

Devices	Manufacturer
Cell sorter Aria III	Becton-Dickenson
EOS 350D digital camera	Canon
Freezing Chamber	Nalgene NUNC
Gallios Flow Cytometer	Beckman Coulter
Gentle MACS Dissociator	Miltenyi Biotec
HeraCell 150i CO2 Incubator	Thermo Scientific
Heraeus Megafuge 16R	Thermo Scientific
Neubauer Counting Chamber	OptikLabor

Purple EasySep Magnet	StemCell Technologies
Reax Top mixer	Heidolph
Refrigerated microfufe Sigma 1-14K	Sigma Laborzentrifugen
Televal 31 microscope	Zeiss
Water bath WNB14 Set	Memmert

Table 10: Consumables

Name	**Manufacturer**
5 mL flow cytometric tubes	Sarstedt
5 mL (12 x 75 mm) polystyrene tubes	Falcon
6-, 12-, 48- well culture dish (flat bottom)	NUNC
15 mL Falcon tube	Sarstedt
15 mL (17 x 100 mm) polystyrene tubes	Falcon
50 mL Falcon tube	Sarstedt
70 µm nylon cell strainers	Greiner
96-well culture dish (round- and v-bottom)	NUNC
C-Tubes	Miltenyi Biotec
Cryo tubes 1.0, 1.8 mL	Sarstedt
Pre-Separation filter 30 µm	Miltenyi Biotec
LD Columns	Miltenyi Biotec
LS Columns	Miltenyi Biotec
MS Columns	Miltenyi Biotec
Pipette tip 5, 10, 25 mL	Sarstedt

Pipette tip 10, 200, 1000 µL	Sarstedt
Syringe 50 mL	B. Braun Melsungen AG
Syringe filter 0.22 µm	Millex-GV
Tissue culture flask 75, 175 cm^2	Sarstedt

Table 11: Software

Name	Manufacturer
FlowJo Software	TreeStar
GraphPad Prism	GraphPad Prism Software
Kaluza Software	Beckman Coulter

2.2 Methods

2.2.1 Blood samples

Buffy coat preparations were obtained from healthy donors at the blood bank of the Universitätsklinikum Köln, Germany. Peripheral blood and bone marrow from healthy adult volunteers, rheumatoid arthritis, EBV, CVID, cancer and trauma patients have also been used in this study. Peripheral blood from cancer patients was obtained immediately prior to surgery. Tonsils from non-malignant tonsillectomies were included as well. Donors gave their consent and all the experiments were approved by our institutional ethical board.

Human peripheral blood mononuclear cells (PBMCs) were isolated using Pancoll density-gradient centrifugation. A maximum of 16 mL whole blood treated with EDTA were diluted with an equal volume of PBS. In another tube, 15 mL of Pancoll solution were carefully covered with a layer of diluted blood, without mixing the phases. After a centrifugation step (1080 g, 20 minutes) at room temperature (RT) the PBMCs were harvested from the white blood cells layer between the plasma sample layer and the Pancoll. The separated PBMCs were washed twice in PBS to remove remaining platelets, serum and Pancoll.

2.2.2 Cell subset enrichment

2.2.2.1 B cell purification

B cells were enriched using positive immunomagnetic selection with human CD19 or CD20 MicroBeads and used fresh at the time of the experiment. The procedure was performed according to the manufacturer's protocol (Miltenyi Biotech, Germany) with minor modifications. PBMCs were resuspended in 40 µL MACS buffer per 1 x 10^7 cells and magnetically labeled with 10 µL CD19 (or CD20) MicroBeads per 1 x 10^7 cells (15 minutes, at RT). Labeled cells were filtered into a MACS Column placed on the magnetic field of the MACS separator. $CD19^+$ (or $CD20^+$) B cells were retained in the magnetic column while unlabeled cells were eluted. Positively selected B cells were washed out from the column, counted and B cell purity was determined. B cell purification by MACs MicroBeads yielded in purities of >96 % $CD20^+$ $CD19^+$ B cells as determined by flow cytometric analysis.

2.2.2.2 B-cell subset isolation by fluorescence activated cell sorting (FACS)

PBMCs were isolated from healthy donors buffy coats and allowed to rest overnight at 4 °C. After 12 hours, B cells were isolated with $CD19^+$ MicroBeads and stained with CD20, CD21 and CD86. CD3 was used to exclude T cells that could remain after B cell enrichment. B cell purity was confirmed after separation. B-cell subsets were separated according to the expression of CD21 and CD86 with the flow cytometry-based cell sorter Aria III (Becton-Dickenson) at the Central Cell Sorting Facility located in the CMMC building at the University Hospital of Cologne, Germany. During isolation and throughout the process cells were kept under sterile conditions and on ice.

2.2.2.3 $CD3^+$ T cell isolation

T cells were purified by negative selection using the human T cell enrichment kit, according to the protocol of the manufacturer (Stem Cell Technologies, Canada). Briefly, cells were resuspended in EasySep medium at a concentration of 5 x 10^7 cells/mL. Cells were incubated for 10 minutes at RT with EasySep Human T Cell Enrichment Cocktail and for additional 5 minutes with EasySep D Magnetic Particles at 50 µL/mL cells. Afterwards, the tube with cells was placed into the EasySep purple magnet for 5 minutes. After the incubation time was ended, the desired cell fraction was poured off into a new tube by inverting the magnet. The negative selected cell suspension was washed and counted. Enrichment of $CD3^+$ T

cells by EasySep Human T cell Enrichment Kit yielded in purities of >96 % $CD3^+$ T cells as determined by flow cytometric analysis.

2.2.2.4 Cell isolation from human tumor tissue

Tissue was obtained from colorectal cancer patients. Fresh unfixed tissue from primary tumor lesions, which were not required for pathological analyzes, were collected and processed immediately after surgical resection (within 12 hours). The samples were provided by an experienced pathologist from the pathology department of the University Hospital of Cologne, Germany, who made sure that the obtained samples were indeed tumor tissue. The fresh tumor tissue was manually minced using a scalpel and then transferred into single cells suspensions using a gentle MACS Dissociator (Miltenyi Biotec). For enzymatic disruption, Tumor Dissociation Enzyme was used and single cell suspensions were obtained by sequential dissociation and incubation according to the company's instructions. Finally, the cells were filtered through 70 µm nylon cell strainers, washed, counted and stained for flow cytometric analysis.

2.2.3 Cell culture

If not described differently, all cells were incubated at 37 °C in a humidified atmosphere with 5 % CO_2. Cell culture was performed at sterile conditions under a safety cabinet with sterile solutions, glass and plastic ware. All centrifugation steps in cell culture were performed in a Heraeus Megafuge 16R (Thermo Scientific).

2.2.3.1 Counting of cells – Trypan Blue exclusion test

For counting, a Neubauer chamber was used. An aliquot of the cell suspension was diluted (10 x) in Trypan Blue Stain 0.4 % to differentiate viable from non-viable cells. Using a light optical microscope with 20 fold magnification, bright, unstained cells were counted viable. Four corner quadrants of the Neubauer chamber were counted completely. The average cell number per quadrant was multiplied by 10^4, resulting in the number of cells per 1 mL. The total cell number was calculated by including the dilution factor and the total volume of the cell suspension.

2.2.3.2 Cryopreservation and thawing of cells

To preserve living cells intact without causing major damage, cells were resuspended in a cold freezing medium at a density of 5-10 x 10^6 cells/mL. Cryotubes were placed into a pre-cooled freezing chamber containing isopropanol for slow freezing. The freezing chamber was stored at -80 °C for 24 hours and then cryotubes were transferred to liquid nitrogen for long-term storage.

For thawing, cryotubes were rapidly removed from nitrogen and put into a water bath at 37 °C until a small ice clump was left in the tube. The cell suspension was then resuspended in an excess of medium and centrifuged at 200 g for 5 minutes.

2.2.3.3 Trypsinization of adherent cells

Adherent cells were washed once with 10 mL of 1 x PBS and 4 mL of Trypsin-EDTA was added for detachment of the cells. Cells were incubated at 37 °C for 5-10

minutes, followed by addition of 5 mL medium containing FBS to stop the trypsinization process. Finally, cells were harvested, washed twice (200 g, 5 minutes) and resuspended in standard medium.

2.2.3.4 Culture of NIH3T3/tCD40L cell line

The NIH3T3/tCD40L cell line is an adherent murine fibroblast cell line expressing the human CD40L that was kindly provided by Dr. Gordon Freeman (DFCI, Boston, MA, USA). Cell passaging was performed twice a week. Briefly, adherent NIH3T3/tCD40L cells were first trypsinized (section 2.2.3.3), then resuspended in 10 mL NIH3T3 standard Medium (Table 4) in order to determine cell number (section 2.2.3.1). To maintain the NIH3T3/tCD40L culture, 1.5 x 10^6 cells were seeded in 10 mL NIH3T3 standard medium supplemented with G-418 (0.7 mg/mL) in a 75 cm^2 culture flask and incubated at 37 °C. To ensure stable expression of CD40L on the transfected cells, flow cytometry was weekly performed using a PE-conjugated anti-human CD154 antibody.

2.2.3.5 Generation of CD40-activated B cells with NIH3T3/tCD40L cell line

CD40-activated B cells were generated as described previously (von Bergwelt-Baildon et al. 2006, Liebig et al. 2009). Briefly, purified $CD19^+$ B cells were cultured on murine NIH3T3/tCD40L feeder cells at a seeding density of 1 x 10^6 cells/mL. NIH3T3/tCD40L feeder cells were previously irradiated at 26 Gy. B cells were cultured in human CD40B medium (Table 6) with 50 U/mL of recombinant human IL-4 (ImmunoTools, Germany) freshly added. Cultures were maintained until

day 21. Expansion of B cells was measured by counting cells twice a week using Neubauer chamber and trypan blue exclusion (section 2.2.3.1). Following CD40L activation CD40B cells were cryopreserved in liquid nitrogen (section 2.2.3.2) for later use in autologous and allogeneic mixed lymphocyte reaction (MLR) (section 2.2.8).

2.2.3.6 Generation of CD40-activated B cells with soluble CD40L

$CD19^+$ B cells were cultivated with multimer human recombinant CD40L (rCD40L) as described previously (Garcia-Marquez et al. 2014). Briefly, B cells were seeded (1 x 10^6 cells/mL) in CD40B medium supplemented with freshly added recombinant human IL-4 (50 U/mL) and human CD40L Multimer kit from Miltenyi Biotec according to manufacturer's instructions (2 µg/mL rCD40L + 10 µg/mL crosslinking antibody, pre-incubated at room temperature for 30 minutes). On day 5, half of the medium was removed and replaced with medium supplemented with fresh rCD40L and IL-4. At day 7 and day 10 the expanding CD40B cells were counted, cell density was adjusted and cells were cultured for further expansion. Cultures were maintained until day 14. Growth of B cells was measured by counting cells on day 7, 10 and 14 using Neubauer chamber and trypan blue exclusion (section 2.2.3.1).

2.2.3.7 Assessment of cell morphology by microscopy

To assess the morphology of B cells during culture, a representative spot was chosen and photographed by using an inverted phase Zeiss Televal 31 microscope fitted with a Canon EOS 350D digital camera.

2.2.4 Phenotype analysis of single cells by FACS

Acquisition and enumeration of cells were performed using a Gallios Flow Cytometer (Beckman Coulter, Pasadena, USA). Single-cell analyzes were performed with the FlowJo software (Tree Star, Ashland, USA) or the Kaluza software (Beckman Coulter, Pasadena, USA). All washing steps were performed with cell wash in a Heraeus Megafuge 16R (Thermo Scientific) at 270 g for 5 minutes at RT.

2.2.5 Surface staining with monoclonal antibodies

To evaluate frequency and phenotype of each B-cell population, PBMCs were stained with antibodies for flow cytometric analyzes. Staining procedure was done with 0.1 – 1 x 10^6 cells in 100 µl cell wash with antibody cocktails (1 µL/antibody, up to 10-parameters) for 20 minutes at 4 °C. Afterwards, cells were washed and resuspended in 150 - 300 µl cell wash depending on the cell number. Monoclonal antibodies used for phenotype analysis, conjugates and companies are listed in table 12. Isotype control antibodies and/or unstained samples were used when appropriate.

For examining Ki-67 expression in each B-cell population, PBMCs were first permeabilized with cold ethanol 70 % at -20 °C for 1 hour. Subsequently, cells were stained with anti-Ki-67 PerCp Cy 5.5 antibody. At the end of the incubation, cells were washed, resuspended in cell staining buffer and analyzed by flow cytometry.

2.2.6 Human monoclonal antibodies used for frequency and conventional phenotype analysis

Table 12: Anti-Human antibodies

Antigen [clone]	Isotype	Labeling	Manufacturer
CD3	Mouse IgG1,K	ECD	Beckman Coulter
	Mouse IgG1,K	PC7	Beckman Coulter
CD4	Mouse IgG1,K	Pacific Blue	BioLegend
CD8	Mouse IgG1,K	PerCP/Cy5.5	BioLegend
CD19	Mouse IgG1,K	Alexa Fluor 780	BioLegend
CD20	Mouse IgG2b, K	Pacific Blue	BioLegend
CD21	Mouse IgG1,K	APC	BioLegend
CD25	Mouse IgG1,K	PE Cy 7	BioLegend
	Mouse IgG1,K	PE	Beckman Coulter
CD27	Mouse IgG1,K	PC 7	Beckman Coulter
CD32	Mouse IgG2b,K	FITC	BD Biosciences
CD43	Mouse IgG1,K	APC	ImmunoTools
CD45	Mouse IgG1,K	Pacific Orange	Beckman Coulter
CD62L	Mouse IgG1,K	ECD	Beckman Coulter
CD80	Mouse IgG1,K	FITC	BioLegend
CD83	Mouse IgG1,K	PE	Caltag
CD86	Mouse IgG1,K	PE	BioLegend
HLA-DR	Mouse IgG1,K	PerCP Cy5.5	eBioscience
IgD	Mouse IgG1,K	FITC	BD Biosciences

IgM	Mouse IgG1,K	PE	BD Biosciences
IgG	Mouse IgG1,K	FITC	BD Biosciences
Ki-67	Mouse IgG1,K	PerCP Cy5.5	BioLegend

The LEGENDScreen Human Cell Screening (PE) Kit was used to further phenotypically characterize the B-cell subsets. The kit containing 332 PE-conjugated monoclonal antibodies to cell surface markers as well as 10 mouse, rat, or Armenian hamster Ig isotype controls was used according to manufactures' instructions to screen expression of all known CD molecules among the B-cell subsets. Briefly, $CD19^+$ B cells were isolated (section 2.2.2.1), stained with CD20, CD21 and CD86 and 0.8 × 10^5 cells were added to each well after the lyophilized antibodies were reconstituted. Cells were then stained for 20 minutes at 4 °C, washed, and fixed with Fixation Buffer. Cells were then washed, resuspended in 160 µL of Cell Staining Buffer, and analyzed by flow cytometry.

2.2.7 Gating strategy for flow cytometry analysis

Flow cytometry generated data were analyzed as follows. Briefly forward and sideward scatter plots were used to gate on lymphocytes and doublets were excluded using time of flight (TOF). Following gating on $CD45^+$ events, the B cells were identified by the expression of CD19 and CD20 (Figure 7). Then, B cells were further subdivided into four subpopulations according to their expression of CD21 and CD86.

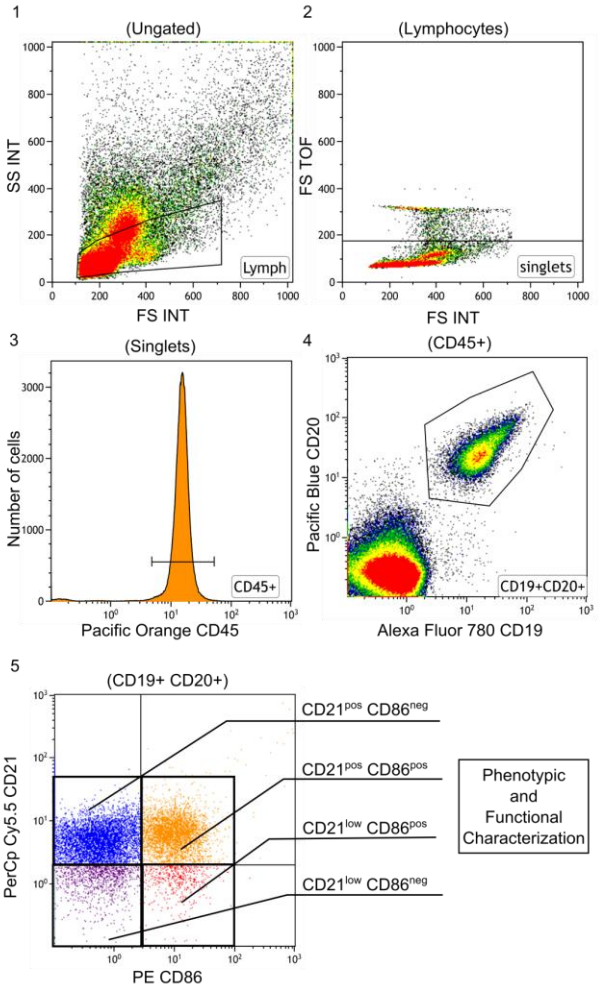

Figure 7. Gating strategy for flow cytometry analysis

In this gating sample, cells were first gated according to the size (-SS- side scatter vs. -FS- forward scatter). On top of each plot and in brackets appears the immediate parent population. At the sides of each plot are shown the antibodies and their respective fluorochromes. (1) The lymphocyte gate (Lymph) is further analyzed to exclude doublets and non-lymphocyte cells with the singlets (2) and CD45 (3) gates, respectively. (4) Within the $CD45^{+}$ lymphocyte population, B cells are gated based on

the expression of CD19 and CD20 and then further subdivided (5) by the expression of CD21 and CD86. Phenotypic and functional characterization of the B-cell subsets described in this work was based on this gating strategy.

2.2.8 Autologous and allogeneic MLR for T cell proliferation analysis

B cells activated with CD40L after 1, 3, 7, 14 and 21 days, cryopreserved and or B-cell subsets sorted from $CD19^+$ B cells based on the expression of CD86 and CD21 which were used as stimulators (1–10 x 10^4 cells/well) with negatively selected autologous or allogeneic T cells (10 x 10^4 cells/well) in a final volume of 200 µL in 96-well round-bottom plates, at 37 °C in a 5 % CO_2 humidified atmosphere. Stimulator B cells were always irradiated (26 Gy) before mixing with T cells. For the autologous MLR, T cells were also stimulated with IL-2 (25 U/mL) and OKT3 (10 µg/mL). As positive control T cells were cultivated in the presence of magnetic $CD3^+$ $CD28^+$ Beads.

Prior to co-culture, purified T cells were labeled with the fluorescent proliferation marker CFSE. Briefly, T cells were resuspended in PBS with 5 % FBS and stained by the addition of 5 µM of CFSE pre-diluted in PBS. Cells were mixed and stained uniformly by agitating the tube constantly for 5 minutes in the dark. After extensive washing to remove excess CFSE, CFSE-labeled T cells were plated in triplicates in RPMI 1640 media supplemented with 10 % FBS, 1 % HEPES, 2 mmol/L L-glutamine with 10% Penicillin/Streptomycin. After 5 days of co-culture (7 days autologous MLR), cells were harvested and stained with the following antibodies for

flow cytometry analysis: CD25 PE, CD62L ECD, CD3 PC7, CD8 PerCp Cy5.5, CD4 Pacific Blue and CD19 Alexa Fluor700 (Table 12).

2.2.9 Analysis of Ca^{2+} mobilization.

For analysis of intracellular Ca^{2+} flux, MACS-purified human $CD20^{+}$ B cells were loaded for 60 minutes at 37 °C with 12 µM Fura-Red acetoxymethyl esters (AM) and 6 µM Fluo-3 AM (Molecular Probes, Eugene, USA) in the presence of 0.2 % Pluronic F-127 (Molecular Probes, Eugene, USA) in calcium flux medium (Table 7) with cells being resuspended every 20 minutes. Afterwards, cells were washed with and resuspended in calcium flux medium. The loaded cells were subsequently stained with antibodies against CD19, CD21, and CD86. After basal Ca^{2+} concentrations were monitored, cells were stimulated with various reagents. The fluorescence Fluo-3/Fura-Red ratio was recorded for the next minutes on a Gallios flow cytometer (Beckman Coulter). The analysis of the kinetics was performed using FlowJo software.

Table 13: Dyes used for the detection of free intracellular Ca^{2+} by flow cytometry

Dye	Excitation (λ_{max})	Emission (λ_{max})	Excitation laser
Fluo-3	503 nm	526 nm (green)	Argon at 488 nm
Fura red	472 nm	637 nm (red)	Argon at 488 nm

2.2.10 Multiplexed phospho-specific flow cytometric profiling (PhosphoFlow)

2.2.10.1 Stimulants used in PhosphoFlow experiments

Cells were stimulated either with 10 µg/mL of soluble CD40L (Miltenyi Biotech, Germany), 10 µg/mL goat $F(ab')_2$ anti-human IgM (µ chain specific) or a combination of CD40L and IgM (5 µg/mL each). In some cases, to amplified downstream signaling, B cells were exposed immediately before stimulation to 3.3 mM H_2O_2. This dose was identified by Irish et al, as one that stimulates little signaling on its own in primary human B cells but effectively inactivates the catalytic cysteine of phosphatases so that subsequent protein tyrosine phosphatase (PTPs)-regulated signals proceed unchecked (Irish et al. 2006). In some experiments, B cells were stimulated with a final concentration of 45 µM of Pervanadate solution for 5 minutes without further stimulation neither with CD40L nor IgM. 1 % FBS in PBS was used as negative stimulation control.

2.2.10.2 Cell stimulation

After isolation, $CD19^+$ B cells were allowed to rest for 2 hours at 37 °C, 5 % CO_2 in AIM-V medium. Thereupon, cells were washed and resuspended in ice cold flow wash buffer (PBS + 1 % FBS) and transferred to 2 mL eppendorf tubes (500 µL containing 5 x 10^6 cells). Before stimulation, samples were plated in the thermo block pre-heated at 37 °C for 3 minutes. Stimulant aliquots (10 µL) were added to B cells and incubated for different time periods. After stimulation, cells were fixed with 500 µL of 4 % PFA (10 minutes) and washed twice with flow wash buffer.

2.2.10.3 Staining and fluorescent-cell barcoding

For fluorescent-cell barcoding pacific blue- and pacific orange- succinimidyl ester (Molecular Probes, Eugene, USA) were prepared at different concentrations (Pacific blue 8-100 pg/µL; Pacific Orange 25-250 pg/µL); 5 µL of each dilution was added per well in V-bottom 96-well plate. Fixed cells were washed and resuspended in 100 µL PBS. Thereupon, 90-95 µL of fixed cells were plated on top of the corresponding barcoding dilution, mixed vigorously and allowed to stain for 20 minutes in the dark at RT. After staining, plate was washed twice with flow wash buffer and barcoded cells were collected together in a 15 mL Falcon tube on ice. Cells were washed again and permeabilized with pre-cooled perm buffer III (BD Bioscience, USA) for 30 minutes at -80 °C. Permeabilized cells were rehydrated and washed twice with flow wash buffer. Samples were then stained with antibodies cocktails in flow wash buffer for 30 minutes at RT. Antibodies in the cocktails included cell surface markers CD20-Alexa Fluor 488 (clone H1(FB1), BD Phosflow), CD86-PE (clone IT2.2, BioLegend) and CD21-PerCpCy5.5 (clone Bu32, BioLegend). Phospho-antibodies were all in Alexa Fluor 647 (BD Phosflow) and included pZAP70 (Y319)/pSYK (Y352), BTK (pY551)&Itk (pY511), pERK (T202/Y204) and NFkB-p65 (pS529). Cells were washed with and resuspended in flow wash buffer before been acquired on a Gallios flow cytometer.

2.2.11 Statistics

Significant differences were calculated by the Student's t -test for paired/unpaired data depending on the group. When multiple groups were compared one-way ANOVA with Tukey´s multiple comparisons test was used according to the case. When groups with more than one variable to analyze were

compared the two-way ANOVA with Tukey´s or Sidak´s multiple comparisons test according to each case were used. When data was compared to a normalized population, the one sample t test was used. P-values of less than 0.05 were considered statistically significant and marked with asterisks: * $p \leq 0.05$, ** $p \leq 0.01$, *** $p \leq 0.001$, **** $p \leq 0.0001$. Mean values and standard deviations (SD) were used unless otherwise stated.

Results

3 RESULTS

3.1 Generation of highly proliferative antigen presenting B cells was achieved by activation via soluble as well as membrane bound CD40L

As described earlier (section 1.4.6), potent antigen-presenting B cells can be generated via CD40 activation. Most common available systems include triggering CD40 with agonist CD40-monoclonal antibodies or the usage of CD40L membrane fractions, as well as CD40L-expressing feeder cells such as Schneider 2 cells (Yoon et al. 2005), NIH3T3/tCD40L cells (Schultze et al. 1995) and 293-CD40L-sCD40L human cell line (Ivanov et al. 2005). The main problem with antibody mediated CD40 stimulation is the weak proliferative response of B cells. The level of B cell activation and proliferation seems to depend on the degree of CD40 crosslinking (Fanslow et al. 1994, Morris et al. 1999, Haswell et al. 2001). Accordingly, the most efficient way to induce B-cell proliferation thus far is through cell membrane-bound CD40L (Ivanov et al. 2005, Yoon et al. 2005). However, the cell-standing systems introduce xenogeneic contaminations that might influence experimental results. Moreover, this has also prevented the translation of the system to the clinic settings. Consequently, a soluble, cell-free CD40L system was established as an effective culture method for generation and expansion of CD40B cells in vitro through the use of a multimerized form of human recombinant CD40 ligand (rCD40L).

The rCD40L system was compared in terms of proliferation, induction of activation markers and immunostimulatory capacity to the well-established and effective membrane-bound CD40L system with NIH3T3 cells.

Purified human $CD19^+$ B cells were activated by culturing them together with either NIH3T3/tCD40L feeder cells or rCD40L in the presence of IL-4 for 14 days. As expected, flow cytometric analysis revealed that stimulation of human B cells via rCD40L induced up-regulation of costimulatory molecules CD80, CD86, HLA-DR and the adhesion molecule CD62L (Figure 8A). Expression levels were always comparable to that observed with NIH3T3/tCD40L cells. The purity of cultures on day 14 was above 96-98 % of $CD19^+$ $CD20^+$ B cells (data not shown). Signaling through CD40L also induced expression of adhesion molecules resulting in the formation of B cell clusters via homotypic adhesion (Figure 8B), which is an important step of B cell activation via CD40 (Klaus et al. 1994). Larger clusters were observed with the rCD40L but in the NHI3T3/CD40L system clusters were more rounded and evenly shaped.

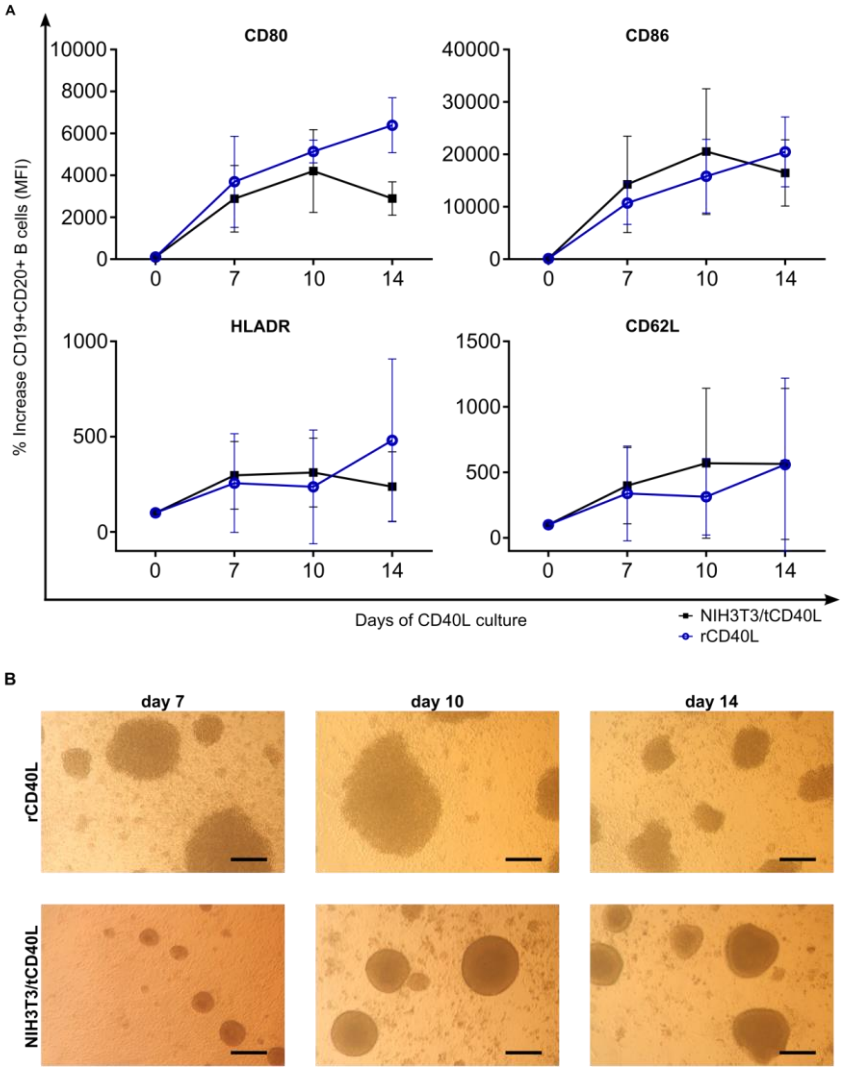

Figure 8. Ligation of B cells by CD40L induced activation and homotypic cluster formation

CD19^{+} B cells from 4 healthy donors were cultured with either soluble rCD40L or NIH3T3/tCD40L feeder cells in the presence of IL-4 for 14 days. B cells were analyzed by flow cytometry. (A) Culture of B cells with rCD40L (blue line) as well as NIH3T3/tCD40L (black line) up-regulated the expression of costimulatory molecules and the adhesion molecule CD62L. Data is represented as the percentage increase of the mean fluorescence intensity (MFI) with standard deviation bars (SD) of each molecule over time. (B) Light microscopy pictures of a representative donor at day 7, 10 and 14 of culture with either rCD40L or NIH3T3/tCD40L showing clustering of B cells. Photos were taken with 5X magnification and size bars are shown (scale bar in all pictures is 100 µm). No significant differences between the two stimuli were detected by two-way ANOVA with Tukey´s multiple comparisons test.

Extensive expansion of human B cells was achieved by stimulation with both rCD40L and NIH3T3/tCD40L. Proliferation rates remained constant until the end of the culture and no differences between the two systems were found. Growth was determined by manually counting cells with trypan blue during the culture as well as with the fluorescent proliferation marker CFSE (Figure 9A and B, respectively). Only a very low expansion rate was observed when rCD40L was not incubated with the cross-linking antibody indicating that cross-linking of the soluble rCD40L is necessary in order to induce proliferation of B cells. As shown in Figure 9B, proliferation of the entire population in response to rCD40L + IL-4 (light grey histograms) was also confirmed by CFSE dilution. Control B cells were cultivated only with IL-4 and as expected no proliferation was observed (dark grey histograms).

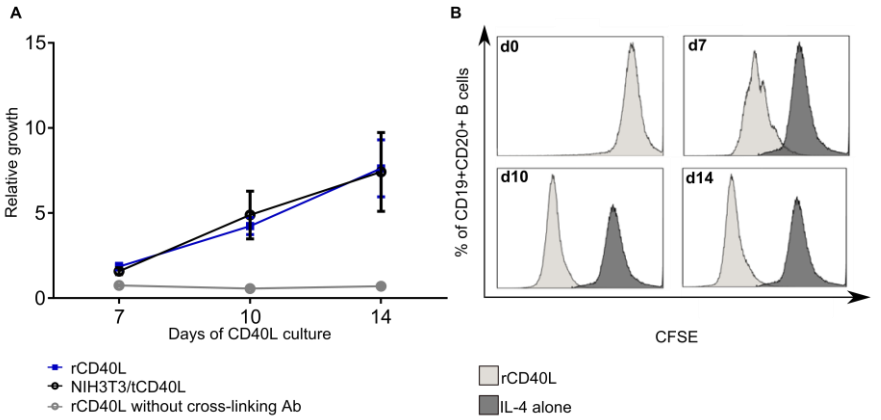

Figure 9. B cell proliferation in response to CD40 ligation

Proliferation of B cells cultivated with CD40L was measured at day 7, 10 and 14. (A) Proliferation of $CD19^+$ B cells cultured with rCD40L, NIH3T3/tCD40L and rCD40L without additional treatment with cross-linking antibody determined by trypan blue exclusion. (n=11, mean ± SEM -standard error of the mean-). (B) Histograms of one representative donor showing CFSE dilution as a consequence of B cell division induced by rCD40L (light grey) compared to B cells stimulated only with IL-4 (dark grey).

As demonstrated by means of an MLR, both CD40L systems were able to generate highly potent APCs that induced activation as determined by CD25 expression and strong proliferation of allogeneic T cells (Figure 10A). Only at a lower B to T cell ratio (1:10) rCD40L-B cells were more efficient inducing T cell proliferation than NIH3T3/tCD40L-B cells (Figure 10B). Non-activated B cells from the same donors were used as negative controls. As positive controls, T cells were cultivated in the presence of activating Dynabeads $CD3^+$ $CD28^+$ (data not shown).

Thus, an effective soluble system was established, in which contamination with xenogeneic components was avoided. Data from these experiments was used to

compare functional and phenotypic characteristics to the CD21^{low} CD86^{pos} peripheral blood B-cell subset. The soluble, cell-free rCD40L system proved to be an efficient method to generate highly potent and proliferating antigen-presenting cells. Moreover, can be used as an in vitro system to study antigen presentation in human B cells and to establish similarities and differences with peripheral blood CD21^{low} CD86^{pos} B lymphocytes.

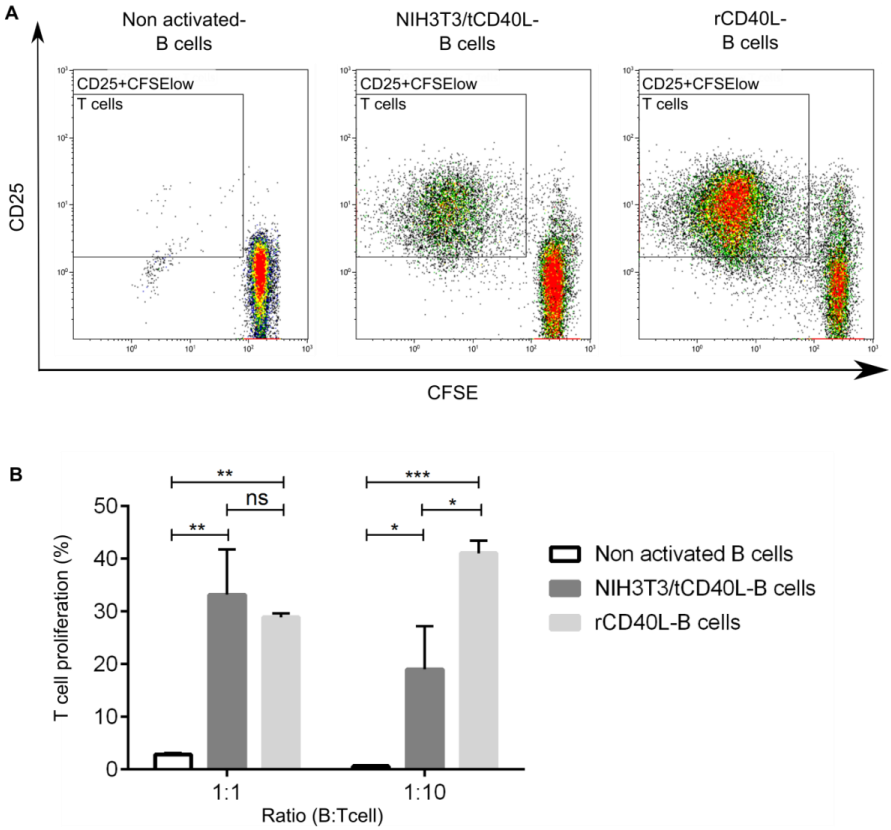

Figure 10. CD40 activated B cells induced strong proliferation of allogeneic T cells

T cells were cocultured either with CD40Bcells (rCD40L-B cells or NIH3T3/tCD40L-B cells) or non-activated B cells at B cell-to-T cell ratios of 1:1 and 1:10. Proliferation of $CD3^+$ T cells was determined after 5 days by means of CFSE dilution. (A) Representative FACS-plots from one representative donor show differences in T cell activation and proliferation when T cells were cultured with non-activated or CD40 activated B cells (ratio 1:1). Activated, proliferating cells were identified by expression of the activation marker CD25 and low CFSE fluorescence. (B) Figure displays the mean and SD bars of the proliferating $CD25^+$ $CFSE^{low}$ T cells from three healthy donors. Significant differences were calculated by one-way ANOVA with Tukey´s multiple comparisons test. Asterisks represent: * $p \leq 0.05$, ** $p \leq 0.01$, *** $p \leq 0.001$.

3.2 Similar distribution of B-cell subsets was found in human peripheral blood, as well as in primary and secondary lymphoid organs

As described in section 1.5 (Figure 5), a novel B-cell subset with similar phenotypic characteristics to CD40B cells, namely reduced expression of CD21 and increased expression of CD86 was previously identified in peripheral blood from healthy donors. In order to determine site-dependent differences in primary and secondary lymphoid organs, samples from non-malignant tonsillectomies and bone marrow from healthy donors were collected and analyzed to search for a similar phenotype. Therefore, by flow cytometry $CD19^+$ $CD20^+$ B cells were classified based on the expression of CD21 and CD86. Bone marrow and tonsils were compared to peripheral blood from a cohort of 41 healthy volunteers. The vast majority of peripheral blood B cells were $CD21^{pos}$ $CD86^{neg}$ B cells (83.97 % ± 7.677). Double positive B cells $CD21^{pos}$ $CD86^{pos}$ constituted 1.57 % ± 0.9564 of the total B cells while the $CD21^{low}$ B cells, further separated into $CD86^{pos}$ and $CD86^{neg}$ subpopulations

made up of 1.193 % ± 0.9720 and 13.27 % ± 7.012, respectively (Figure 11A). A similar distribution of the subsets was found in bone marrow (Figure 11B) and tonsils (Figure 11C). Interestingly, the proportion of activated, $CD21^{pos}$ $CD86^{pos}$ and $CD21^{low}$ $CD86^{pos}$ B cells was increased in the tonsils (25.52 % ± 12.26 and 2.553 % ± 2.279, respectively). This could be explained by the fact that these donors underwent tonsillectomies due to inflammation of the tonsils.

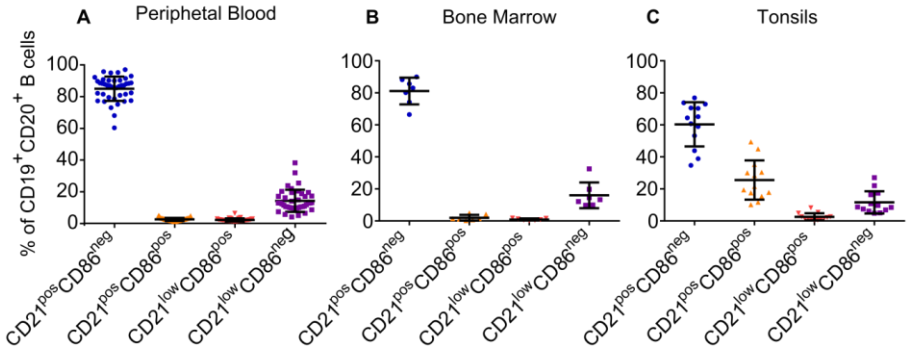

Figure 11. Frequency of B-cell subsets in human peripheral blood, bone marrow and lymphoid tissue.

Lymphocytes from peripheral blood and bone marrow from 41 and 7 healthy volunteers respectively, and 13 tonsils from non-malignant tonsillectomies were analyzed by flow cytometry. Shown are scatter plots representing the frequency of $CD19^{+}$ $CD20^{+}$ B-cell subsets according to the expression of CD21 and CD86 in (A) peripheral blood, (B) bone marrow and (C) tonsils. Bars denote the mean ± SD. Percentages of cells for each subset are calculated out of the total $CD19^{+}$ $CD20^{+}$ B cells.

To study inter-individual differences in the frequency of the four B-cell subsets, the healthy cohort was divided by gender and age. The age of the subjects varied from 18 to 89 years, with an average of 44 years. The $CD21^{low}$ $CD86^{pos}$ B-cell

population showed a clear gender difference (Figure 12A). After matching subjects by age it became obvious that in individuals below age 50 women had significantly higher percentage of $CD21^{low}$ $CD86^{pos}$ B cells than men (1.412 % ± 0.8015 against 0.7030 % ± 0.3412, respectively) (p=0.0334, n=10). However, in people aged 50 and older the percentage of $CD21^{low}$ $CD86^{pos}$ B cells was not significantly different (p=0.0927, n=7). This could indicate that hormonal differences might affect the homeostasis of this B-cell subset and that the gender difference disappears after women reach menopause. Despite the gender-dependent differences, the composition of the B-lymphocyte population in peripheral blood did not show age-dependent changes (Figure 12B).

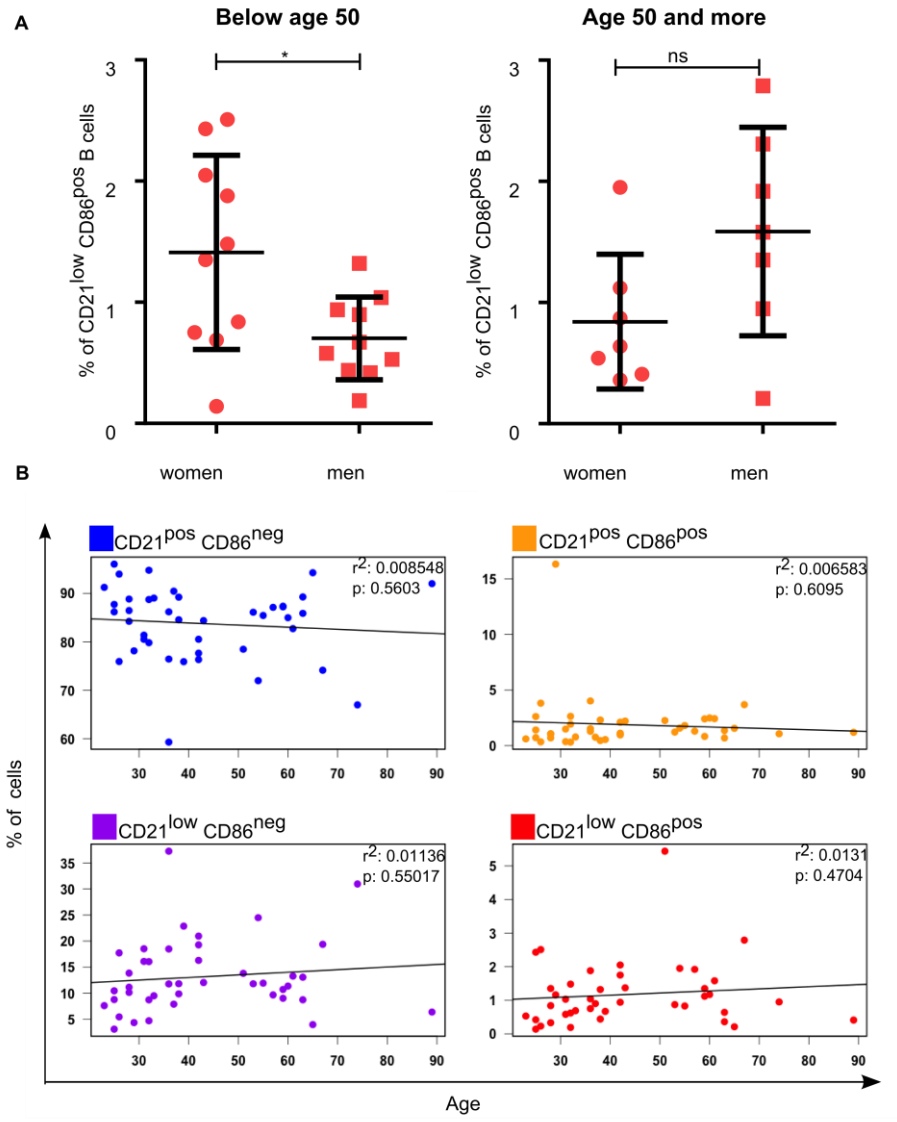

Figure 12. Individual variation in the frequency of B-cell subsets

Gender and age differences were evaluated in peripheral blood from healthy volunteers. $CD19^+$ $CD20^+$ B cells were divided into four B-cell subsets according to the

expression of CD21 and CD86. (A) Frequency of $CD21^{low}$ $CD86^{pos}$ B cells was analyzed comparing age-matched men and women younger than 50 years (n=10) and older (n=7). Significance was calculated with a paired t test and exact p values are given in the text. (B) Changes on the composition of the four B-cell subsets as a function of age. The lines represent the linear regression curve. The corresponding coefficient of determination (r^2) and significance values (p) for each population are indicated in each plot.

3.3 Phenotypic characterization of the four B-cell subsets

More detailed phenotypic analysis of cell size, proliferative status, stage of maturation and expression of activation molecules and chemokine receptors revealed characteristic differences between the four B-cell subsets.

3.3.1 $CD21^{low}$ $CD86^{pos}$ B cells were significantly larger than the other subsets

The cell size of the four subsets differed significantly (Figure 13). Consistent with the assumption that they represent activated B cells, both $CD21^{pos}$ $CD86^{pos}$ and $CD21^{low}$ $CD86^{pos}$ B cells were significantly larger than $CD86^{neg}$ subsets. The largest cells were $CD21^{low}$ $CD86^{pos}$ B cells with an MFI of the forward scatter signal (FSS) of 314.5 ± 6.491, followed by $CD21^{pos}$ $CD86^{pos}$ with 278.2 ± 7.707, the double negatives $CD21^{low}$ $CD86^{neg}$ with 257 ± 9.328 and the smaller were $CD21^{pos}$ $CD86^{neg}$ B cells with 249.9 ± 6.649 (n=4; mean ± SD).

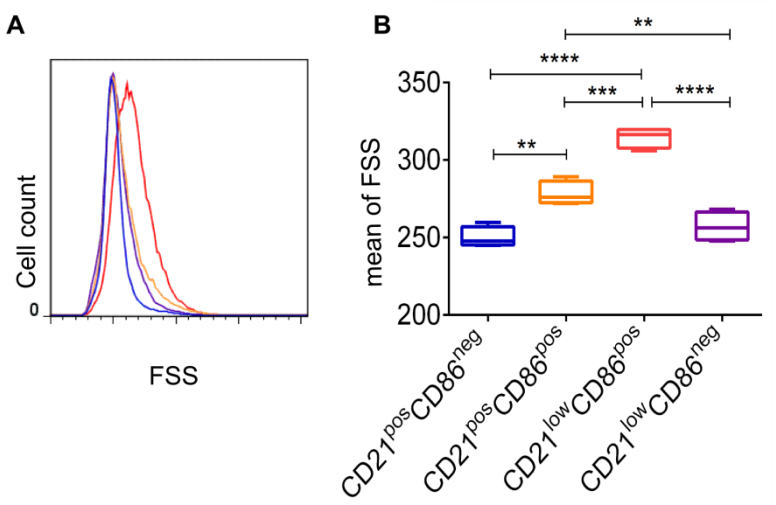

Figure 13. CD21^{low} CD86^{pos} B cells were larger than B cells from the other three cell subsets

CD19^{+} CD20^{+} B cells were divided into four B-cell subsets according to the expression of CD21 and CD86 and analyzed by flow cytometry to determine cell size. (A) Representative donor histograms of cell size of the four B-cell subpopulations. Lines are color-coded for each subset corresponding to the colors in (B). (B) Box plot of the cell size (n=4) calculated with the MFI of the forward scatter signal (FSS). Band inside the box represents the median and whiskers are minimum and maximum value. Significant differences were calculated by one-way ANOVA with Tukey´s multiple comparisons test. Asterisks represent: ** $p \leq 0.01$, *** $p \leq 0.001$, **** $p \leq 0.0001$.

3.3.2 CD21^{pos} CD86^{pos} and CD21^{low} CD86^{pos} B-cell subsets were actively proliferating

Generally, cells have to increase their cell mass in order to progress through the cell cycle (Polymenis and Schmidt 1999). The Ki-67 human proliferation marker was used in order to determine the growth fraction of each B-cell subset. Ki-67 is a

protein strictly associated with cell proliferation. Hence, during interphase (G_1, S, G_2) the antigen is exclusively detected within the nucleus, whereas in mitosis most of the protein is relocated to the surface of the chromosomes. More importantly, the protein is absent from resting cells (G(0)) (Scholzen and Gerdes 2000). This makes it an excellent marker for determining the proportion of proliferating cells within each B-cell subset. Consistent with the cell size analysis, Ki-67 staining revealed that both $CD21^{pos}$ $CD86^{pos}$ and $CD21^{low}$ $CD86^{pos}$ B-cell subsets contained a significant larger fraction of proliferating cells compared to $CD21^{pos}$ $CD86^{neg}$ ($p \leq 0.05$) (Figure 14). In the $CD21^{low}$ $CD86^{pos}$ subset, 17.42 % ± 6.168 of the cells showed higher rates of proliferation as measured by Ki-67 expression while 9.478 % ± 2.827 of the cells were proliferating in the $CD21^{pos}$ $CD86^{pos}$ subset. On the other hand, in the $CD86^{low}$ subset very few cells were positive for Ki-67 with 0.1175 % ± 0.026 of $CD21^{pos}$ cells and 2.120 % ± 1.195 of $CD21^{low}$ cells (n=4; mean ± SD).

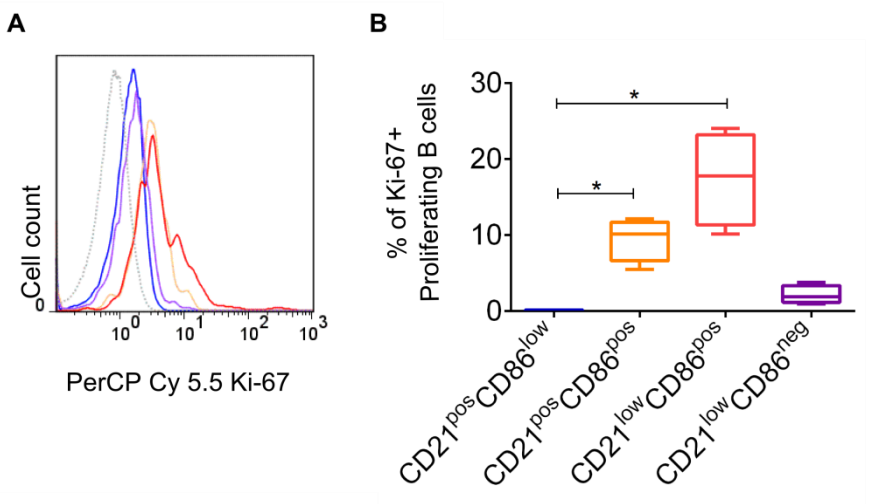

Figure 14. CD21^{low} CD86^{pos} B-cell subset had a higher proportion of proliferating cells

CD19^{+} CD20^{+} B cells were divided into four B-cell subsets according to the expression of CD21 and CD86 and analyzed by flow cytometry to determine proliferation status by Ki-67. (A) Representative donor histograms of Ki-67 expression of the four B-cell subpopulations and isotype control (dotted grey line). Lines are color-coded for each subset corresponding to the colors in (B). (B) Box plot of the amount of cells expressing Ki-67 in each subset (n=4, band inside the box represents the median and whiskers are minimum and maximum value). Significant differences were calculated by one-way ANOVA with Tukey´s multiple comparisons test. Asterisks represent: * $p \leq 0.05$.

3.3.3 CD21^{low} CD86^{pos} B-cell subset contained mostly antigen experienced IgM^{neg} IgD^{neg} class-switched B cells

B-cell subsets also differed with regard to their stage of maturation. CD21^{pos} B-cell subsets consisted primarily of IgM^{pos} IgD^{pos} naïve B cells (68.367 % ± 9.642 of CD86^{neg} and 70.797 % ± 19.806 of CD86^{pos} subset), whereas CD21^{low} CD86^{pos} B-cell subset contained significantly more antigen experienced IgM^{neg} IgD^{neg} class-switched B cells (53.440 % ± 21.874; $p \leq 0.0001$) (Figure 15). The CD21^{low} CD86^{neg} B-cell subpopulation, on the other hand, consisted of a mixture of naïve and class-switched B cells (42.109 % ±13.605 IgM^{pos} IgD^{pos} and 34.337 % ± 18.099 were IgM^{neg} IgD^{neg}) (n=4; mean ± SD).

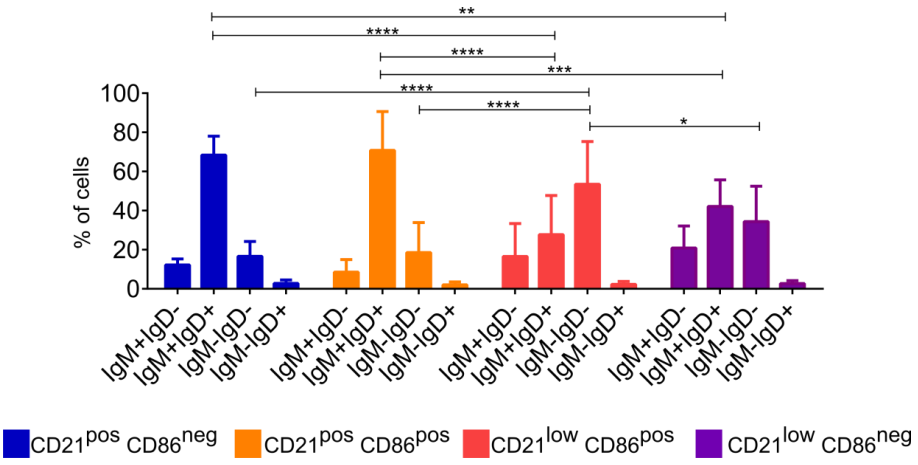

Figure 15. CD21^{low} CD86^{pos} subset consisted primarily of IgM^{neg} IgD^{neg} class-switched B cells

CD19+ CD20+ B cells were divided into four B-cell subsets according to the expression of CD21 and CD86 and analyzed by flow cytometry to determine maturation status according to the expression of IgM and IgD. Bar charts represented the percentage of each subset expression of both IgM and IgD (n=7). Significant differences were calculated by two-way ANOVA with Tukey´s multiple comparisons test. Asterisks represent: * $p \leq 0.05$, ** $p \leq 0.01$, *** $p \leq 0.001$, **** $p \leq 0.0001$.

3.3.4 Expression of cell surface molecules among B-cell subsets

In analogy to in vitro generated CD40B cells (section 3.1), CD21^{low} CD86^{pos} B cells expressed high levels of activation markers such as the costimulatory molecules CD80 and CD86 and had high expression of MHC class II (HLA-DR) (Figure 16A) (n=16) (Schultze et al. 1997). Interestingly, CD62L, which is expressed primarily by naïve B cells (Morrison et al. 2010) was differentially expressed on CD21^{pos} and CD21^{low} subsets. CD62L, which is a molecule involved in early phases of migration through

high endothelial venules allowing transmigration into tissues, was down-regulated in both $CD21^{low}$ subsets (n=13) (Figure 17A, lower right panel). Additionally and consistent with the hypothesis that $CD21^{low}$ $CD86^{pos}$ and $CD21^{pos}$ $CD86^{pos}$ B-cell subsets are antigen experienced, a significantly higher proportion of $CD27^{+}$ B cells was found in $CD86^{pos}$ subsets compared to $CD86^{low}$ subsets (n=16, $p \leq 0.001$) (Figure 16B, upper panel). Moreover, the cell-surface glycoprotein CD43, described to be expressed only on a subpopulation of naïve B cells, was expressed on 84.77 % ± 13.48 of $CD21^{low}$ $CD86^{pos}$ and 72.03 % ± 16.43 of $CD21^{pos}$ $CD86^{pos}$ B cell (n=3). In contrast, only 7.967 % ± 2.918 and 15.34 % ± 9.455 of $CD21^{pos}$ $CD86^{neg}$ and $CD21^{low}$ $CD86^{neg}$ expressed CD43, respectively (Figure 16B, lower panel). The role of CD43 is not fully established, but it is believed to have a major function during later stages of B cell differentiation (Bjorck et al. 1991). Moreover, in human systems, CD43 has been described to be up-regulated upon activation stimuli, therefore should be considered as an "activation antigen" (Griffin et al. 2011).

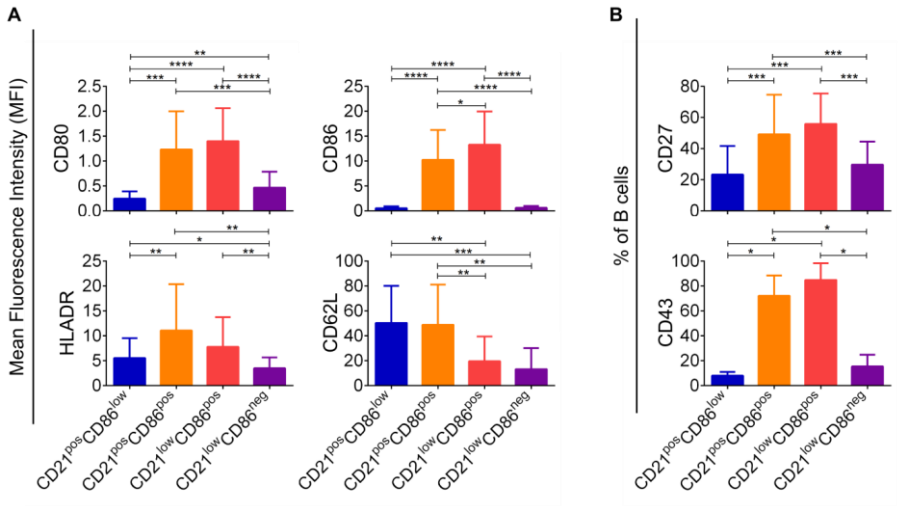

Figure 16. B-cell subsets differed in terms of expression of several cell surface molecules

PBMCs from healthy donors were analyzed by flow cytometry. $CD19^+$ $CD20^+$ B cells were divided into four B-cell subsets according to the expression of CD21 and CD86. Expression of each marker (MFI) was determined. (A) MFI of molecules associated with antigen presentation such as CD80 (n=16), CD86 (n=16), HLA-DR (n=15) and the adhesion molecule CD62L (n=13). Data is represented as the MFI ± SD. (B) Bar chart showing the amount of cells (expressed as percentage -%- of B cells) that express CD27 (n=16) or CD43 (n=3). Significant differences were calculated by one-way ANOVA with Tukey´s multiple comparisons test. Asterisks represent: * $p \leq 0.05$, ** $p \leq 0.01$, *** $p \leq 0.001$, **** $p \leq 0.0001$.

As shown in figure 17, phenotyping of B cells with LEGENDScreen Human Cell Screening (PE) Kit further confirmed these results. Additionally, relative to the other B-cell subsets, $CD21^{low}$ $CD86^{pos}$ B cells expressed lower levels of inhibitory receptors CD22 and CD32 (FcγRIIb) (n=2). $CD21^{low}$ $CD86^{neg}$ B cells on the other hand were characterized by a high expression of CD32 and a low expression of CD80, CD86, HLA-DR, and CD22.

CD32 binds IgG-immune complexes and exerts its inhibitory function by suppressing or blocking BCR signaling via its immunoreceptor tyrosine-based inhibitory motif (ITIM) upon simultaneous binding to the BCR (Nimmerjahn and Ravetch 2008). Besides, CD22 binds to CD45R isoforms on T cells and down-modulates B cell activation threshold through its association with PTP-1C (SHP-1) (Toba et al. 2002).

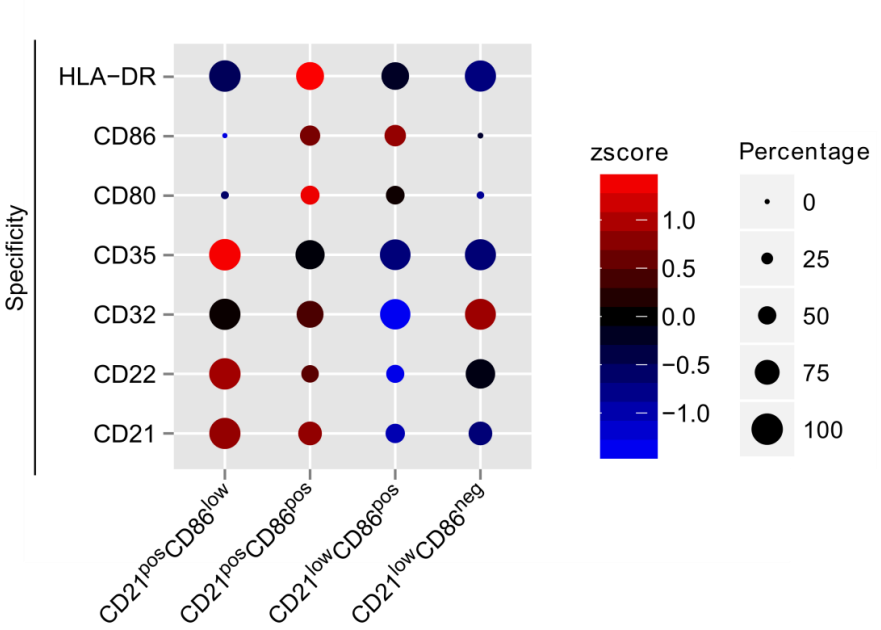

Figure 17. CD21^{low} CD86^{pos} B cells expressed lower levels of the inhibitory receptors CD22, and CD32

Purified CD19^{+} B cells from healthy donors were stained according to manufactures' instructions with the LEGENDScreen Human Cell Screening (PE) Kit and analyzed by flow cytometry to determine the expression of several markers. The size of the dots indicates the percentage of B cells positive for the respective cell marker. Color of the dots represents the z-score normalized average expression level of the indicated markers. Blue color denotes low expression, red color denotes high expression. The z-score is a statistical measurement of a score's relationship to the mean in a group of scores. A z-score of 0, means that the score has the same value than the mean. The positive and negative numbers, indicate whether the value is above or below the mean and by how many standard deviations. The numbers represent the z-score. One donor out of 2 independent experiments is shown.

3.3.5 Expression of molecules involved in cell trafficking among B-cell subsets

During the course of a normal immune response, lymphocytes continuously circulate between blood and tissues and rapidly accumulate at sites of inflammation (von Andrian and Mempel 2003). Molecules involved in this process of cell trafficking include cell adhesion molecules (such as selectines and integrins), chemokines and ectoenzymes (enzymes with catalytic domains outside the plasma membrane) (Salmi and Jalkanen 2005). Since CD40B cells were proven to induce chemotaxis of both $CD4^+$ and $CD8^+$ T cells by expression of a pattern of chemokines (see section 1.4.6) and to home to secondary lymphoid organs (Klein-González et al. 2010), the expression of relevant markers was evaluated in peripheral blood B-cell subsets.

$CD21^{low}$ $CD86^{pos}$ B cells displayed a chemokine receptor profile that appears to favor migration to sites of inflammation in peripheral tissues. They expressed high levels of CXCR3 and adhesion molecules CD18, CD11a and CD11b while expressing low levels of lymph node homing receptors CCR7, CXCR4 and CD62L (Figure 18 and Figure 16). On the other hand, $CD21^{pos}$ $CD86^{pos}$ B cells expressed predominantly lymph node homing receptors CCR7, CXCR4, and CD62L (Figure 18 and Figure 16). In contrast, $CD21^{pos}$ $CD86^{neg}$ and $CD21^{low}$ $CD86^{neg}$ B cells were characterized by down-regulation of these trafficking molecules.

CD39, described first as an activation marker (Maliszewski et al. 1994) and then as an ectoenzyme (Kaczmarek et al. 1996), is a nucleoside triphosphate diphosphohydrolase that regulates cell trafficking by modulating adenosine levels in the body due to their involvement in adenosine triphosphate (ATP) metabolism (Salmi and Jalkanen 2005). Therefore, CD39 expressing cells migrate towards

gradients at inflammation sites where ATP has been released (Antonioli et al. 2013). Interestingly, $CD21^{low}$ $CD86^{pos}$ B cells also expressed high levels of CD39 on their surface (Figure 18).

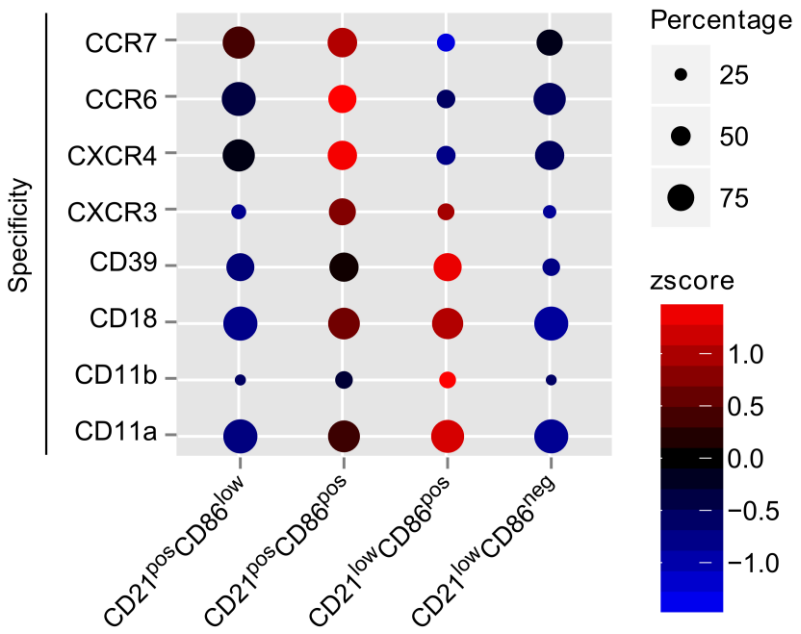

Figure 18. Expression of molecules involved in cell trafficking

Purified $CD19^+$ B cells from healthy donors were stained according to manufactures' instructions with the LEGENDScreen Human Cell Screening (PE) Kit and analyzed by flow cytometry to determine the expression of several migration markers. The size of the dots indicates the percentage of B cells positive for the respective cell marker. $CD19^+$ $CD20^+$ B cells were divided into four B-cell subsets according to the expression of CD21 and CD86. The size of the dots indicates the percentage of B cells positive for the respective cell marker. Color of the dots represents the z-score normalized average expression level of the indicated markers. Black color denotes low

expression, red color denotes high expression. The z-Score was calculated as described above. One donor out of 2 independent experiments is shown.

3.4 Isolation of B-cell subsets via fluorescence activated cell sorting (FACS)

Based on their phenotypic characteristics and the in vitro results of the CD40L experiments (section 3.1, Figure 10), it was expected that $CD21^{pos}$ $CD86^{pos}$ and $CD21^{low}$ $CD86^{pos}$ B cells would have a higher antigen-presenting capacity compared to $CD21^{pos}$ $CD86^{neg}$ and $CD21^{low}$ $CD86^{neg}$ B cells. In order to assess the antigen-presenting capacity, the four B-cell subsets were isolated using FACS according to the expression of CD21 and CD86.

Direct sorting of B-cell subsets from PBMCs by expression of CD21 and CD86 was not possible. The purity after isolation was never higher than 30 % especially in the $CD86^{pos}$ B-cell subsets (data not shown). Therefore, a pre-separation step for B-cell enrichment was included. In order to disturb the B cells as less as possible the pre-separation was done with a negative selection kit for B cells. Nevertheless, using this method most of the $CD21^{low}$ $CD86^{pos}$ B cells were lost in the process of separation. By screening the B-cell subsets for the molecules used for negative selection, a high expression of CD43 was found to be expressed by the majority of $CD21^{low}$ $CD86^{pos}$ B cells. CD43 is used to deplete T lymphocytes, monocytes and granulocytes, but has been also described to be expressed on a small fraction of B cells that happened to include most of the $CD21^{low}$ $CD86^{pos}$ and $CD21^{pos}$ $CD86^{pos}$ B cells (Figure 19).

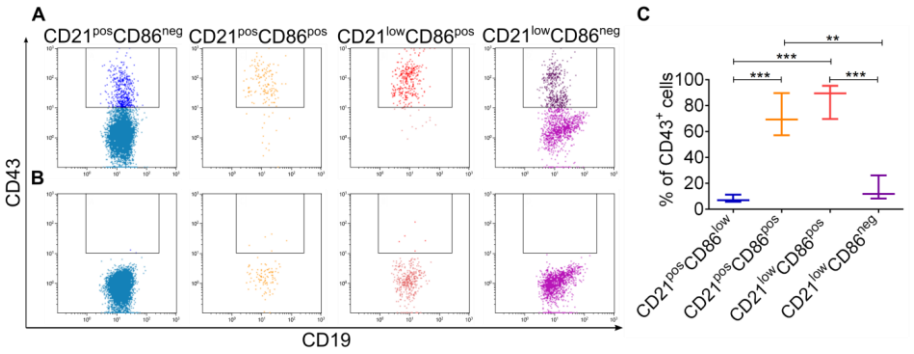

Figure 19. The majority of CD21^{low} CD86^{pos} and CD21^{pos} CD86^{pos} B cells expressed CD43 on their surface

CD19^{+} CD20^{+} B cells were divided into four B-cell subsets according to the expression of CD21 and CD86 and were analyzed by flow cytometry to determine expression of CD43. (A, B) Representative donor plots. (A) Positive cells for CD43 are marked in the square. (B) Plots with the appropriate isotype control for each subset. (C) Box plot showing the percentage of cells that express CD43 in each B-cell fraction. Horizontal middle line represents the median and whiskers are minimum and maximum value (n=3). Significant differences were calculated by one-way ANOVA with Tukey´s multiple comparisons test. Asterisks represent: ** $p \leq 0.01$, *** $p \leq 0.001$.

Since most of the commercial kits available for negative selection of untouched B cells contain CD43 in their mix, a CD19^{+} positive magnetic selection was performed. Purity of CD19^{+} CD20^{+} B cells after CD19^{+} selection was always more than 98% (data not shown). The combination of CD19^{+} selection with subsequent cell sorting resulted in sufficient numbers of the B-cell subpopulations with a good purity (Figure 20). For sorting, CD3 antibody was included to eliminate possible contaminating T cells.

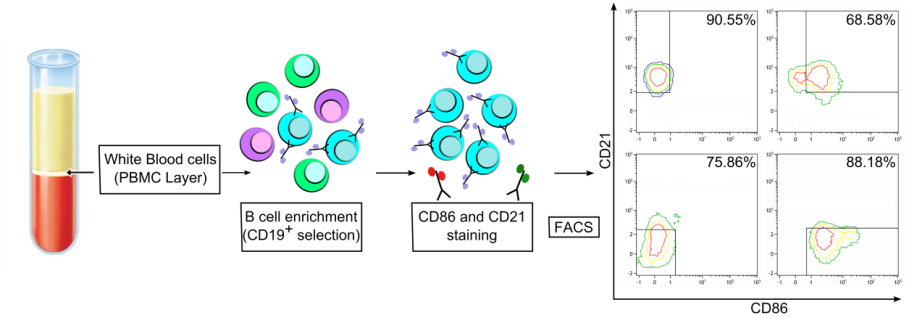

Figure 20. Isolation on B-cell subsets via FACS

B cells were purified from PBMCs via CD19 positive selection, incubated with CD3, CD20, CD21, CD86 and sorted by FACS according to the expression of CD21 and CD86. Purity of the cells after sorting is shown in the graph as a percentage of the total cell number for each fraction.

3.5 $CD21^{pos}$ $CD86^{pos}$ and $CD21^{low}$ $CD86^{pos}$ B cells were potent antigen-presenting cells

In order to proliferate, T cell required two main signals; first, activation via binding of the specific antigen to the TCR in the context of MHC and second, costimulatory signals through binding of CD80 and CD86 expressed on APCs to the receptor CD28 on the T cell surface (Chambers 2001).

Assessment of the antigen-presenting capacity of B-cell subsets was done by means of an MLR. In order to reduce as much as possible cross-activation of T cells by allogeneic interactions, autologous T cells were used (Hausmann et al. 2000). In the autologous MLR system, the first signal is provided by the addition of OKT3. The target of OKT3 is the CD3 molecule, which is assembled together with the TCR

heterodimer. The TCR polypeptides themselves have very short cytoplasmic tails and all proximal signaling events are mediated through the CD3 molecule. Therefore, engagement of CD3 by OKT3 initiates a signaling cascade that mimics the antigen-specific response causing T cell mitogenesis (Norman 1995, Lin and Weiss 2001). The OKT3 concentration was titrated in previous experiments and was combined with a sub-optimal concentration of IL-2, which did not induce T cell proliferation in the absence of costimulation (data not shown). Costimulation was the second signal and was provided by the APCs.

FACS-purified and irradiated B-cell subsets were cultured with CFSE-labeled autologous $CD3^{+}$ T cells. As shown in Figure 21A and B, among the four different subsets, $CD21^{low}$ $CD86^{pos}$ B cells showed the strongest T cell-stimulatory activity which was significantly higher than that induced by $CD21^{pos}$ $CD86^{neg}$ and $CD21^{low}$ $CD86^{neg}$ B cells ($p \leq 0.05$, n=3). In line with the results from in vitro CD40B cells, the $CD21^{low}$ $CD86^{pos}$ B-cell subset showed the strongest immunostimulatory capacity and $CD21^{pos}$ $CD86^{pos}$ B cells showed an intermediate immunostimulatory activity, which was higher than that of $CD21^{pos}$ $CD86^{neg}$ B cells and $CD21^{low}$ $CD86^{neg}$ B cells. Figure 21C shows flow cytometric plots of T cells from one representative donor cultivated with the different controls used to determined baseline stimulation.

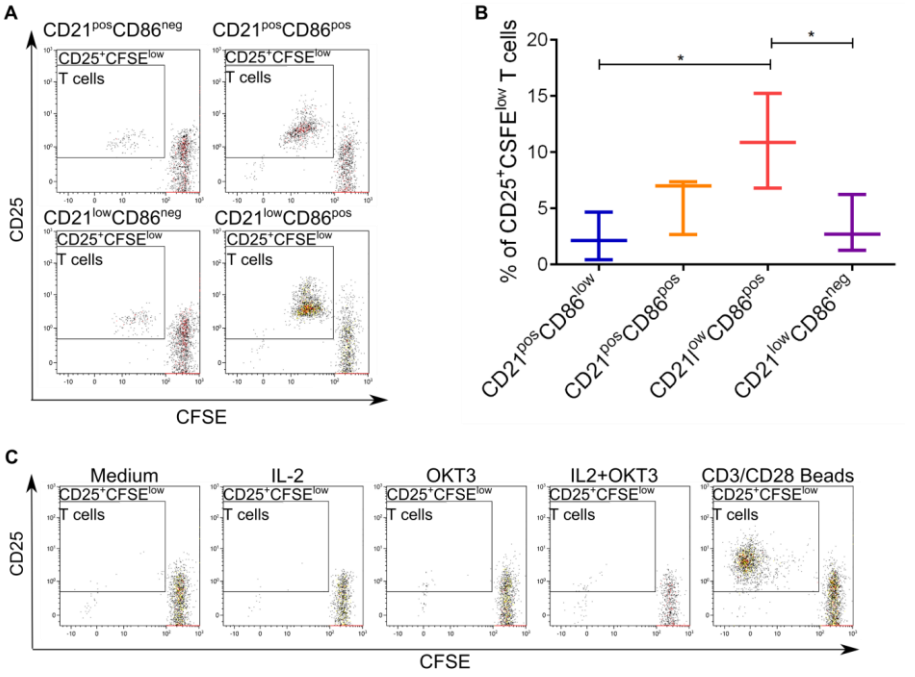

Figure 21. Mixed lymphocyte reaction with purified B-cell subpopulations and autologous T cells

Sorted B cells were incubated with CFSE-labeled autologous $CD3^+$ T cells for 7 days and proliferation and activation of T cells were evaluated by CFSE dilution and up-regulation of CD25, respectively. (A) Dot plot showing T cell proliferation ($CD25^+$ $CFSE^{low}$ T cells) in response to each B-cell subset of one representative donor. (B) Box plot with the percentage of T cell proliferation in response to each B-cell subset of 3 donors from independent experiments. Horizontal middle line represents the median and whiskers are minimum and maximum value. (C) Representative FACS plots of T cells cultivated with the different controls (same donor from (A)). Significant differences were calculated by one-way ANOVA with Tukey´s multiple comparisons test. Asterisks represent: *$p \leq 0.05$.

3.6 Triggering of BCR poorly induced calcium flux in CD21^{low} B-cell subsets

Calcium signaling is important for B cell activation, proliferation, differentiation and function (Dolmetsch et al. 1997). After BCR crosslinking by antigen, downstream molecules such as SYK and BTK are phosphorylated, which in turn leads to activation of PLCγ2 (Kurosaki and Hikida 2009). Activated PLCγ2 hydrolyses phosphatidylinositol 4,5-bisphosphate (PIP_2) to diacylglycerol and inositol-1,4,5-trisphosphate (IP3). The resulting IP3 binds to its receptor, which is itself a Ca^{2+}-permeable ion channel mediating a transient calcium release from intracellular stores in the endoplasmic reticulum (ER) (Foerster et al. 2010). Due to the small size of the ER, increase in intracellular Ca^{2+} concentration is only moderated and transient.

Since the amplitude of the calcium response after BCR stimulation is dependent on the stage of B cell differentiation (Antony et al. 2007, Engelke et al. 2007) and varies among B-cell subpopulations (Foerster et al. 2010), a calcium flux assessment was performed in the four subpopulations separately, with regards to B-cell subset-specific differences in the initiation of cellular signaling cascade. Due to the low frequency of cells in each B-cell subset, a flow cytometric method was established to identify changes in free intracellular Ca^{2+} and to assess both basal status and the response to several stimuli. To do so, Fluo-3 AM and Fura Red AM fluorescent dyes were used. Fluo-3 is a dye which emission is 100-200 times brighter in the presence of Ca^{2+} than its Ca^{2+} -free form (Burchiel et al. 2000). In contrast, Fura Red AM experiences fluorescence quenching when Ca^{2+} is bound. Therefore, by analyzing the ratio of the two fluorescence emissions (Fluo-3 green to Fura Red

emission ratio) the sensitivity is increased (Novak and Rabinovitch 1994, Mounho and Burchiel 1998). These AM dyes are permeable to the cell membrane; however Pluronic F-127 was used to increase the penetration of dyes into the cell. Once in the cytoplasm, the AM esters are cleaved by esterases and dyes become sensitive to calcium (Burchiel et al. 2000).

Monitoring of both the calcium basal level and the flux of intracellular calcium after BCR triggering was done. $CD21^{low}$ $CD86^{pos}$ B cells had significantly higher basal intracellular calcium levels (0.320 ± 0.1522) than the other B-cell subsets (Figure 22A and B -red line-) ($p \leq 0.05$). $CD21^{low}$ $CD86^{neg}$ B cells also had higher basal calcium levels (0.2240 ± 0.03912) than $CD21^{pos}$ $CD86^{neg}$ (0.1260 ± 0.06427) and $CD21^{pos}$ $CD86^{pos}$ (0.1420 ± 0.08672) B lymphocytes (Figure 22).

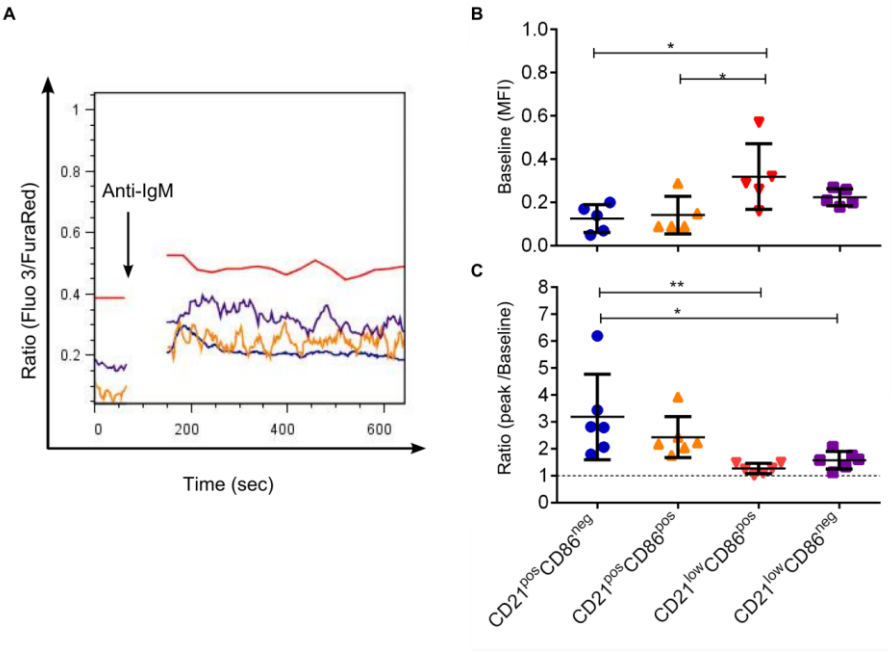

Figure 22. Baseline cytosolic calcium levels and response to BCR stimulation in the four B-cell subsets

Purified B cells were incubated with the fluorescent calcium indicators Fura-Red AM and Fluo-3 AM for 60 min and analyzed by flow cytometry. $CD19^+$ $CD20^+$ B cells were divided into four B-cell subsets according to the expression of CD21 and CD86 (A) FACS plot of one representative donor calcium release in response to BCR signaling. Basal levels of calcium were recorded for 60 sec and then cells were stimulated with anti-IgM antibody. Shown is one representative donor with color-coded lines for each B-cell subset. Black arrow indicates the moment when stimulation with anti-IgM antibody was added to the sample (B) Baseline level of intracellular calcium before stimulation (MFI of Fluo3/FuraRed ratio) (n=5). (C) The scatter plot shows the BCR-mediated calcium flux expressed as the ratio of the peak and baseline fluorescence (MFI of Fluo3/FuraRed ratio) in the four different B-cell subsets (n=6, mean ± SD). Significant differences were calculated by one-way ANOVA with Tukey´s multiple comparisons test. Asterisks represent: *$p \leq 0.05$, ** $p \leq 0.01$.

Analysis of the response to BCR stimulation also showed a differential response among the subsets (Figure 22A and C). The amplitude of the response was calculated normalizing the peak value after stimulation to the baseline. Therefore, the minor the difference between baseline and peak stimulation, the closest was the value to 1. In $CD21^{pos}$ $CD86^{neg}$ and $CD21^{pos}$ $CD86^{pos}$ BCR engagement was followed by a rapid increase in intracellular calcium (3.190 ± 1.587 and 2.439 ± 0.7653, respectively) (Figure 22A and C). In contrast, in $CD21^{low}$ $CD86^{pos}$ and $CD21^{low}$ $CD86^{neg}$ BCR cross-linking failed to trigger a calcium release (1.270 ± 0.1963 and 1.585 ± 0.3263, respectively). Collectively, these results showed that $CD21^{low}$ $CD86^{pos}$ and $CD21^{low}$ $CD86^{neg}$ B cells have an impaired calcium signaling. The higher intracellular calcium level before stimulation of $CD21^{low}$ $CD86^{pos}$ B cells and their decreased incremental response to BCR engagement might be related to their activated state.

To determine whether the impaired calcium signal release found on $CD21^{low}$ $CD86^{pos}$ cells was also observed in in vitro generated long term activated CD40B cells, the calcium response of CD40B cells against non-activated B cells (resting B cells) was examined. Although baseline levels of intracellular calcium were higher in CD40B cells, BCR cross-linking elicited intracellular calcium signals of comparable duration to resting B cells (Figure 23A). Unlike expected, no differences in amplitude of the calcium response to anti-IgM were seen compared to resting B cells (n=3, normalized to baseline) (Figure 23B). Thus, BCR stimulation elicited a rise in intracellular Ca^{2+} in both CD40B cells and non-activated B cells.

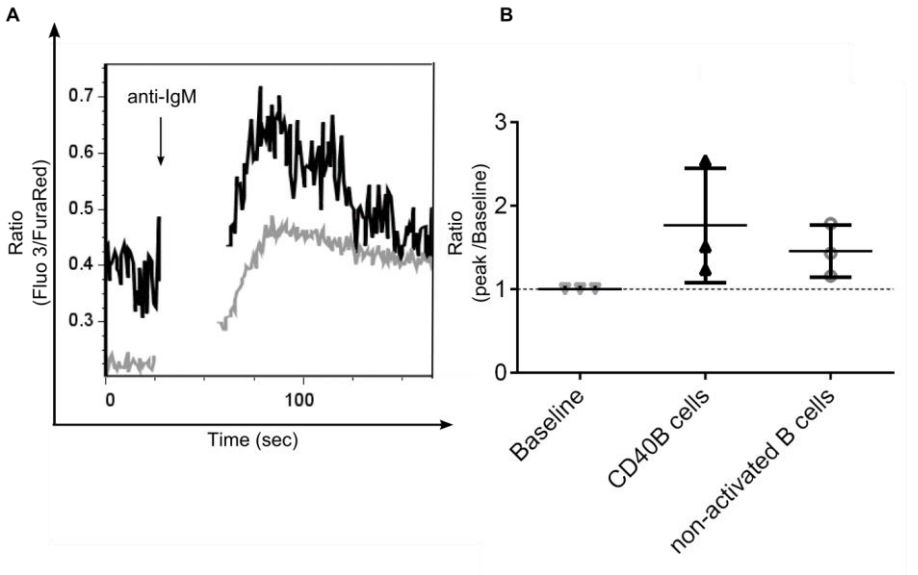

Figure 23. BCR-triggering induced calcium flux on CD40B cells

CD40 activated B cells after 21 days of culture and non-activated B cells from the same donors were incubated with the fluorescent calcium indicators Fura-Red AM and Fluo-3 AM for 60 min. Basal levels of calcium were recorded for 30 sec, cells were stimulated with anti-IgM and analyzed by flow cytometry. (A) Calcium release

of pre-treated CD40B cells (black line) or non-activated B cells (grey line) of one representative donor stimulated with anti-IgM (black arrow). (B) The scatter plot shows the calcium flux response to stimulation expressed as the ratio of the peak and baseline fluorescence (MFI of Fluo3/FuraRed ratio) in CD40B cells or non-activated B cells (n=3, mean ± SD).

CD40 ligation on B cells regulates several important functions such as induction of proliferation, immunoglobulin class switch, antibody secretion, rescue from apoptosis and also has a role in the development of GCs and the survival of memory B cells (Wykes 2003). However, the focus of the investigation of CD40 and CD40L interactions in most of the studies are mainly related to the NF-κB and c-jun N-terminal kinase signaling pathways while there is little information concerning the early events of signaling such as calcium flux (Schwabe et al. 2001, Zarnegar et al. 2004). Therefore and due to the importance of calcium signaling in nearly every aspect of cellular life, intracellular calcium levels after CD40 ligation were investigated to analyze B-cell subset-specific differences. Recording of baseline calcium levels confirmed the results described previously in figure 22 that B-cell subsets differ in terms of intracellular calcium levels. However, unlike the response obtained after BCR engagement, CD40 ligation did not induced the release of intracellular calcium stores (Figure 24 A and B).

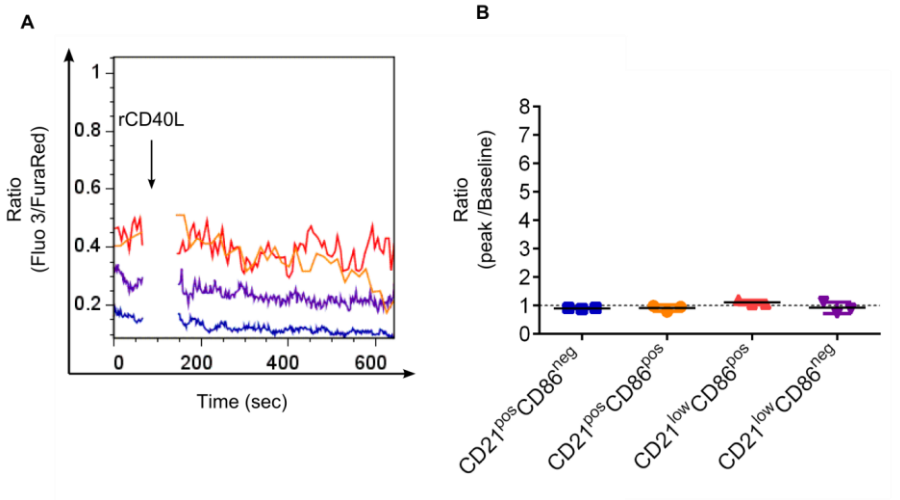

Figure 24. CD40L stimulation induced no calcium flux in B-cell subsets

Purified B cells were incubated with the fluorescent calcium indicators Fura-Red AM and Fluo-3 AM for 60 min. Basal levels of calcium were recorded for 60 sec, cells were stimulated with cross-linked rCD40L and analyzed by flow cytometry. $CD19^+$ $CD20^+$ B cells were divided into four B-cell subsets according to the expression of CD21 and CD86. (A) Calcium release in response to cross-linked rCD40L binding of one representative donor with color-coded lines for each B-cell subset. The black arrow indicates the moment when stimulation with rCD40L was added to the sample (B) The scatter plot shows the calcium flux response to rCD40L expressed as the ratio of the peak and baseline fluorescence (MFI of Fluo3/FuraRed ratio) in four different B-cell subsets (n=3, mean ± SD).

Since no release of calcium from intracellular stores was detected after CD40L stimulation, the question arose if CD40 signaling acts through opening of plasma membrane calcium channels. Therefore, B cells were stimulated again with CD40L, but this time $CaCl_2$ was added as a source of extracellular calcium to a final concentration of 5 mM. Changes in intracellular calcium were only detectable when $CaCl_2$ was added to the medium (Figure 25), suggesting that CD40 ligation acts

through regulation of calcium influx from extracellular space rather than through release from endoplasmic stores.

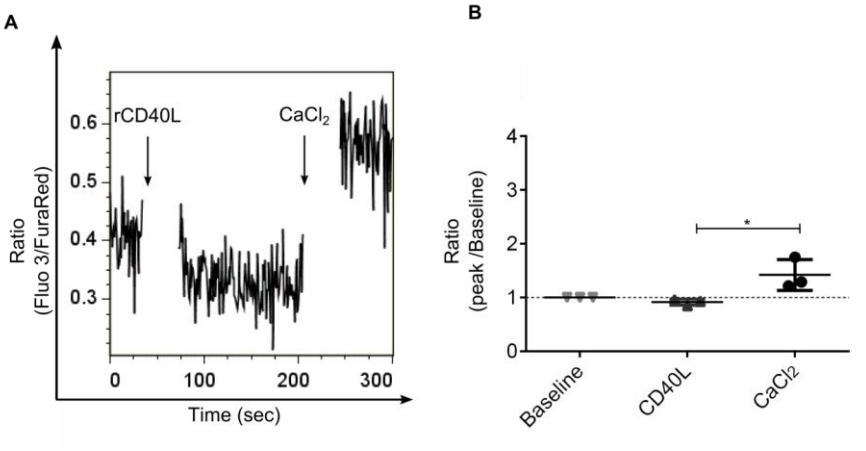

Figure 25. Addition of extracellular calcium induced signaling after CD40 ligation on B cells

Purified B cells were incubated with the fluorescent calcium indicators Fura-Red AM and Fluo-3 AM for 60 min. Basal levels of calcium were recorded for 30 sec, cells were stimulated with cross-linked rCD40L followed by $CaCl_2$ as a source of extracellular calcium and analyzed by flow cytometry. (A) Calcium release of B cells of one representative donor stimulated first with rCD40L and then $CaCl_2$. The black arrow indicates the moment when cross-linked rCD40L and $CaCl_2$ were added to the sample (B) The scatter plot shows the calcium flux response to CD40L or $CaCl_2$ compare to the baseline expressed as the ratio of the peak and baseline fluorescence (MFI of Fluo3/FuraRed ratio) in B cells (n=3, mean ± SD). Significant differences were calculated by one-way ANOVA with Tukey´s multiple comparisons test. Asterisks represent: *$p \leq 0.05$.

Similarly, when B cells were splitted into B-cell subsets according to expression of CD21 and CD86 no differences in terms of CD40L response after $CaCl_2$ were detected among the subsets (Figure 26). All B-cell subsets increased the

concentration of intracellular calcium once the extracellular source was added to the sample.

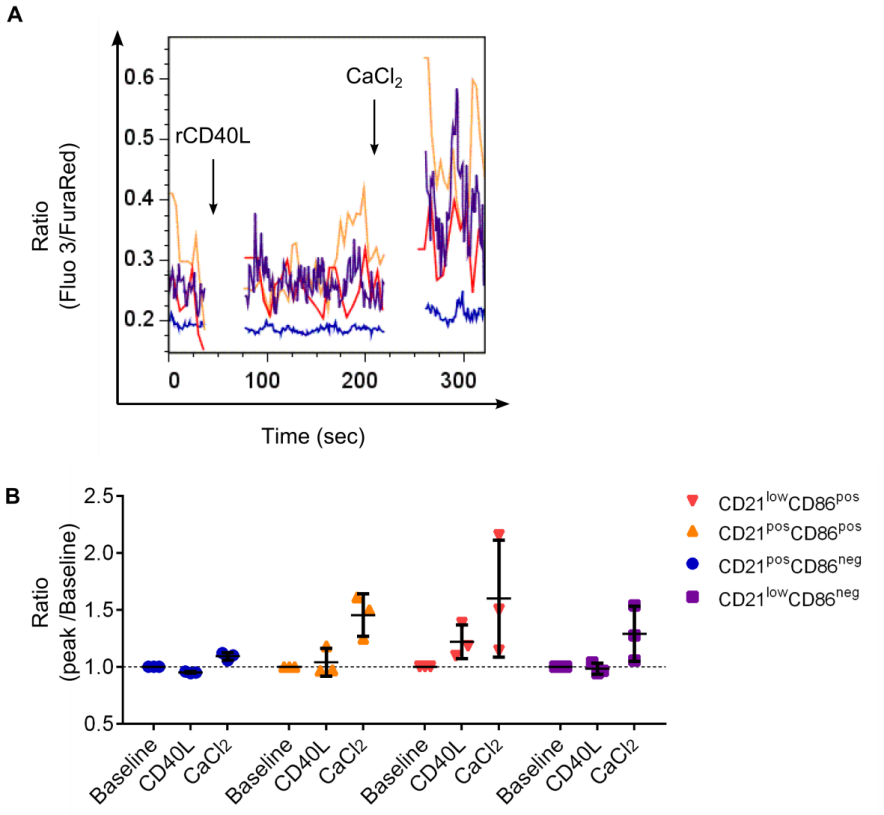

Figure 26. Addition of extracellular calcium induced signaling after CD40 ligation on B-cell subsets

B cells from above experiment were divided into 4 B-cell subsets according to the expression of CD21 and CD86 and calcium flux was analyzed individually in each population after CD40L and $CaCL_2$ stimulation. (A) Calcium release of B-cell subsets of one representative donor stimulated first with rCD40L and then $CaCl_2$ was added. Subpopulations are color-coded as described before. Black arrows indicate the moment when rCD40L and $CaCl_2$ were added to the sample (B) The scatter plot

shows the calcium flux response to CD40L or $CaCl_2$ compare to the baseline expressed as the ratio of the peak and baseline fluorescence (MFI of Fluo3/FuraRed ratio) in each subset (n=3, mean ± SD). No significant differences were detected by two-way ANOVA with Tukey´s multiple comparisons test

Next, CD40-activated B cells were compared to non-activated B cells in order to evaluate if the pre-activation status influences the calcium response after a second brief CD40 ligation. As expected, in both B-cell types there was no calcium flux release from intracellular stores after CD40L (Figure 27). On the contrary, it appears that there was less intracellular free calcium after CD40 ligation. However, when extracellular calcium was added, intracellular calcium in both CD40B and resting B cells augmented. Nevertheless, amplitude of the calcium response after $CaCl_2$ was significantly higher in non-activated B cells compared to CD40B cells ($p \leq 0.05$) (Figure 27B).

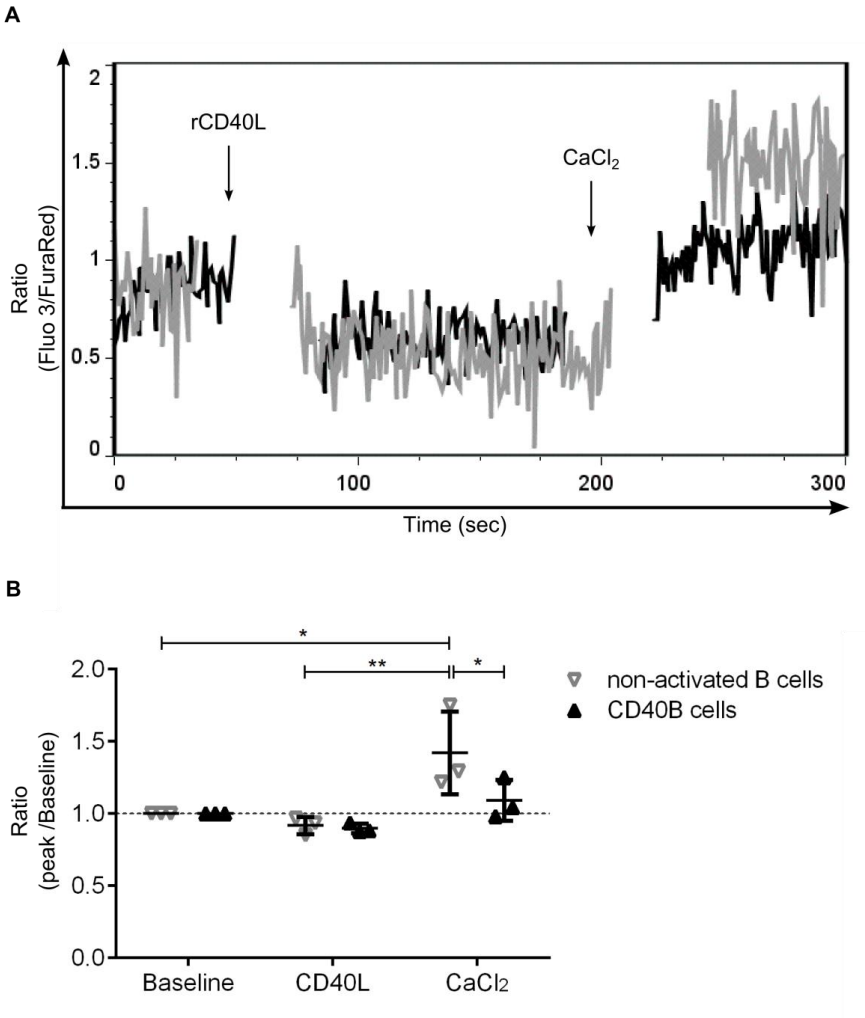

Figure 27. CD40B cells were unresponsive to brief CD40L stimulation

CD40 activated B cells after 21 days of culture and non-activated B cells from the same donors were incubated with the fluorescent calcium indicators Fura-Red AM and Fluo-3 AM for 60 min. Basal levels of calcium were recorded for 30 sec, cells were stimulated with CD40L followed by $CaCl_2$ as a source of extracellular calcium and analyzed by FACS. (A) Calcium release of pre-treated CD40B cells (black line) or

non-stimulated B cells (grey line) of one representative donor stimulated first with CD40L and then with $CaCl_2$. Black arrows indicate the moment when stimulation with CD40L or $CaCl_2$ was added to the sample. (B) The scatter plot shows the calcium flux response to CD40L or $CaCl_2$ respectively expressed as the ratio of the peak and baseline fluorescence (MFI of Fluo3/FuraRed ratio) in CD40B cells or non-stimulated B cells (n=3, mean ± SD). Significant differences were calculated by two-way ANOVA with Sidak´s multiple comparisons test. Asterisks represent: *$p \leq 0.05$, ** $p \leq 0.01$.

3.7 $CD21^{pos}$ $CD86^{pos}$ subsets exhibited increased constitutive SYK, BTK and ERK phosphorylation and decreased response to BCR mediated stimulation

Signals transmitted via the BCR are central events during B cell development, survival, immune responsiveness and differentiation of B lymphocytes (Benschop and Cambier 1999, King and Monroe 2000, Niiro and Clark 2002). An understanding of the signaling circuitry within a cell type can provide important insights into its function. Therefore the signaling state was assessed with regards to the phosphorylation status of important signaling cascades in the four B-cell subpopulations. To this end, a multiplexed phospho-specific flow cytometric profiling was performed to detect basal as well as activation-induced signaling of intracellular molecules involved in B cell activation such as pZAP/SYK, BTK, pERK. Phosphorylated ZAP/SYK and BTK represent BCR proximal signaling events, whereas phosphorylated ERK, is a downstream effector protein (Figure 28) (Mackay et al. 2010). The balance of these signals determines the fate of the cell (Niiro and Clark 2002).

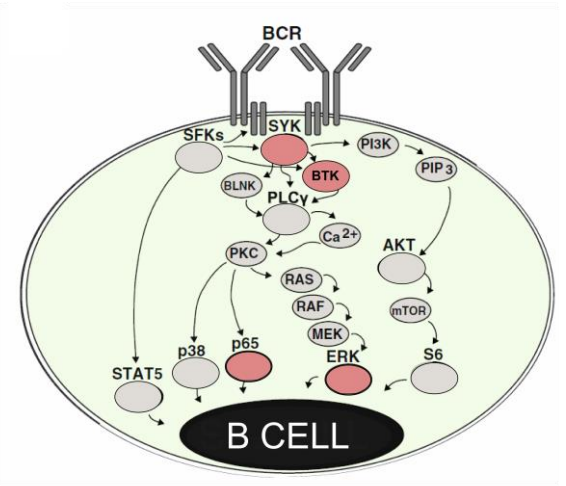

Figure 28. BCR induced signaling

Overview of the signaling after BCR stimulation. Investigated phospho-proteins are marked in red color. Adopted from (Blix et al. 2012).

These results confirmed previously observed patterns of BCR-induced phosphorylation and revealed novel differences within the four B-cell subsets. First, differences in the basal phospho-protein levels were evaluated. For this purpose, samples from 11 healthy donors were analyzed by flow cytometry. The fold change in MFI was calculated as a transformed ratio as described by Irish et at (Irish 2014). Phospho-proteins in unstimulated B-cell subsets were normalized to the MFI of phospho-protein in $CD21^{pos}$ $CD86^{neg}$ B cells of the corresponding sample. Analysis of the baseline phosphorylation of pZAP/SYK, BTK, and pERK revealed that the $CD21^{pos}$ $CD86^{pos}$ B subset displayed a higher baseline phosphorylation than the other three B-cell subsets (Figure 29A). The most pronounced differences in baseline phosphorylation were present between the $CD21^{pos}$ $CD86^{pos}$ and the $CD21^{low}$

CD86^{pos} B cells, which differed within basal phosphorylation of all three signaling molecules (Figure 29A and B). It is important to stress that the basal levels of phospho-proteins for the CD86^{pos} subsets were more heterogeneous compared to CD86^{neg} subsets as some of them showed only small changes while others had either higher or lower basal levels (Figure 29B).

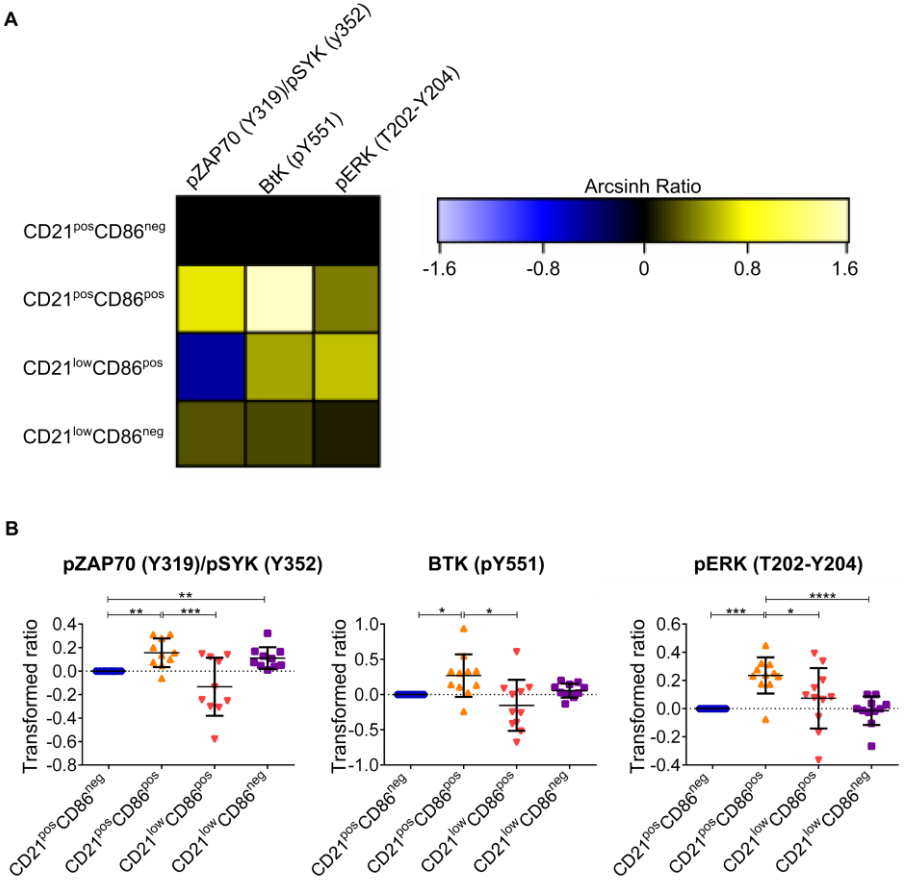

Figure 29. Elevated basal levels of phospho-proteins in CD21^{pos} CD86^{pos} B-cell subset

Purified B cells were stained for intracellular phospho-proteins and analyzed by flow cytometry. (A) Heatmap shows basal level (unstimulated) of pZAP70/SYK, BTK, and pERK in one representative donor. Heatmap was calculated using the arcsinh ratio of means normalized to the $CD21^{pos}$ $CD86^{neg}$ population. (B) Scatter plots of the basal level of 3 phosphoproteins in B-cell subsets (n=11, mean ± SD). Unstimulated samples were used for analysis of basal level of phospho-proteins. The transformed ratio was calculated with $\log_{10}$ (X MFI / $CD21^{pos}$ $CD86^{neg}$ MFI) as described by Irish et al (Irish 2014). Significant differences were calculated by one sample t test to the normalized $CD21^{pos}$ $CD86^{neg}$ B cells and one-way ANOVA with Tukey´s multiple comparisons for the other 3 groups. Asterisks represent: *p ≤ 0.05, ** p ≤ 0.01, *** p ≤ 0.001, **** p ≤ 0.0001.

Next, phosphorylation of several signaling proteins downstream of BCR, 3, 15 and 30 minutes post BCR cross-linking were assessed (n=7). The change in MFI was calculated as described above and each subset-time point was normalized to the respective baseline MFI, i.e. before stimulation baseline MFI was set to 0. With regards to the BCR-triggered phosphorylation of pZAP/SYK and pERK, $CD21^{pos}$ $CD86^{neg}$ showed the largest increase after stimulation. On the contrary, the other three B-cell subsets showed a decreased response (Figure 30). Particularly, $CD21^{pos}$ $CD86^{pos}$ B lymphocytes failed to phosphorylate either ZAP/SYK and ERK after BCR cross-linking compared to the normal response of $CD21^{pos}$ $CD86^{neg}$. Although after BCR stimulation mean phosphorylation of pZAP/SYK in $CD21^{low}$ $CD86^{pos}$ was lower than that of the other three cell subsets, differences were not significant due to inter-donor variations (3 min p=0.2033, 15 min p= 0.0786 and 30 min p=0.0857 respectively, compared to $CD21^{pos}$ $CD86^{neg}$ subset). Importantly, phosphorylation of ERK after 15 min was significantly impaired in both $CD86^{pos}$ subsets. In terms of BTK phosphorylation only minor changes were detected among B-cell subsets (Figure 30).

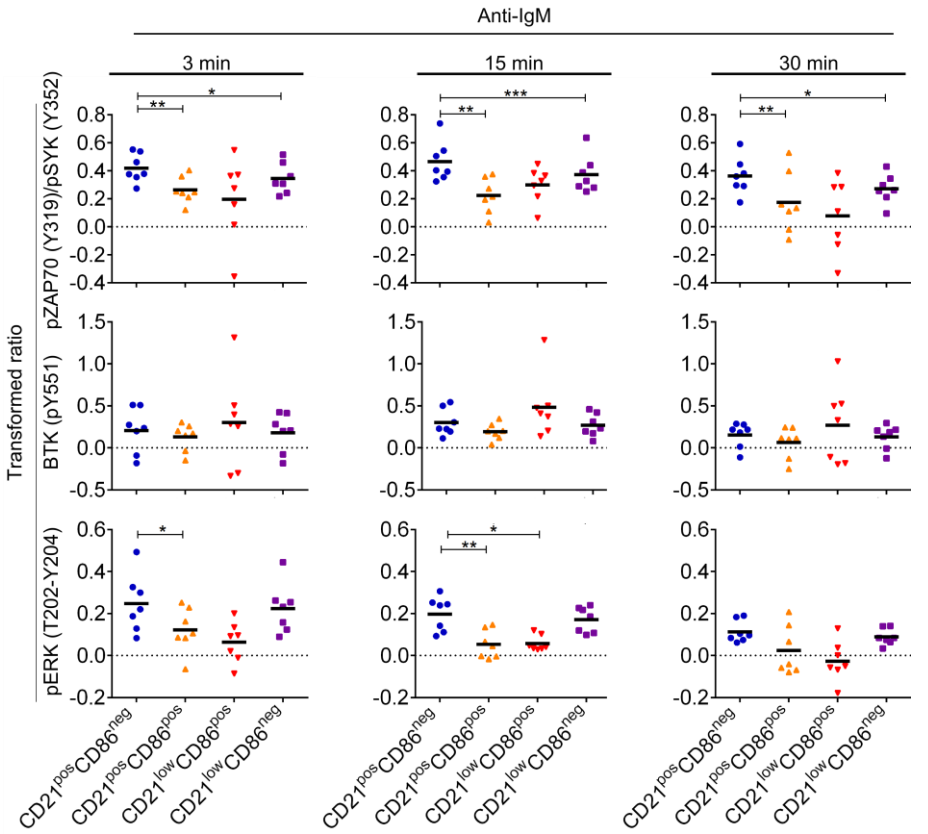

Figure 30. BCR induced signaling was impaired in all but CD21^{pos} CD86^{neg} B-cell subset

Flow cytometry analysis of phosphorylation after BCR cross-linking of key signaling proteins downstream BCR. Purified B cells were stimulated with BCR cross-linking (anti-IgM) for 3, 15 and 30 min. (A) Scatter plots showing the differences in the response after BCR stimulation among the four B-cell subsets defined by the expression of CD21 and CD86 (n=7, mean). Changes in MFI were calculated as described above and expressed as transformed ratio normalized to time-point 0 (before stimulation) of the corresponding sample. Significant differences were calculated to CD21^{pos} CD86^{neg} B cells by one-way ANOVA with Dunnet´s multiple

comparisons post and adjusted p value. Asterisks represent: *p ≤ 0.05, ** p ≤ 0.01, *** p ≤ 0.001.

Signaling after BCR triggering is controlled by dephosphorylation of key molecules by PTPs that terminate the signal (Blix et al. 2012). A low dose of H_2O_2 can regulate BCR-induced PTP activity and therefore modulates the quantity and length of the signaling (Irish et al. 2006). Addition of 3.3 mM of H_2O_2 without BCR-cross linking led to no significant phosphorylation of B cells in the absence of BCR stimulation (data not shown). When H_2O_2 was added immediately before BCR crosslinking, striking differences in BCR-induced signaling of pZAP/SYK and pERK were observed among the subsets (Figure 31A, B). $CD21^{low}$ $CD86^{pos}$ B cells showed significantly low and transient phosphorylation of ZAP/SYK and ERK proteins over time compared to the other subsets (Figure 31A and C). They also showed reduced phosphorylation of BTK phosphorylation that did not reach significant levels (Figure 31C). The pattern of phosphorylation observed in $CD21^{pos}$ $CD86^{pos}$ was similar to that of $CD21^{low}$ $CD86^{pos}$ B cells. Thus, these results suggest that $CD86^{pos}$ subsets have impaired BCR-induced signaling and that inhibition of H_2O_2-sensitive phosphatase activity cannot restore signaling in these cells. In contrast, signaling in $CD21^{low}$ $CD86^{neg}$ B cells was restored after treatment and was no longer different to that of $CD21^{pos}$ $CD86^{neg}$ B cells. Furthermore, the amplitude of the change in MFI of all investigated phospho-proteins was higher for all subsets compared with the BCR stimulation without H_2O_2 suggesting that H_2O_2-sensitive phosphatases are required to control the magnitude of the response (see also Figure 30).

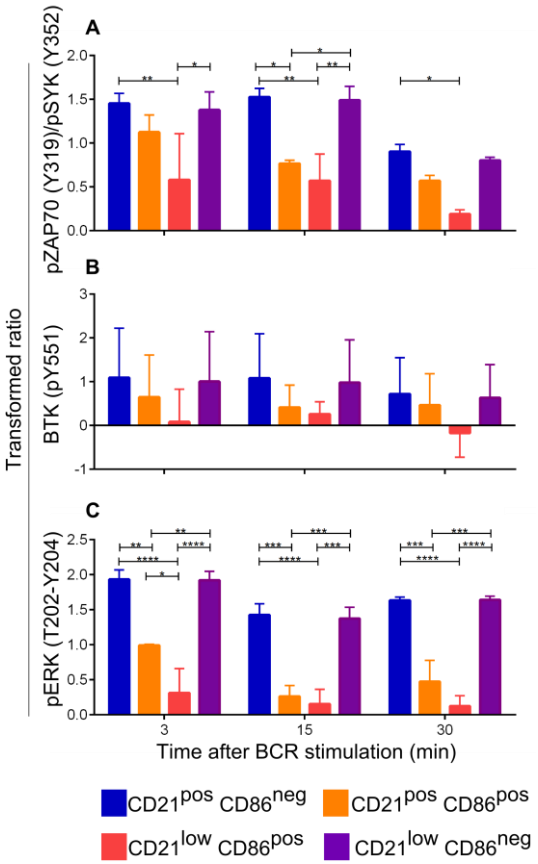

Figure 31. Impaired BCR-induced signaling in CD86^{pos} subsets was not restored by inhibition of H_2O_2 - sensitive phosphatases

Purified B cells were stimulated with a combination of BCR cross-linking (anti-IgM) and H_2O_2 for 3, 15 and 30 min. Cells were stained for intracellular phospho-proteins and analyzed by flow cytometry. Bar chart showing the differences in the response after BCR + H_2O_2 stimulation among the four B-cell subsets of (A) pZAP/SYK, (B) pERK and (C) BTK (n=2, mean ± SD). Changes in MFI were calculated as described above and expressed as transformed ratio normalized to time-point 0 (before stimulation) of the corresponding sample. Significant differences were calculated by one-way ANOVA with Tukey´s multiple comparisons test and adjusted p value. Asterisks represent: *p ≤ 0.05, ** p ≤ 0.01, *** p ≤ 0.001, **** p ≤ 0.0001.

Next, phosphatase activity was completely blocked with pervanadate, a rapidly acting inhibitor (Wienands et al. 1996). As previously showed in figure 29, only CD21^{pos} CD86^{pos} B cells had elevated basal levels of pZAP70/SYK, BTK, and pERK while CD21^{low} CD86^{neg} B cells had elevated baseline of pZAP70/SYK. Surprisingly, upon addition of pervanadate there was a marked increase in the level of pZAP70/SYK only in CD21^{low} CD86^{pos} B cells. As shown in Figure 32, 5 minutes

after pervanadate treatment, CD21^{low} CD86^{pos} B cells contained 2.3-fold more pZAP70/SYK than CD21^{pos} CD86^{neg} ($p \leq 0.05$) and 2.6-fold more than CD21^{low} CD86^{neg} B cells ($p \leq 0.05$) (Figure 32). The mild increase in phosphorylation of pZAP70/SYK in CD21^{pos} CD86^{pos} B cells was not significantly different to any other subset (1.3-fold to CD21^{pos} CD86^{neg} and 1.5-fold to than CD21^{low} CD86^{neg} B cells). The other two phospho-proteins were assessed and no differences among the subsets were detected (data not shown).

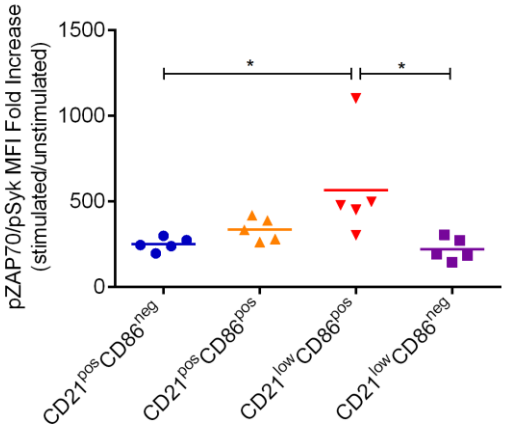

Figure 32. Pervanadate was required for pZAP/SYK phosphorylation in CD21^{low} CD86^{pos} subset

Purified B cells were stimulated with pervanadate for 5 min. Cells were stained for intracellular pZAP/SYK and analyzed by flow cytometry. Scatter plots showing the fold increase phosphorylation of pZAP/SYK after pervanadate treatment compared to unstimulated B-cell subsets (n=5, mean ± SD). Significant differences were calculated by one-way ANOVA with Tukey´s multiple comparisons. Asterisks represent: *$p \leq 0.05$.

3.8 Impaired CD40 signaling in CD21^{low} B-cell subsets

CD40 ligation in B cells activates both arms of the NF-κB pathways. Therefore baseline phosphorylation of NF-κB-p65 (n=11) and CD40L-induced phosphorylation of ERK and NF-κB-p65 were analyzed (n=7). Expression of NF-κB-p65 (pS529) in unstimulated B-cell subsets was normalized to the MFI of phospho-protein in CD21^{pos} CD86^{neg} B cells of the corresponding sample. Analysis of the baseline phosphorylation of NF-κB-p65 revealed that the CD21^{pos} CD86^{pos} B subset displayed a higher baseline phosphorylation than CD21^{low} CD86^{pos} B cells, however not different to that of CD21^{pos} CD86^{low} B cells (Figure 33).

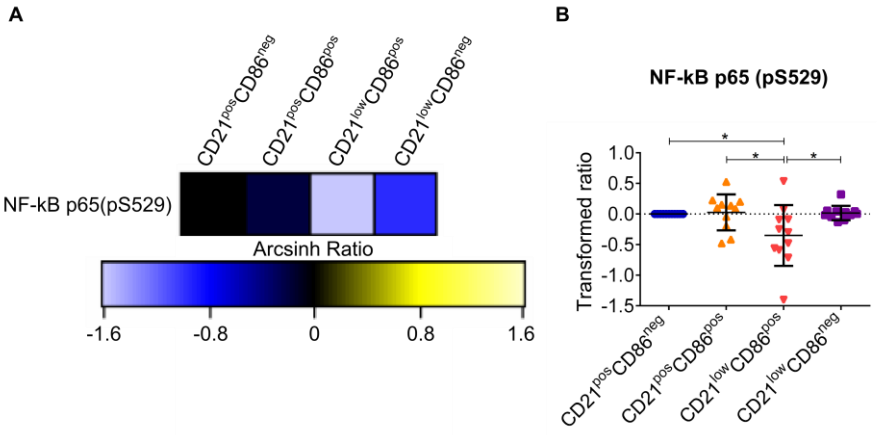

Figure 33. Baseline phosphorylation of NF-κB-p65

Purified B cells were stained for intracellular NF-κB-p65 and analyzed by flow cytometry. (A) Heatmap show basal level (unstimulated) of NF-κB-p65 in one representative donor. Heatmap was calculated using the arcsinh ratio of means normalized to the CD21^{pos} CD86^{neg} population. (B) Scatter plots of the basal level of NF-κB-p65 in B-cell subsets (n=11, mean ± SD). Unstimulated samples were used for analysis of basal level. The transformed ratio was calculated as described before.

Significant differences were calculated by one sample t test to the normalized $CD21^{pos}$ $CD86^{neg}$ B cells and one-way ANOVA with Tukey´s multiple comparisons for the other 3 groups. Asterisks represent: *p ≤ 0.05.

Phosphorylation of ERK and NF-ĸB-p65 was analyzed after 3, 15 and 30 min of CD40L stimulation. After 15 min, $CD21^{pos}$ $CD86^{neg}$ B cells have the strongest increase in both molecules (Figure 34, upper and lower middle panels). Nevertheless, the phosphorylation of ERK reached a maximum after 15 min of CD40L stimulation, which occurred later than that observed by cross-linking of BCR (Figure 30, pERK, left panel -3min-). At this time (15 min) $CD21^{low}$ $CD86^{pos}$ B cells had significantly less CD40L-induced pERK (p=0.0148) and decreased NF-ĸB-p65 (p=0.3721) compared to $CD21^{pos}$ $CD86^{neg}$ B cells (Figure 34 middle panels). Mean relative MFI levels of pERK and NF-ĸB-p65 in $CD21^{low}$ $CD86^{pos}$ B cells were 94% and 63.1% lower than in $CD21^{pos}$ $CD86^{neg}$ B cells, respectively. At this time-point $CD21^{low}$ $CD86^{neg}$ B cells had also significantly less CD40L-induced NF-ĸB-p65 (p=0.0421) and less pERK (p=0.2177) compared to $CD21^{pos}$ $CD86^{neg}$ B cells (Figure 34, middle panels). A similar pattern was seen after 30 min stimulation. Interestingly, in $CD21^{low}$ $CD86^{pos}$ cells phosphorylation pattern of NF-ĸB-p65 over the time of stimulation was highly heterogeneous among donors. The phosphorylation of NF-ĸB-p65 was bimodal, with some responding very quickly and others not responding at all. This could suggest that CD40L-induced phosphorylation of NF-ĸB-p65 might be differentially regulated in different subsets of $CD21^{low}$ $CD86^{pos}$ cells e.g. IgD^{pos} vs. IgD^{neg} subsets. Therefore, no significant differences were observed when compared to $CD21^{pos}$ $CD86^{neg}$ B cells (Figure 34, lower panels). Altogether, CD40L signaling was impaired in $CD21^{low}$ B-cell subsets compared to $CD21^{pos}$ $CD86^{neg}$ B cells.

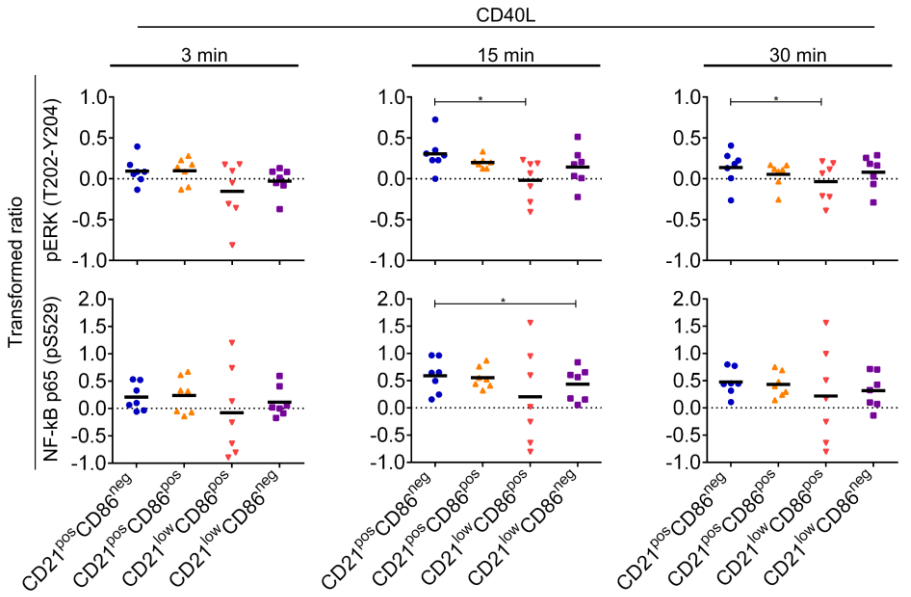

Figure 34. Impaired phosphorylation of pERK and NF-kB-p65 after CD40L stimulation in CD21^{low} B-cell subsets

Purified B cells from healthy donors were stimulated with CD40L for 3, 15 and 30 minutes and the expression of pERK and NF-kB-p65 was measured by flow cytometry. Shown are scatter plots of the differences in the response after CD40L stimulation among the four B-cell subsets defined by the expression of CD21 and CD86 (n=7, mean). Changes in MFI were calculated as described above and expressed as transformed ratio normalized to time-point 0 (before stimulation) of the corresponding sample. Significant differences were calculated by one-way ANOVA with Dunnet´s multiple comparisons test to CD21^{pos} CD86^{low} and adjusted p value. Asterisks represent: *p ≤ 0.05.

3.9 Combined CD40 engagement and BCR stimulation restored signaling in CD21^{low} CD86^{pos} subset

BCR signaling by presentation of antigenic peptides by T cells to mature B cells usually leads to engagement of CD40, which in turn promotes GC formation and differentiation (Calderhead et al. 2000). Therefore, an experiment to identify cross-talk between these two pathways was performed. Purified B cells were stimulated with a combination of anti-IgM and cross-linked, multimerized soluble CD40L for 0, 3, 15 and 30 min (n=6). As previously described, IgM stimulation induced considerable and sustained phosphorylation of ZAP70/SYK and ERK on CD21^{pos} CD86^{low} B cells but not on the other subsets (Figure 30, ZAP70/SYK and ERK panels). In contrast, combination of BCR + CD40 signaling restored pZAP70/SYK in CD21^{pos} CD86^{pos} B cells after 3 min stimulation (Figure 35, upper left panel). Signaling was sustained until 15 min and lost after 30 min stimulation (Figure 35, upper middle and right panels respectively). In CD21^{low} CD86^{pos} B-cell subset, combined stimulation induced low phosphorylation of ZAP70/SYK (Figure 35, upper left panel -3 min-) that was not different to that observed by BCR cross-linking alone (Figure 30, upper left panel). Interestingly, phosphorylation was sustained and increased with time, after 30 min reaching 3.8 times higher levels than that observed by anti-IgM stimulation alone (Figure 35 and Figure 30 respectively, upper right panels). In this subset, combination of both stimuli induced a delayed but great phosphorylation of BTK (Figure 35, BTK panels) that was not observed by BCR cross-linking alone (Figure 30, BTK panels). In a similar way, after 30 min, ERK was phosphorylated.

Doble-negative CD21^{low} CD86^{neg} B cells had a delayed phosphorylation of ZAP70/SYK and BTK that was much more pronounced than that observed by BCR-cross linking alone (Figure 35, ZAP70/SYK and BTK panels).

Finally, NF-kB-p65 was phosphorylated in all subsets but to a lesser extent on CD21^{pos} CD86^{pos} B cells (Figure 35, NF-kB-p65 middle and right panel; p=0.0377 and p=0.0355 respectively).

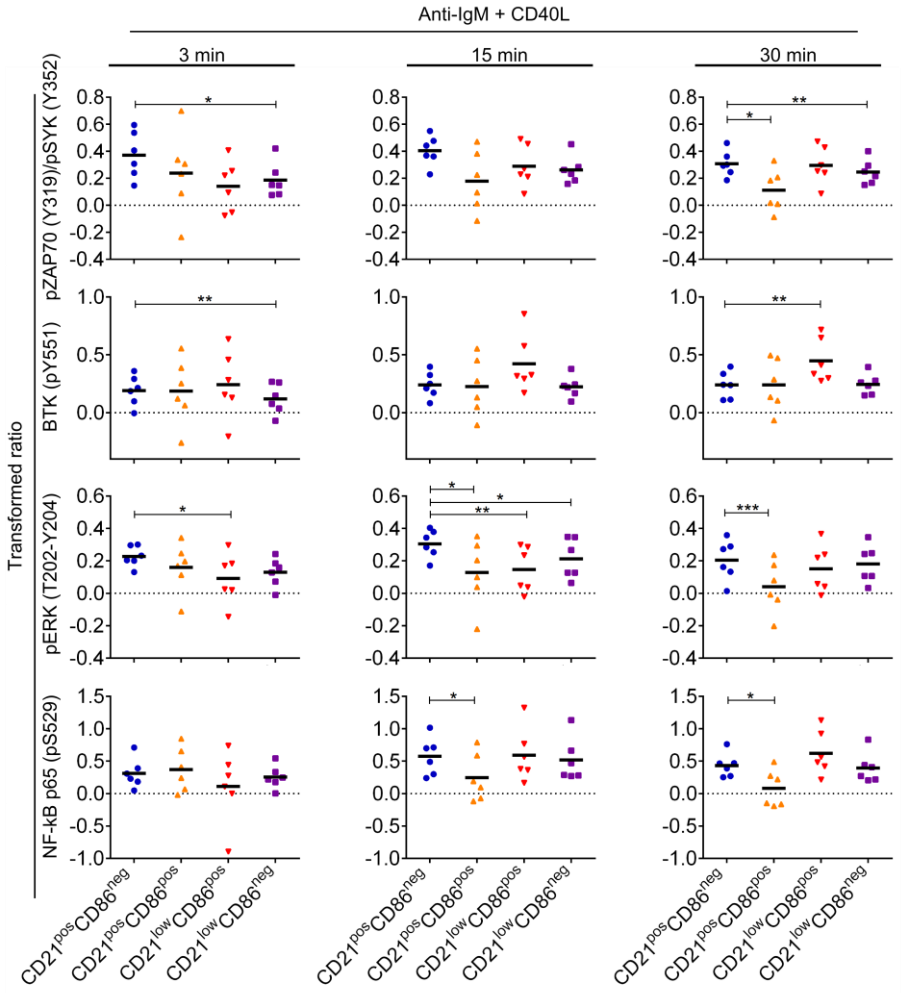

Figure 35. Combination of BCR and CD40 ligation restored signaling on CD21^{low} CD86^{pos} B cells

Purified B cells from healthy donors were stimulated with a combination of CD40L and anti-IgM for 3, 15 and 30 minutes and the expression of phospho-proteins was measured by flow cytometry. Shown are scatter plots of the differences in the response after stimulation among the 4 B-cell subsets defined by the expression of CD21 and CD86 (n=6, mean). Changes in MFI were calculated as described above and expressed as transformed ratio normalized to time-point 0 (before stimulation) of the corresponding sample. Significant differences were calculated by one-way ANOVA with Dunnet´s multiple comparisons test to $CD21^{pos}$ $CD86^{neg}$ and adjusted p value. Asterisks represent: *p ≤ 0.05, ** p ≤ 0.01, *** p ≤ 0.001, **** p ≤ 0.0001.

3.10 CD21 and CD86 delineated four functionally distinct peripheral blood B-cell subsets

The phenotypic and functional characteristics described so far, suggest that peripheral blood B-cell subsets defined by the expression of CD21 and CD86 represent four functionally distinct B-cell subsets. Figure 36 summarizes the findings of the phenotypic and functional features of the four subsets. They differ in terms of the expression of activation and costimulatory molecules, cell size, proliferative status, antigen presentation capacity and responsiveness to BCR stimulation measured by Ca^{2+} flux and phospho-specific flow cytometric profiling. The figure suggests a hypothetical model for their function-based categorization. The majority of B cells consist of the $CD21^{pos}$ $CD86^{neg}$ B-cell subset, which is mostly composed of conventional resting B cells and is therefore subsequently abbreviated as B_{conv}. After short activation, B_{conv} up-regulate costimulatory molecules and become $CD21^{pos}$ $CD86^{pos}$ B cells that seem to represent recently activated B cells (B_{react}), which - after prolonged activation - differentiate into highly immunostimulatory, antigen-experienced $CD21^{low}$ $CD86^{pos}$ B cells (B_{APC}). On the contrary, $CD21^{low}$ $CD86^{neg}$ B cells appear to be functionally inactivated B cells (B_{inact}). The model is consistent with the

in vitro results that suggest that CD21^{low} CD86^{pos} highly immunostimulatory B cells can arise from resting B cells driven by prolonged BCR and CD40L stimulation (Figure 5C; section 1.5). However, in vivo the origin of CD21^{low} B-cell subsets remains unclear.

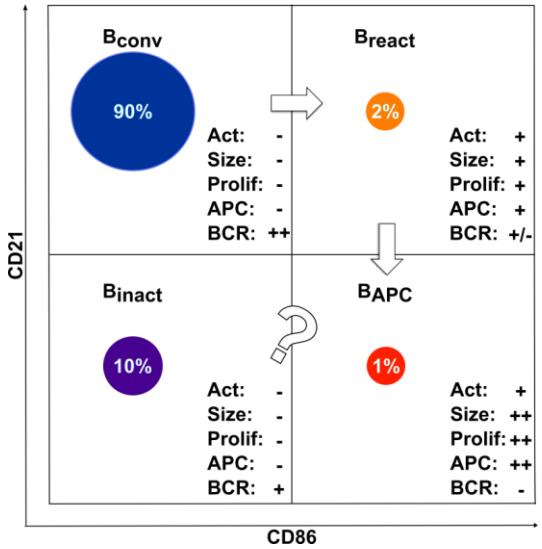

Figure 36. Hypothetical model for the function-based categorization of B-cell subsets divided by the expression of CD21 and CD86

Summary of the similarities and differences found in the four B-cell subsets in terms of activation (Act), cell size (size), proliferative status (Prolif), antigen presentation capacity (APC) and responsiveness to BCR stimulation (BCR). The model suggests that B_{conv}, which are conventional resting B cells after short-term activation become B_{react}, which in turn after prolonged stimulation downregulate CD21 and become B_{APC}. B_{inact} have features of inactivated cells.

3.11 B_{APC} were increased following vaccination

In order to better understand the changes in B-cell subsets in response to an antigenic challenge, peripheral blood from healthy donors before and after vaccination with either influenza or hepatitis B vaccine was obtained (n=8). Following vaccination there was a significant increase in the frequency of circulating B_{APC} (p=0.0243) (Figure 37A). The increase was only transient and occurred within a short time window of 7 days after vaccination. All other B-cell subsets remained unchanged throughout the first two weeks (Figure 37A). This vaccine-induced surge in B_{APC} suggested that this B-cell subset plays a role in the initiation and regulation of the normal immune response to foreign antigens. In order to confirm the results, one year later with the seasonal influenza vaccination, a cohort with 10 healthy donors was evaluated before and one week after vaccination. Figure 37B shows that effectively, after 7 days of antigenic challenge, frequency of B_{APC} increased. It might be that the time frame for increase in the frequency of B_{react} was lost since this might happen shortly after vaccination.

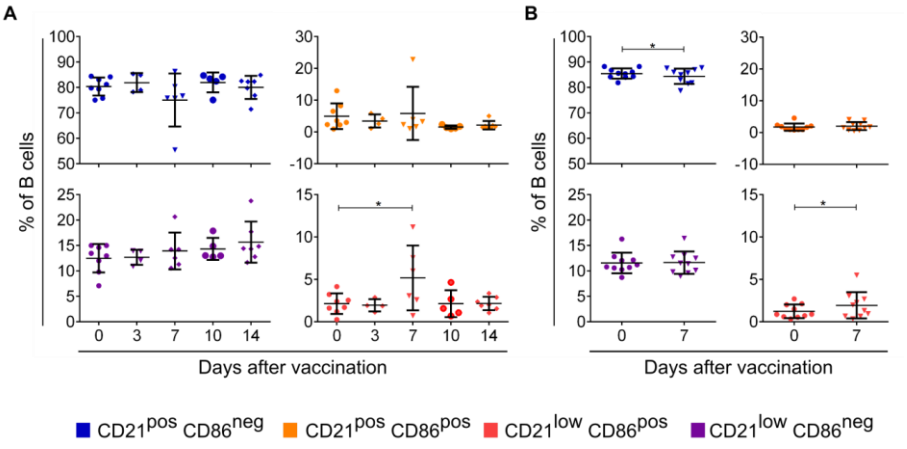

Figure 37. B_{APC} were increased following vaccination

Peripheral blood from healthy donors was collected before and after 3, 7, 10 and 14 days of vaccine. (A) Scatter plots showing the dynamics in cell frequency after vaccination with either influenza (n=7) or hepatitis B (n=1) vaccine. Significant differences were calculated by one-way ANOVA with Tukey´s multiple comparisons test. Asterisks represent: *p ≤ 0.05. (B) Scatter plots from a validation cohort to verify increase of B_{APC} after 7 days of influenza vaccination (n=10, mean ± SD). Significant differences were calculated to day 0 (before vaccination) by paired t-test. Exact p values are given in the text.

3.12 EBV-infected human B-lymphocytes gain a $CD21^{low}$ $CD86^{pos}$ phenotype in vivo

The experiments and analysis performed up to now were done in healthy donors. Therefore, to determine whether and how the four B-cell subsets are disturbed in human disease, peripheral blood from patients with clinically relevant immune-related conditions were analyzed.

As described in Figure 36, B cell activation through CD40 ligation leads to changes in phenotype that first generated $CD21^{pos}$ $CD86^{pos}$ and after prolonged activation $CD21^{low}$ $CD86^{pos}$ B cells. The central role of CD40-mediated signaling for B cell activation and survival is further supported by the fact that EBV hijacks the B cell signaling machinery to immortalize B cells and promote its own survival and spread (Imadome et al. 2003). EBV is a human lymphotropic herpesvirus that is associated with several malignancies such as infectious mononucleosis and lymphoproliferative malignancies such as HIV-related lymphoma, Burkitt lymphoma, Hodgkin disease, and nasopharyngeal carcinoma (Adler et al. 2002). B lymphocytes are infected by EBV through the binding of gp350/220 to CD21, which is followed by internalization of the virus (Roberts et al. 1996). Transformation of B cells by EBV occurs via LMP1 (latent membrane protein-1), which is encoded by the virus and mimics CD40-

meadiated signals (Uchida et al. 1999, Peters et al. 2010). In addition LMP2A provides developmental and survival advantage through a surrogate BCR-like signal to infected B cells (Anderson and Longnecker 2008).

It was thus a logical next step to investigate the B cells in the peripheral blood of patients with EBV reactivation. Since EBV-infected B cells become activated and are efficient APCs, they are quickly eliminated by host T cells. Therefore, EBV transformed B cells would hence only be expected to be present in immunocompromised individuals (Thorley-Lawson 2005). Consequently, peripheral blood B cells of patients, who underwent hematopoietic stem cell transplantation and had an elevated level of EBV copy numbers detected during routine monitoring, were analyzed. In some severely immune compromised patients, who developed an EBV-reactivation after allogeneic stem cell transplantation, expansion of a $CD21^{low}$ $CD86^{pos}$ B-cell population was indeed identified (37.30 % ± 34.18) (Figure 38). This subpopulation showed similar phenotypic features as in vitro generated long-term CD40-activated B cells and the $CD21^{low}$ $CD86^{pos}$ B-cell population that was described early in this work in peripheral blood from healthy subjects.

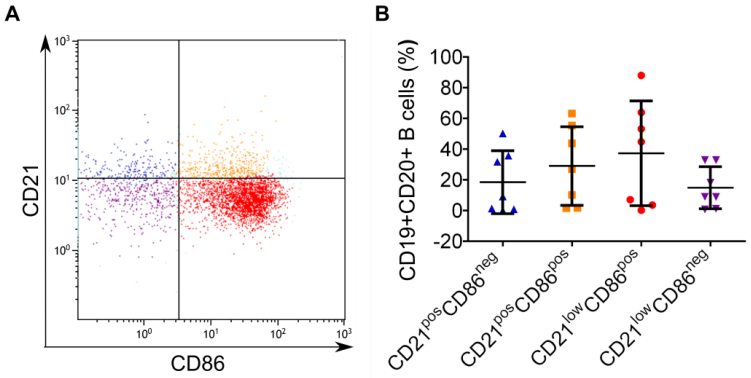

Figure 38. B_{APC} were increased in patients with EBV reactivation following allogeneic stem cell transplantation

Results of the analysis of peripheral blood from 7 patients with EBV reactivation following allogeneic stem cell transplantation. (A) Exemplary FACS plot of a patient with EBV-reactivation after allogeneic stem cell transplantation. (B) Scatter plot of the frequency of B-cell subsets in patients with EBV-reactivation after allogeneic stem cell transplantation (n=7, mean ± SD).

3.13 The balance of CD21^{low} B cells was altered in patients with inflammatory diseases

In order to continue the analysis of the B-cell subset homeostasis during disease, some prototypic inflammatory conditions were chosen. As a model for an acute inflammatory condition, patients with acute traumatic fractures were selected (Bastian et al. 2011, Claes et al. 2012). Compared to healthy controls peripheral blood of patients with acute traumatic fractures contained an increased percentage of the B_{react} B-cell subset (p= 0.0018, n=20) (Figure 39).

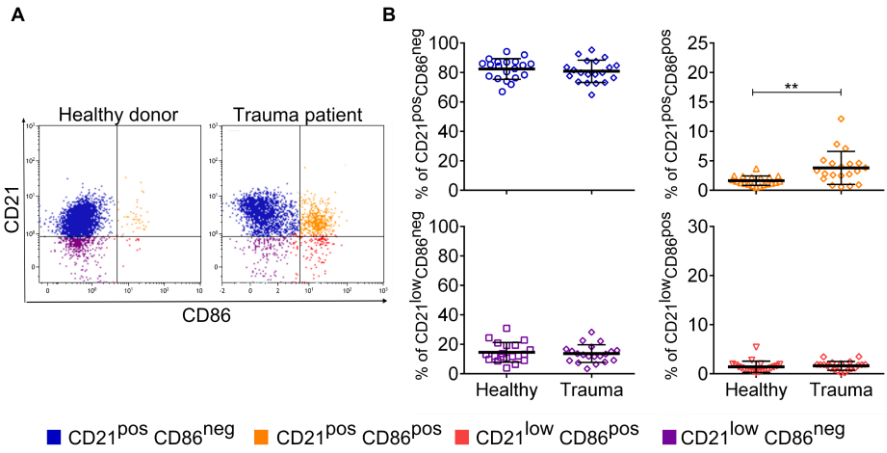

Figure 39. B_{react} were increased in patients with acute traumatic fractures

Results of the analysis of peripheral blood of 20 patients with acute traumatic fractures compared with healthy donors. (A) Exemplary FACS plot of a healthy donor and a patient with a trauma, both donors are male. (B) Scatter plot of the frequency of B-cell subsets in patients compared to healthy donors (n=20, mean ± SD). Significant differences were calculated by unpaired t-test. Exact p values are given in the text.

Rheumatoid arthritis is one of the most common autoimmune diseases and affects approximately 1% of the world's population (Finnegan et al. 2012). Active rheumatoid arthritis is associated with profound inflammation and autoimmune destruction of joints and other tissues. An important role that B cells plays in the pathogenesis of rheumatoid arthritis has beed demonstrated by the observation that B cell depletion with the monoclonal anti-CD20 antibody rituximab has proven to be an effective therapeutic approach for this autoimmune disease (Edwards et al. 2004, Samuels et al. 2005). Hence, frequency of the four B-cell subsets in rheumatoid arthritis was analyzed. Patients with rheumatoid arthritis had a higher frequency of $CD21^{pos}$ $CD86^{pos}$ B_{react} (3.233 % ± 3.916) compared to controls (1.552% ± 0.9637) (p=0.0055) (Figure 40A and B). Moreover, frequency of $CD21^{low}$ $CD86^{pos}$ B_{APC} (2.909 % ± 3.828) was also increased in arthritis patients compared to controls (1.206 % ± 0.988) (p=0.0044) (Figure 40A and B). Interestingly, synovial B cells in the joint fluid of two patients with rheumatoid arthritis consisted to a large part of B_{APC} (62.62 % ± 9.914) (Figure 40C).

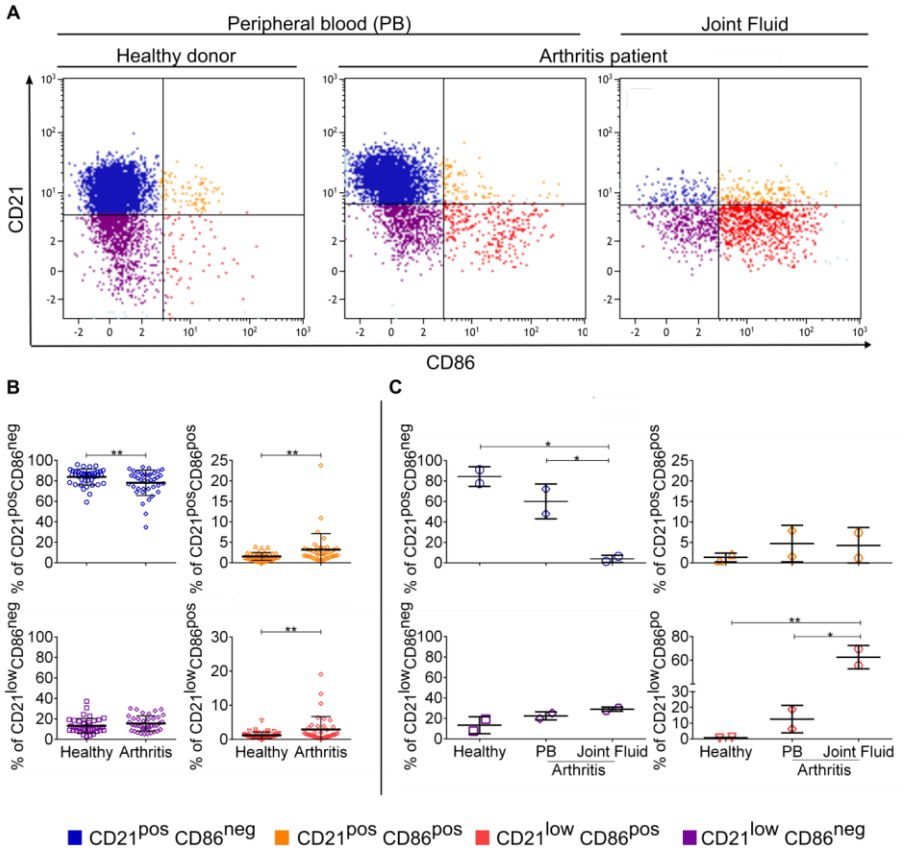

Figure 40. B_{react} and B_{APC} were increased in patients with rheumatoid arthritis

Results of the analysis of peripheral blood of 39 patients with rheumatoid arthritis (2 patients from whom was possible to obtain fluid from the joint) compared to healthy donors. (A) Exemplary FACS plot of a healthy donor, a patient with arthritis and joint fluid from the same patient, both donors were male and approximately of the same age (21 and 23 years respectively). (B) Scatter plot of the frequency of B-cell subsets in patients compared to healthy donors (n=39, mean ± SD). Significant differences were calculated by unpaired t-test. Exact p values are given in the text. (C) Scatter plot of the frequency of B-cell subsets in 2 healthy donors, 2 patients peripheral blood (PB) and joint fluid from the same patients (n=2, mean ± SD). Significant

differences were calculated by one-way ANOVA with Tukey´s multiple comparisons test. Asterisks represent: *$p \leq 0.05$, ** $p \leq 0.01$.

Several recent papers have highlighted an unexpected role for B cells in solid tumors. It has been described in colorectal cancer that B cells constitute a significant proportion of the infiltrate within the tumor microenvironment (Shimabukuro-Vornhagen et al. 2014). Analysis of 22 tumor specimens from patients with colorectal cancers (CRC) revealed that $CD21^{low}$ $CD86^{pos}$, $CD21^{pos}$ $CD86^{pos}$ and $CD21^{low}$ $CD86^{neg}$ B cells were enriched within the tumor tissue compared to the peripheral blood of colorectal cancer patients and healthy controls (Figure 41 A and B).

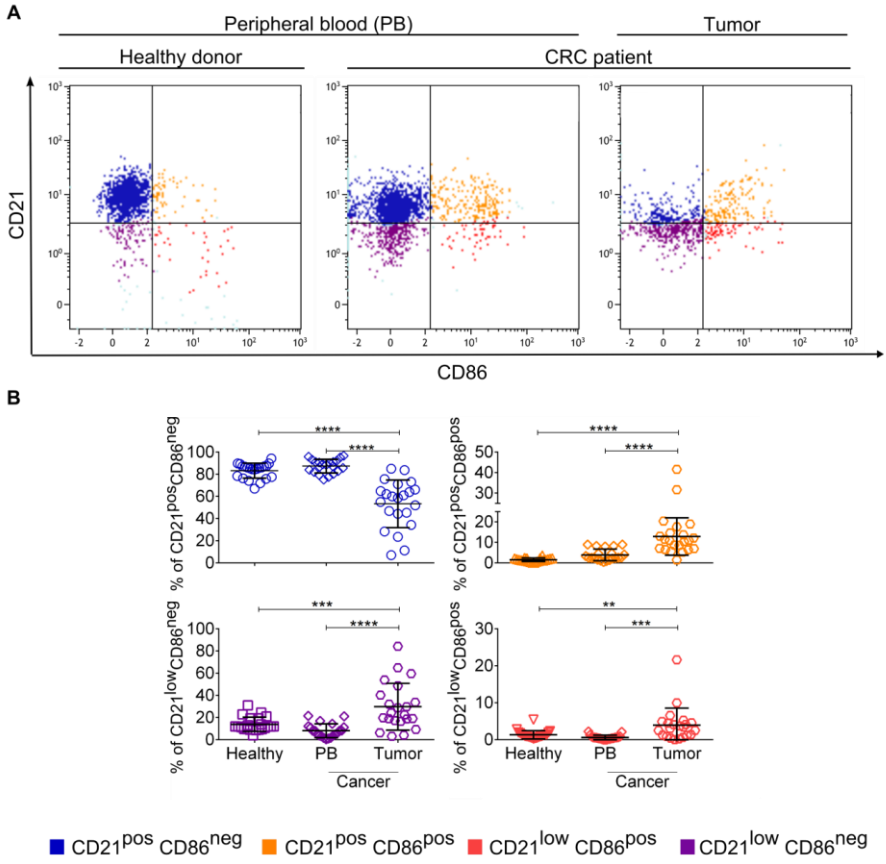

Figure 41. B_{react}, B_{APC} and B_{inact} were increased in tumors specimens of CRC patients

Results of the analysis of peripheral blood and tumor samples of 22 patients with CRC cancer compared to healthy donors. (A) Exemplary FACS plot of the peripheral B cells from a healthy donor, a patient with CRC and B cells from the tumor of the same patient, both donors were male and approximately of the same age (57 and 70 years respectively). (B) Scatter plot of the frequency of B-cell subsets in patients peripheral blood and tumor compared to healthy donors (n=22, mean ± SD). Significant differences were calculated by one-way ANOVA with Tukey´s multiple comparisons test. Asterisks represent: * $p \leq 0.05$, ** $p \leq 0.01$, *** $p \leq 0.001$, **** $p \leq 0.0001$.

Discussion

4 DISCUSSION

To date, most of the studies have been focused on the role of antigen presentation by B cells in mouse models (Lanzavecchia 1985, Janeway et al. 1987, Ron and Sprent 1987, Rivera et al. 2001, Crawford et al. 2006, Bouaziz et al. 2007). In humans, the study of the role that B lymphocytes play as antigen-presenting cells has been hampered by the lack of a phenotypically well defined subset. Therefore, the functional and phenotypic characterization of the recently discovered human B cell subset resembling CD40B cells and the establishment of a new soluble system to generate immunostimulatory B cells, helped to elucidate the role of this novel population in the human immune system both in health and disease.

4.1 Soluble rCD40L system to generate antigen-presenting B cells

During the past years, several in vitro models have been established to generate potent antigen-presenting B cells via activation through CD40. The most reliable and potent systems to generate CD40-activated B cells turned out to be those that express the ligand on a cell surface (Banchereau et al. 1991, Banchereau and Rousset 1991, Schultze et al. 1997, Liebig et al. 2009). Nevertheless, a cell-standing CD40L system containing xenogeneic components has several disadvantages. It not only incorporates a source of contamination that could interfere with experimental observations but also represents a limitation to transfer the system to the clinical settings.

In this work, the tested soluble human rCD40L proved to be as potent as the well-known NIH3T3/tCD40L system at inducing activation and proliferation of B cells with the advantage of elimination of xenogeneic contaminations. Therefore, development of this efficient rCD40L is an important step to facilitate the potential

use of CD40B cells in human clinical trials. Moreover, previously described features of CD40B cells were confirmed by the characterization of activated B cells generated by both CD40L systems. They both up-regulated the expression of HLA-DR, CD80 and CD86 and had high capacity to induce activation and proliferation of allogeneic T cells (Schultze et al. 1997).

The importance of clustering of the CD40L was evidenced by low proliferation rate of B cells induced by CD40L in the absence of the cross-linking antibody. Although CD40L is found in vivo on the cell surface as homotrimer, it has been shown that homotrimerization is necessary but not sufficient for maximal activity (Haswell et al. 2001). Therefore, clustering of CD40 is required for optimal CD40 signaling (Fanslow et al. 1994, Morris et al. 1999, Stone et al. 2006, Naito et al. 2013).

Moreover, by using this in vitro model for generation of CD40B cells it was possible to compare and confirm similarities between B_{APC} and long term activated CD40B cells. They resemble each other in terms of high expression of costimulatory molecules CD80 and CD86, low expression of CD21 and CD32 and more importantly, both are highly efficient antigen-presenting B cells and induced activation and expansion of T cells. All these features are recognized to be characteristics of professional antigen-presenting B cells (Rodríguez-Pinto 2005). Therefore, these results suggest that CD40-activated human B cells represent a valuable in vitro model to study the properties of B_{APC}.

Additionally, in the future, this in vitro model could be applied to develop B_{APC}-based targeted therapies. In diseases such as arthritis where a high frequency of B_{APCs} was observed, therapeutic agents that specifically deplete these cells might result in the amelioration of the symptoms.

4.2 The CD21^{low} population

To date, populations characterized by a low expression of CD21 have been described in several pathological conditions such as CVID, SLE, hepatitis B, viremic HIV infection and rheumatoid arthritis (Warnatz et al. 2002, Wehr et al. 2004, Moir et al. 2008, Rakhmanov et al. 2009, Isnardi et al. 2010, Charles et al. 2011, Visentini et al. 2012). An increase in the frequency of CD21^{low} B cells is the reflection of the disturbance in the homeostasis of circulating subsets in such diseases. This homeostasis is maintained under physiological conditions by controlled pro- and anti-inflammatory forces. When the balance is disrupted, alterations in the frequency of subsets are evident.

Most of the functional assays done to characterize the CD21^{low} population described in such diseases revealed that they are functionally attenuated (Rakhmanov et al. 2009), anergic (Isnardi et al. 2010) or exhausted (Moir et al. 2008) B cells. Nevertheless, none of the groups studied the function of CD21^{low} population in healthy individuals.

In this study, healthy donor-derived peripheral blood B cells classified in four subsets according to the expression of CD21 and CD86 were characterized phenotypically and functionally. Low frequencies of CD21^{low} B cells were detected in healthy donors, but surprisingly, these B cells were further separated into two functionally different subpopulations by the expression of CD86.

4.3 Functional and phenotypic characterization of B cells classified by the expression of CD21 and CD86 revealed striking differences among subsets

In addition to the differential expression of CD21 and CD86 surface molecules, B-cell subsets differed in several other features.

4.3.1 $CD21^{pos}$ $CD86^{neg}$ B_{conv} subset

Like naive B cells, $CD21^{pos}$ $CD86^{neg}$ B_{conv} cells were characterized by a small cell size, low frequency of $Ki\text{-}67^{+}$ cycling cells, absence of expression of activation, costimulatory and memory markers and a non-switched IgM^{pos} IgD^{pos} phenotype (Duty et al. 2009). Furthermore, they were positive for the BCR-associated regulator CD22 that is expressed on mature B cells (Tedder et al. 1997). Moreover, since they expressed neither the T cell costimulatory molecule CD80 nor CD86, when cultivated with autologous T cells they induced very low stimulation. As expected B_{conv} showed low basal calcium and phosphorylation levels and a robust response after stimulation evidenced by calcium and phosphorylation signaling (Duty et al. 2009).

These phenotypic and functional characteristics corresponded to mature resting B cells that were recirculating throughout the body and had not yet encounter their cognate antigen.

4.3.2 $CD21^{pos}$ $CD86^{pos}$ B_{react} subset

In agreement with previous data on activated B cells, double positive B_{react} subset showed a characteristic phenotype with increased expression of CD80, CD86, CD43 and HLA-DR (Sarkar et al. 1980, Azuma et al. 1993, Boussiotis et al. 1993, Griffin

et al. 2011). Up-regulation of these molecules coincided with an increased cell size and a higher frequency of proliferating Ki-67^{+} cells compared to other populations (Sarkar et al. 1980). Additionally, most of B_{react} cells were CD27 positive. Interestingly, most of the cells in the B_{react} subset had a "natural effector" phenotype described by Brekowska et al., by expression of CD27^{+} IgM^{pos} IgD^{pos} B cells (Berkowska et al. 2011). Berkowska et al., characterized these cells by a limited proliferation, reduced replication history and SHM levels compared to GC B cells. They also found them in CD40L-deficient patients. As a result, the authors concluded that this phenotype is expressed by B cells that were derived (at least in part) from systemic GC-independent responses. However, the origin of these cells is controversial, since another group has reported that they could be derived from T-cell-dependent GC reactions (Seifert and Kuppers 2009). From the in vitro results of CD40L activation obtained in this study, it could be hypothesized that B_{react} are activated B cells that had recently encountered their cognate antigen. They are probably trafficking towards the secondary lymphoid organs, where usually they encounter both antigen bound to follicular DCs and CD40L-mediated T-cell help. At this point, at least part of them will undergo further selection and class-switch recombination in the GC reaction.

Consistently, B_{react} expressed higher levels of receptors CD62L, CCR7 and CXCR4 than B_{APC} and B_{inact} which have been associated with migration to lymph nodes (Butcher and Picker 1996, Gunn et al. 1999, Hiller and Chu 2011). Additionally, B_{react} expressed CCR6 which has been shown to be transiently up-regulated after activation (Wiede et al. 2013). Moreover, and consistent with the hypothesis that the immunostimulatory activity increases with the duration of the stimulus and decreasing expression of CD21, the antigen-presenting capacity of B_{react} was intermediate between B_{conv} and B_{APC}.

Analysis of the basal phosphorylation in B_{react} showed active ZAP70/SYK, BTK and pERK, which might suggest that they are actively in cell cycle (Gururajan et al. 2006). This is consistent with the high rate of proliferation observed by Ki-67 analysis. In this subset, changes in phosphorylation after stimulation were lower compared to B_{conv} in part because these cells had a higher basal level of activation.

Moreover, since Ca^{2+} signaling was not impaired in this B-cell subset, it can be suggested that the constitutive phosphorylation of the analyzed elements was independent of PLCɣ2. However, further signaling analysis have to be performed to elucidate the pathway that controls such activated state.

Taken together, these characteristics might suggest that the B_{react} subset developmentally represents a transitional stage between B_{conv} and B_{APC}.

4.3.3 $CD21^{low}$ $CD86^{pos}$ B_{APC} subset

$CD21^{low}$ $CD86^{pos}$ B_{APC} subset shares some characteristics with B_{react} cells. They both had increased cell size and a higher proportion of proliferating cells compared to the B_{conv} and B_{inact} subsets. They both over-express CD80, CD86, CD43 and HLA-DR consistent with an activated phenotype. These characteristics are in agreement with the in vitro results of CD40B cells (section 3.1). Therefore, $CD21^{low}$ $CD86^{pos}$ B_{APC} seems to represent activated B cells that have undergone continuous or repeated stimulation. Presumably, constant stimulation through BCR and the influence of other pro-inflamatory signals, such as CD40 ligation, could have lead to this activated phenotype.

It is probable that the effect of the activation stimuli was potentiated by the down-modulation of inhibitory receptors i.e. CD32 (FcγRIIb) and CD22, seen on this

subset. Thus, reduced levels of these proteins would have resulted in a lower threshold for B cell activation. Consistently, recent data suggests that the aberrant expression and function of CD32 on B cells is important in the pathogenesis of various autoimmune diseases (Nimmerjahn and Ravetch 2008, Smith and Clatworthy 2010). More specifically, in a mouse model was shown that CD32 gene deficiency increases both the susceptibility to autoimmunity and disease severity (Bolland and Ravetch 2000, Nakamura et al. 2003).

In line with the hypothesis that B_{APC} underwent several rounds of stimulation, most of the cells in this subset expressed CD27, recognized to be a marker for human memory B cells (Agematsu et al. 2000). Since, memory B cells are mainly generated in secondary lymphoid organs in GC reactions after antigen encounter, it can be suggested that most of the B_{APC} are antigen experienced. Furthermore, the analysis of their class-switched profile confirmed this result. Classical memory B cells are $CD27^{+}$ class-switched IgM^{neg} IgD^{neg} that are derived from T cell-dependent responses, have high levels of activation and costimulatory molecules and an extensive replication history (Good et al. 2009, Berkowska et al. 2011). Such characteristics correspond to the majority of B_{APC}, which as proposed by van Zelm et al., are features of cells that already underwent additional immune responses in secondary and tertiary antigen encounters (van Zelm et al. 2007). Interestingly, the switched IgM^{pos} B_{APC} subset could either arise through a GC-independent route, as proposed by Taylor et al., or as described by Klein et al., they could be early emigrants from a primary GC response without participating long enough in the reaction for isotype switching to occur (Klein et al. 1997, Taylor et al. 2012). Either way, B_{APC} subset seems to be composed of antigen-experienced cells.

Excitingly, an additional feature shared by CD40B cells and B_{APC} was detected. They both displayed a higher expression of the integrins CD11a/CD18 and CD11b which are involved in migration from peripheral blood to sites of inflammation (Barrett et al. 1991, Kawai et al. 2011). These results suggest that migration capacity of B_{APC} out of peripheral blood is markedly superior compared to the other three B-cell subsets. However, based on their chemokine receptor profile, B_{APC} appears to be poised to home to sites of inflammation in peripheral tissues, while CD40B cells have been described to home to secondary lymphoid organs (Klein-González et al. 2010). In this way, B_{APC} expressed high levels of CXCR3, CD39, CD18, CD11a and CD11b and low levels of the lymph node homing receptors CCR7, CXCR4 and CD62L. Interestingly and consistent with the notion that B_{APC} home to peripheral tissue, it was found in the synovial fluid from two rheumatoid arthritis patients that the majority of the B cell infiltration was of the phenotype $CD21^{low}$ $CD86^{pos}$ B_{APC}. Consistently, the frequency of these B cells was also increased in tumors of CRC patients.

Therefore, B_{APC} possessed the phenotypic characteristics of antigen-experienced post-germinal center B cells. They might represent a transitional stage between GC B cells and plasma cells. Besides, they still express CD20, which is lost during differentiation at the plasmablast stage (Jego, Bataille et al. 2001) and they did not express CD138 (data not shown), which is acquired by differentiated plasma cells (Klein and Dalla-Favera 2007). Antibody secretion by B_{APC} remains to be tested.

In agreement with the fact that B_{APC} expressed more costimulatory molecules than other subsets, it was not surprising that they exhibited the most efficient antigen-presenting capacity as tested by means of an autologous MLR. This is consistent with the in vitro findings described here and by others that showed that CD40B cells possessed a potent immunostimulatory activity (Faassen et al. 1995).

Thus, $CD21^{low}$ $CD86^{pos}$ B_{APC} subset efficiently stimulated autologous T cells. More importantly, this functional characteristic was mainly restricted to the $CD21^{low}$ $CD86^{pos}$ B-cell subset.

Signaling analysis after BCR-stimulation revealed that B_{APC} as well as B_{inact} not only had an increased basal calcium level but a poor calcium release after further BCR-stimulation. This is in line with one study where analysis of calcium signaling on $CD21^{low}$ B cells from healthy donors revealed that this population had physiologically lower Ca^{2+} signaling response than the naïve IgD^{pos} B cells after BCR-crosslinking (Foerster et al. 2010). Since this attenuated response was not seen in the other two B-cell subsets (B_{react} and B_{conv}) it is thus tempting to speculate that the defect in the mechanism regulating Ca^{2+} in $CD21^{low}$ subpopulations is specific for mature, class-switched B cells. The low calcium response seen in these subsets, cannot be attributed to the low expression of CD21 itself since Thiel et al. reported that a patient with a genetic CD21 deficiency that abolished surface expression of the protein had normal calcium flux (Thiel et al. 2012). They found that in CD21-deficient B cells, calcium flux triggered by C3d-containing immune-complex was completely abolished while the response triggered directly through the BCR alone was completely normal, indicating that CD21 is not required for generating a Ca^{2+} signal.

Moreover, as previously described by Galibert et al., BCR stimulation of long term activated CD40B cells induced a substantial calcium release comparable to that of non-activated B cells, even though like B_{APC}, CD40B cells exhibited higher basal calcium levels (Galibert et al. 1996). These results suggest that the proximal events of BCR signaling transduction, e.g. activation of PLCγ2, are operative in CD40-activated B cells, which might not be the case for the B_{APC} subset.

One potential mechanism that could account for reduced BCR responsiveness of B_{APC} could be a high constitutive downstream signaling. To address this issue, specific mediators of intracellular signaling were analyzed by multi-parameter phosphoflow and revealed that B_{APC} were less responsive to BCR stimulation compared to B_{conv}. This result coupled to the high calcium baseline and low calcium release suggested signs of previous activation. However, activation should be reflected in basal phosphorylation of intracellular mediators. Surprisingly, analysis of the baseline activation of intracellular signaling elements did not provide evidence of constitutive activation in B_{APC} subset, but yet downstream signaling was interrupted as evidenced by the poor BCR-induced phosphorylation of ERK compared to B_{conv} cells. This phenomenon was not mediated by a high phosphatase activity, since treatment with H_2O_2 was not able to restore the BCR-signaling propagation in this subset. An additional explanation might be that signaling elements in $CD21^{low}$ $CD86^{pos}$ B_{APC} are being actively and continuously phosphorylated and dephosphorylated. To test this hypothesis, phospho-proteins were evaluated in the presence of pervanadate. Pervanadate is a rapidly acting phosphatase inhibitor (Wienands et al. 1996), which have been also shown to activate intracellular tyrosine kinases that are normally retained in inactivated state by dephosphorylation (Trudel et al. 1991, Teshima et al. 1994). Interestingly, pervanadate treatment increased the baseline level of pZAP70/SYK only in the B_{APC} subset. As proposed by Holodick et al., these results might suggest that ZAP70/SYK is being continually and rapidly phosphorylated, and just as rapidly dephosphorylated (Holodick et al. 2009). This suggests that in B_{APC}, phosphorylated ZAP70/SYK protein is persistently turning over and hence steadily signaling. Consistently, inhibition of ZAP70/SYK has shown promising results in rheumatoid arthritis patients characterized by B-cell hyperactivity (Ghosh and Tsokos 2010).

Since individual signaling pathways are not acting alone but interconnecting and influencing each other to lead to a biological response, cross-talk between BCR and CD40L stimulation was evaluated in the four B-cell subpopulations. When B cells were stimulated with CD40L alone, both $CD21^{low}$ subsets showed impaired signaling of the canonical pathway NF-κB (p65) and ERK. However, concurrent activation with both stimuli was able to restore signaling in $CD21^{low}$ subsets, which was translated in a delayed but greater phosphorylation of SYK, BTK, ERK and NF-κB-p65 that was higher on B_{APC} than in B_{inact}. This result indicates that B_{APC} exhibited a higher sensitivity to CD40-mediated signaling when combined with BCR stimulation. It might be that simultaneous stimulation activates an alternate pathway that circumvents the early events (i.e. calcium flux) that were shown to be disrupted in $CD21^{low}$ subsets to ultimately lead to phosphorylation of ERK and NF-κB. This is in line with a previous report in which an alternate pathway in PLCγ2-inhibited B cells stimulated with CD40L was described (Mizuno and Rothstein 2005). Collectively, the signaling assays demonstrate that B_{APC} are in an activated state and that the four B-cell subpopulations exhibited differential downstream activation of the signaling pathways.

4.3.4 $CD21^{low}$ $CD86^{neg}$ B_{inact} subset

$CD21^{low}$ $CD86^{neg}$ B_{inact} subset represented most of the $CD21^{low}$ B-cell compartment. In contrast to B_{APC}, they were characterized by a small cell size, low proliferative rate as measured by Ki-67 positivity, low expression of costimulatory molecules, high expression of CD32, down-regulation of trafficking molecules and a very low capacity to induced T cell activation.

The absence of chemokine and trafficking receptors was previously reported in $CD21^{low}$ anergic B cells, suggesting that down-regulation of these receptors is likely to exclude them from follicles, to recruit them in GCs or to favor their eventual elimination in specific compartments (Cyster et al. 1994, Cyster and Goodnow 1995, Isnardi et al. 2010). Altogether, B_{inact} subset expressed a set of molecules that might help to prevent their activation.

Most of these features have been associated with mouse anergic B cells (Cambier et al. 2007). In fact, an anergic, autoreactive $CD21^{low}$ population with these characteristics was previously described in CVID and SLE patients and in persons infected with HIV and HCV (Wehr et al. 2004, Moir et al. 2008, Rakhmanov et al. 2009, Charles et al. 2011). They represented a population of autoreactive B cells that escaped central tolerance mechanisms and were silenced in the periphery by an induced state of lethargy, probably as a result of an antigenic challenge (self- or viral) in the absence of costimulatory signals that sustained their activation (Cambier et al. 2007).

In mouse anergic B cells, down-regulation of CD21 was associated with an increased BCR signaling threshold and an inability to be activated (Hartley et al. 1993, Nguyen et al. 1997). Moreover, as reported by Lyubchenko et al., cross-linking of CD21 and BCR was enough to overcome B cell anergy (Lyubchenko et al. 2007). By using an Ars/A1 murine model of B cell anergy independent of CD21 down-regulation, they studied the effects of complement-mediated signaling in anergic B cells. They found that unlike BCR stimulation alone, BCR/CD21 costimulation of anergic Ars/A1 B cells led to calcium mobilization in vitro and the production of autoantibodies in vivo. These findings further suggest that CD21 down-regulation contributes to B cell anergy in mice and humans. In addition to the low expression of CD21, the up-regulation of the inhibitory cell surface receptor CD32 could as well be

influencing the functional consequences of the BCR signaling response (Nimmerjahn and Ravetch 2008).

Furthermore, B_{inact} cells were constitutively phosphorylated in tyrosine residues Y319 and Y352 on ZAP70/SYK compared to B_{conv} cells. This is in contrast to the results of Visentini et al., who described an exhausted marginal zone-like $CD21^{low}$ B-cell population with attenuated BCR signaling but constitutive activation of ERK in healthy donors as well as in hepatitis C virus (HCV)-associated mixed cryoglobulinemia (Visentini et al. 2012). However, their population was characterized by the expression of a V_H1-69-encoded idiotype and although they indicated to be a $CD21^{low}$ subset, it was actually a mixture of $CD21^{low}$ and $CD21^{pos}$ B cells. In the $CD21^{low}$ $CD86^{neg}$ B_{inact} subset, constitutive expression of ZAP70/SYK was not accompanied by constitutive expression of activated forms of signaling mediators that would be expected if phosphorylation of ZAP70/SYK were produced by cell "activation". Moreover, after BCR stimulation, downstream induced phosphorylation of ERK was triggered. For these reasons, the presence of pZAP70/SYK and the higher baseline Ca^{2+} level in this subset might be the reflection of isolated ZAP70/SYK activation, possibly as a result of aberrant Src family kinase activity, or as a reflection of previous activation events that have long since run their course and are no longer present. Consistently, overexpression of phosphatases evidenced by the restored BCR-signaling after H_2O_2 treatment might be the reason why constitutive activation of ZAP70/SYK was not inducing accumulation of pERK in this subset.

These results corroborate earlier findings that the $CD21^{low}$ B-cell subset predominantly consists of functionally impaired B cells with features consistent with an anergic or exhausted state. Therefore, $CD21^{low}$ $CD86^{neg}$ B cells seem to represent the healthy counterpart to the anergic-exhausted and expanded population

described by others in CVID, SLE, hepatitis B, viremic HIV infection and rheumatoid arthritis (Warnatz et al. 2002, Wehr et al. 2004, Moir et al. 2008, Rakhmanov et al. 2009, Isnardi et al. 2010, Charles et al. 2011, Visentini et al. 2012).

4.4 Calcium flux signaling in B cells after CD40L stimulation

There is little information available concerning the early events of signaling after CD40 ligation. Therefore, signaling of calcium was analyzed in the four B cell-subsets after CD40L stimulation. Interestingly, in this setting, CD40L acted independently of intracellular calcium release from endoplasmic stores and induced no calcium response in any of the studied B-cell populations.

These results were surprising since at least one study showed that binding of CD40 elicited PLCγ2 activation on B cells and increased IP3 kinase activity, which in turn is essential for calcium release from ER stores (Kashiwada et al. 1996). Nevertheless, studies done with $PI3K^{-/-}$ mice reported normal PLCγ2 phosphorylation after stimulation, although Ca^{2+} mobilization was only 25 % of normal (Clayton et al. 2002). Therefore, normal tyrosine phosphorylation of PLCγ2 does not necessarily imply full PLCγ2 activation. Additionally, another study showed that CD40 engagement on pro-B-, pre-B-I, pre-B-II, or activated mature tonsillar B cells but not on naïve mature B cells resulted in enhanced tyrosine phosphorylation and a rapid increase in the production of IP3 (Uckun et al. 1991). The CD40 receptor signaling they detected, occurred in buoyant tonsillar B cells consisting predominantly of IgM^{neg} GC B cells as well as in immature IgM^{neg} B-cell precursors, but not in strongly IgM^{pos} dense tonsillar B cells. This is consistent with another study, which showed that anti-CD40 mAb did not induce an increase in tyrosine phosphorylation in dense

tonsillar B cells even though this population is highly responsive to IgM stimulation (Lane et al. 1990).

Therefore, general conclusions should be taken with care, because most of the studies were performed with different cellular models. It might be that signaling through CD40L on B cells is dependent on the developmental as well as activation stage of the B-cell subset or that peripheral blood B cells are responding to CD40L in an independent fashion from calcium release from intracellular stores.

Interestingly, when a source of extracellular calcium was included, an increase in the Ca^{2+} response of B cells was observed in all the studied populations. This result suggests that the Ca^{2+} signaling after CD40L relies on mechanisms regulating Ca^{2+} influx from the extracellular space downstream of PLCγ2 activation and IP3 receptor-mediated release of Ca^{2+} from ER stores.

4.5 B-cell subset homeostasis is disturbed in some diseases

After phenotypic and functional analysis of the four B-cell subsets in healthy individuals, it was clear that B_{conv}, B_{react}, B_{APC}, and B_{inact} populations are functionally different and possesses unique features. Since the current literature shows that many inflammatory diseases in humans are accompanied by a perturbation of the balance of the $CD21^{low}$ B-cell compartment, it was not surprising to find an imbalance in the homeostatic state of the four B-cell subsets in the selected medical conditions. Therefore, acute inflammation (trauma patients) resulted in an increase in $CD21^{pos}$ $CD86^{pos}$ B_{react} while $CD21^{low}$ $CD86^{pos}$ B_{APCs} were increased in autoimmune diseases (rheumatoid arthritis) as well as in cancer as a model for chronic inflammatory condition. These results are in line with the hypothesis that B_{react} are generated after

short stimulation and that prolonged CD40 or BCR stimulation leads to the accumulation of B_{APCs}.

It is important to note that the classification of B cells by the expression of CD21 and CD86 further dissected the $CD21^{low}$ B-cell population previously described to be composed of anergic, exhausted, auto-reactive B cells into two subsets with distinct functions. On the one hand, $CD21^{low}$ $CD86^{neg}$ B_{inact} with the exhausted phenotype seems to represent the subset previously described in CVID patients (Warnatz et al. 2002) while $CD21^{low}$ $CD86^{pos}$ B_{APC} with an activated phenotype and potent antigen-presenting capacity were found to be increased in rheumatoid arthritis patients. Interestingly, it was previously described that CVID but not rheumatoid arthritis patients contain elevated serum levels of B cell-activating factor (BAFF), which has been associated with an increased survival of auto-reactive B cells in mice, likely contributing to the accumulation of these cells in CVID patients (Lesley et al. 2004). Moreover, CVID patients who display higher frequencies of $CD21^{low}$ B cells are more susceptible to develop autoimmune syndromes (Isnardi et al. 2010). This suggests that accumulation of $CD21^{low}$ $CD86^{neg}$ B_{inact} cells may contribute to the development of autoimmunity in humans. Immune reactions may create a favorable environment in which tolerance is broken and $CD21^{low}$ $CD86^{neg}$ B_{inact} cells are eventually activated to $CD21^{low}$ $CD86^{pos}$ B_{APC}. Thus, both $CD21^{low}$ B-cell subsets seem to arise from antigen-experienced B lymphocytes. In the case of B_{APC}, additional T cell help was received through CD40-mediated signals allowing them to become fully activated inflammatory effector B cells while B_{inact} received no or insufficient T cell help.

The expanded population of B_{APC} found in rheumatoid arthritis patients might be favoring a more productive interaction with pathogeneic T cells. In mice for example, it has been shown that antigen-specific B cells with high expression of MHC

class II, and costimulatory molecules CD80 and CD86 are required for the induction of arthritis (O'Neill et al. 2005). As mentioned above, presumably repeated stimulation of autoantigens through BCR plus the influence of other proinflammatory signals, such as cytokines or CD40L stimulation, gave rise to this activated phenotype, which has been reported in other diseases such as systemic sclerosis (Sato et al. 2004), asthma (Hofer et al. 1998) and irritable bowel syndrome (Ohman et al. 2009). The described absence of inhibitory molecules on B_{APC} might account for this phenomenon since such regulatory molecules provide a negative feedback that limits the ongoing self-reactive humoral responses (Catalan et al. 2010). In fact, in an SLE mouse model, restoration of the expression of CD32 on B cells diminished the symptoms and reverted the secretion of autoantibodies (McGaha et al. 2005).

Interestingly, in healthy individuals a higher percentage of B_{APC} was observed in women compared to men of the same age, an observation which is in line with a previous report that women have a higher risk of developing autoimmune disease (Amur et al., 2012).

In the observed conditions a shift in the balance towards the B_{APC} subset could be indicating the generation of an inflammatory B cell response. Indeed as observed with the influenza vaccinated cohort, the B_{APC} subset was increased 7 days after vaccination indicating the involvement of this B-cell population during the course of the physiologic immune response to vaccines. This is consistent with an study from Jahnmatz et al., in which after 7 and 14 days of intranasal vaccination with an attenuated *Bordetella pertussis* vaccine they found an increase in $CD21^{low}$ $CD27^{pos}$ B cells (Jahnmatz et al. 2014). Although the antigen-specificity of the B cells was not investigated, it is most likely that such increase on B_{APC} was induced by the vaccine, since the frequency of the other B-cell subsets was not altered.

Each condition was associated with a characteristic imbalance of the homeostatic state within the B-cell compartment. Acute inflammation resulted in an increase in B_{react} while a shift towards the B_{APC} subset could indicate the generation of an inflammatory B cell response, like response to vaccination or disease activity in human autoimmune disease. The data demonstrated that there are important alterations in the homeostasis of peripheral blood B-cell subsets involving the expression of the costimulatory molecules CD86 and CD21 in chronic and acute diseases, suggesting that these cells indeed play a role during the course of an immune response.

This research project has important clinical implications. The analysis of the frequency of each B-cell subpopulation could serve as a promising biomarker for disease activity and response to treatment in many immune-mediated diseases. Furthermore, dysregulated subsets could be therapeutically targeted as an effective approach for the treatment of many B-cell mediated immune pathologies. In this way, depletion of B cells using monoclonal anti-CD20 antibodies has been shown to be an effective therapeutic strategy in several medical conditions including cancer, autoimmune diseases, graft-versus-host disease, and transplant rejection (McLaughlin et al. 1998, Shimabukuro-Vornhagen et al. 2009, Barnett et al. 2013, Bindea et al. 2013, Pateinakis and Pyrpasopoulou 2014). However, B cell subset-specific therapies would be advantageous. Unfortunately, the cell surface markers described here to characterize the subpopulations are not suitable for targeting these subsets. Further research should be done in order to identify specific-cell surface markers that are amenable for a therapeutic depletion of these subsets with monoclonal antibodies. In addition, the establishment of the novel soluble model to generate CD40-activated B cells showed to be an effective in vitro model to produce

large amounts of B_{APC}. In the future, this model could be used for the development of B_{APC}-specific targeted therapies.

4.6 Conclusion

Taken together, the data presented in this work demonstrated that human B-cell subsets divided by the expression of CD21 and CD86 represent phenotypic and functionally different B-cell populations. In vitro data sustained the hypothesis that $CD21^{pos}$ $CD86^{pos}$ subset can develop from resting naïve B cells after T cell help through CD40L and that prolonged stimulation results in down-regulation of CD21. Therefore, it is tempting to suggest that in vivo $CD21^{low}$ $CD86^{pos}$ B_{APC} likewise arise from $CD21^{pos}$ $CD86^{pos}$ B_{react} by sustained BCR- and CD40-driven activation. Collectively, the results provide a conceptual framework for the division of human B cells into functional subsets.

Both $CD21^{low}$ B-cell subsets seem to arise from antigen-experienced B lymphocytes. They were proven to be functionally different and to differ in the expression of several molecules and inhibitory receptors. $CD21^{low}$ $CD86^{pos}$ B_{APC} were shown to be fully activated memory B cells with a strong immunostimulatory capacity while $CD21^{low}$ $CD86^{neg}$ B_{inact} subset contained primarily inactivated B cells, which displayed evidence of exhaustion or anergy. Additionally, B_{APC} were increased in patients with autoimmune diseases and cancer indicating that they might play a role in the induction of pathogenic responses. Hence, it could be suggested that in autoimmunity, breaking of tolerance mechanisms might be contributing to the pathogenesis of the disease by the activation of auto-reactive $CD21^{low}$ $CD86^{neg}$ B_{inact} that eventually would become $CD21^{low}$ $CD86^{pos}$ B_{APC}.

It is important to mention that in order to further dissect the molecular mechanisms that determine the development of $CD21^{low}$ $CD86^{pos}$ B_{APC} an analogue to this B-cell subset have to be identified in a mouse model. The main problem is that in mice and humans the expression of CD21 is regulated differently (McGaha et al. 2005). In the human system, two separate genes which lie in close vicinity on chromosome 1q encode CD21 and CD35 (Fujisaku et al. 1989). However, in mice these two proteins are encoded within the *CR2* locus and are generated from one gene by means of differential splicing (Erdei et al. 2009). Therefore, there are no available knockout mice for only one of these proteins, and thus the phenotype might not reflect the phenotype of human B cells lacking only CD21.

Furthermore, major differences between the two species have been identified in terms of the genetic background, tissue distribution, cytoplasmic sequences and their role in B cell functions (Jacobson and Weis 2008). Therefore, in order to identify the murine counterpart to human B_{APC} another set of marker have to be determined that is characteristic for the mouse B_{APC} subset. Identification of the murine counterpart will enable more detailed studies on the molecular regulation of this subset.

References

REFERENCES

Acosta-Rodriguez, E. V., L. Rivino, J. Geginat, D. Jarrossay, M. Gattorno, A. Lanzavecchia, et al. (2007). "Surface phenotype and antigenic specificity of human interleukin 17-producing T helper memory cells." Nat Immunol **8**(6): 639-646.

Adler, B., E. Schaadt, B. Kempkes, U. Zimber-Strobl, B. Baier and G. W. Bornkamm (2002). "Control of Epstein–Barr virus reactivation by activated CD40 and viral latent membrane protein 1." Proc Natl Acad Sci U S A **99**(1): 437-442.

Agematsu, K., S. Hokibara, H. Nagumo and A. Komiyama (2000). "CD27: a memory B-cell marker." Immunology Today **21**(5): 204-206.

Ahmadi, T., A. Flies, Y. Efebera and D. H. Sherr (2008). "CD40 Ligand-activated, antigen-specific B cells are comparable to mature dendritic cells in presenting protein antigens and major histocompatibility complex class I- and class II-binding peptides." Immunology **124**(1): 129-140.

Ait-Oufella, H., O. Herbin, J. D. Bouaziz, C. J. Binder, C. Uyttenhove, L. Laurans, et al. (2010). "B cell depletion reduces the development of atherosclerosis in mice." J Exp Med **207**(8): 1579-1587.

Allen, C. D., K. M. Ansel, C. Low, R. Lesley, H. Tamamura, N. Fujii, et al. (2004). "Germinal center dark and light zone organization is mediated by CXCR4 and CXCR5." Nat Immunol **5**(9): 943-952.

Allen, C. D., T. Okada and J. G. Cyster (2007). "Germinal-center organization and cellular dynamics." Immunity **27**(2): 190-202.

Allman, D., R. C. Lindsley, W. DeMuth, K. Rudd, S. A. Shinton and R. R. Hardy (2001). "Resolution of three nonproliferative immature splenic B cell subsets reveals multiple selection points during peripheral B cell maturation." J Immunol **167**(12): 6834-6840.

Allman, D. and D. Northrup (2007). "Giving B cell tolerance the 'TSLiP'." Nat Immunol **8**(5): 481-483.

Anderson, L. J. and R. Longnecker (2008). "EBV LMP2A provides a surrogate pre-B cell receptor signal through constitutive activation of the ERK/MAPK pathway." The Journal of general virology **89**(Pt 7): 1563-1568.

Annunziato, F., L. Cosmi, V. Santarlasci, L. Maggi, F. Liotta, B. Mazzinghi, et al. (2007). "Phenotypic and functional features of human Th17 cells." J Exp Med **204**(8): 1849-1861.

Antonioli, L., P. Pacher, E. S. Vizi and G. Haskó (2013). "CD39 and CD73 in immunity and inflammation." Trends in molecular medicine **19**(6): 355-367.

Antony, P., K. Hoek, B. Sarmah and W. N. Khan (2007). "Micro-scale flow cytometry-based and biochemical analysis of lipid signaling in primary B cell subpopulations." Biol Proced Online **9**: 73-83.

Ardeshna, K. M., A. R. Pizzey, N. S. Thomas, S. Orr, D. C. Linch and S. Devereux (2000). "Monocyte-derived dendritic cells do not proliferate and are not susceptible to retroviral transduction." Br J Haematol **108**(4): 817-824.

Asokan, R., J. Hua, K. A. Young, H. J. Gould, J. P. Hannan, D. M. Kraus, et al. (2006). "Characterization of human complement receptor type 2 (CR2/CD21) as a receptor for IFN-alpha: a potential role in systemic lupus erythematosus." J Immunol **177**(1): 383-394.

Aubry, J. P., S. Pochon, P. Graber, K. U. Jansen and J. Y. Bonnefoy (1992). "CD21 is a ligand for CD23 and regulates IgE production." Nature **358**(6386): 505-507.

Aucher, A., E. Magdeleine, E. Joly and D. Hudrisier (2008). "Capture of plasma membrane fragments from target cells by trogocytosis requires signaling in T cells but not in B cells." Blood **111**(12): 5621-5628.

Azuma, M., D. Ito, H. Yagita, K. Okumura, J. H. Phillips, L. L. Lanier, et al. (1993). "B70 antigen is a second ligand for CTLA-4 and CD28." Nature **366**(6450): 76-79.

Banchereau, J., F. Bazan, D. Blanchard, F. Briere, J. P. Galizzi, C. van Kooten, et al. (1994). "The CD40 antigen and its ligand." Annu Rev Immunol **12**: 881-922.

Banchereau, J., P. de Paoli, A. Valle, E. Garcia and F. Rousset (1991). "Long-term human B cell lines dependent on interleukin-4 and antibody to CD40." Science **251**(4989): 70-72.

Banchereau, J. and F. Rousset (1991). "Growing human B lymphocytes in the CD40 system." Nature **353**(6345): 678-679.

Barnett, A. N., V. G. Hadjianastassiou and N. Mamode (2013). "Rituximab in renal transplantation." Transpl Int **26**(6): 563-575.

Barratt-Boyes, S. M., M. I. Zimmer, L. A. Harshyne, E. M. Meyer, S. C. Watkins, S. Capuano, 3rd, et al. (2000). "Maturation and trafficking of monocyte-derived dendritic cells in monkeys: implications for dendritic cell-based vaccines." J Immunol **164**(5): 2487-2495.

Barrault, D. V. and A. M. Knight (2004). "Distinct sequences in the cytoplasmic domain of complement receptor 2 are involved in antigen internalization and presentation." J Immunol **172**(6): 3509-3517.

Barrett, T. B., G. Shu and E. A. Clark (1991). "CD40 signaling activates CD11a/CD18 (LFA-1)-mediated adhesion in B cells." J Immunol **146**(6): 1722-1729.

Bastian, O., J. Pillay, J. Alblas, L. Leenen, L. Koenderman and T. Blokhuis (2011). "Systemic inflammation and fracture healing." J Leukoc Biol **89**(5): 669-673.

Benschop, R. J. and J. C. Cambier (1999). "B cell development: signal transduction by antigen receptors and their surrogates." Curr Opin Immunol **11**(2): 143-151.

Berkowska, M. A., G. J. Driessen, V. Bikos, C. Grosserichter-Wagener, K. Stamatopoulos, A. Cerutti, et al. (2011). "Human memory B cells originate from three distinct germinal center-dependent and -independent maturation pathways." Blood **118**(8): 2150-2158.

Bindea, G., B. Mlecnik, M. Tosolini, A. Kirilovsky, M. Waldner, A. C. Obenauf, et al. (2013). "Spatiotemporal dynamics of intratumoral immune cells reveal the immune landscape in human cancer." Immunity **39**(4): 782-795.

Bjorck, P., B. Axelsson and S. Paulie (1991). "Expression of CD40 and CD43 during activation of human B lymphocytes." Scand J Immunol **33**(2): 211-218.

Blix, E. S., J. M. Irish, A. Husebekk, J. Delabie, L. Forfang, A. M. Tierens, et al. (2012). "Phospho-specific flow cytometry identifies aberrant signaling in indolent B-cell lymphoma." BMC Cancer **12**: 478.

Boackle, S. A., V. M. Holers and D. R. Karp (1997). "CD21 augments antigen presentation in immune individuals." Eur J Immunol **27**(1): 122-129.

Bolland, S. and J. V. Ravetch (2000). "Spontaneous autoimmune disease in Fc(gamma)RIIB-deficient mice results from strain-specific epistasis." Immunity **13**(2): 277-285.

Bonilla, F. A. and H. C. Oettgen (2010). "Adaptive immunity." J Allergy Clin Immunol **125**(2 Suppl 2): S33-40.

Bouaziz, J.-D., K. Yanaba, G. M. Venturi, Y. Wang, R. M. Tisch, J. C. Poe, et al. (2007). "Therapeutic B cell depletion impairs adaptive and autoreactive CD4(+) T cell activation in mice." Proc Natl Acad Sci U S A **104**(52): 20878-20883.

Bouaziz, J. D., K. Yanaba, G. M. Venturi, Y. Wang, R. M. Tisch, J. C. Poe, et al. (2007). "Therapeutic B cell depletion impairs adaptive and autoreactive CD4+ T cell activation in mice." Proc Natl Acad Sci U S A **104**(52): 20878-20883.

Boussiotis, V. A., G. J. Freeman, J. G. Gribben, J. Daley, G. Gray and L. M. Nadler (1993). "Activated human B lymphocytes express three CTLA-4

counterreceptors that costimulate T-cell activation." Proceedings of the National Academy of Sciences **90**(23): 11059-11063.

Brandtzaeg, P. and F. E. Johansen (2005). "Mucosal B cells: phenotypic characteristics, transcriptional regulation, and homing properties." Immunol Rev **206**: 32-63.

Bretscher, P. A. (1999). "A two-step, two-signal model for the primary activation of precursor helper T cells." Proc Natl Acad Sci U S A **96**(1): 185-190.

Broere, F., S. Apasov, M. Sitkovsky and W. van Eden (2011). A2 T cell subsets and T cell-mediated immunity. Principles of Immunopharmacology. F. P. Nijkamp and M. J. Parnham, Birkhäuser Basel**:** 15-27.

Brouns, G. S., E. de Vries and J. Borst (1995). "Assembly and intracellular transport of the human B cell antigen receptor complex." Int Immunol **7**(3): 359-368.

Burchiel, S. W., B. S. Edwards, F. W. Kuckuck, F. T. Lauer, E. R. Prossnitz, J. T. Ransom, et al. (2000). "Analysis of free intracellular calcium by flow cytometry: multiparameter and pharmacologic applications." Methods **21**(3): 221-230.

Burrows, P. D., R. P. Stephan, Y. H. Wang, K. Lassoued, Z. Zhang and M. D. Cooper (2002). "The transient expression of pre-B cell receptors governs B cell development." Semin Immunol **14**(5): 343-349.

Butcher, E. C. and L. J. Picker (1996). "Lymphocyte homing and homeostasis." Science **272**(5258): 60-66.

Calderhead, D. M., Y. Kosaka, E. M. Manning and R. J. Noelle (2000). "CD40-CD154 interactions in B-cell signaling." Curr Top Microbiol Immunol **245**(2): 73-99.

Cambier, J. C., S. B. Gauld, K. T. Merrell and B. J. Vilen (2007). "B-cell anergy: from transgenic models to naturally occurring anergic B cells?" Nat Rev Immunol **7**(8): 633-643.

Campbell, K. S., E. J. Hager, R. J. Friedrich and J. C. Cambier (1991). "IgM antigen receptor complex contains phosphoprotein products of B29 and mb-1 genes." Proc Natl Acad Sci U S A **88**(9): 3982-3986.

Caraux, A., B. Klein, B. Paiva, C. Bret, A. Schmitz, G. M. Fuhler, et al. (2010). "Circulating human B and plasma cells. Age-associated changes in counts and detailed characterization of circulating normal CD138- and CD138+ plasma cells." Haematologica **95**(6): 1016-1020.

Carrasco, Y. R., S. J. Fleire, T. Cameron, M. L. Dustin and F. D. Batista (2004). "LFA-1/ICAM-1 interaction lowers the threshold of B cell activation by facilitating B cell adhesion and synapse formation." Immunity **20**(5): 589-599.

Carsetti, R., M. M. Rosado and H. Wardmann (2004). "Peripheral development of B cells in mouse and man." Immunol Rev **197**: 179-191.

Catalan, D., O. Aravena, F. Sabugo, P. Wurmann, L. Soto, A. M. Kalergis, et al. (2010). "B cells from rheumatoid arthritis patients show important alterations

in the expression of CD86 and FcgammaRIIb, which are modulated by anti-tumor necrosis factor therapy." Arthritis Res Ther **12**(2): R68.

Cella, M., F. Sallusto and A. Lanzavecchia (1997). "Origin, maturation and antigen presenting function of dendritic cells." Curr Opin Immunol **9**(1): 10-16.

Cerny, A., A. W. Hugin, H. Bazin, S. Sutter, H. Hengartner and R. M. Zinkernagel (1988). "Anti-Listeria monocytogenes immunity in mu-suppressed mice: a comparison of treatment with conventional hyperimmune rabbit anti-mouse IgM and affinity-purified, monoclonal rat anti-mouse IgM." Med Microbiol Immunol **177**(3): 123-131.

Cerny, A., S. Sutter, H. Bazin, H. Hengartner and R. M. Zinkernagel (1988). "Clearance of lymphocytic choriomeningitis virus in antibody- and B-cell-deprived mice." J Virol **62**(5): 1803-1807.

Chambers, C. A. (2001). "The expanding world of co-stimulation: the two-signal model revisited." Trends Immunol **22**(4): 217-223.

Chang, H. C., L. Han, R. Goswami, E. T. Nguyen, D. Pelloso, M. J. Robertson, et al. (2009). "Impaired development of human Th1 cells in patients with deficient expression of STAT4." Blood **113**(23): 5887-5890.

Chaplin, D. D. (2010). "Overview of the immune response." Journal of Allergy and Clinical Immunology **125**(2): S3-S23.

Charles, E. D., C. Brunetti, S. Marukian, K. D. Ritola, A. H. Talal, K. Marks, et al. (2011). "Clonal B cells in patients with hepatitis C virus-associated mixed

cryoglobulinemia contain an expanded anergic CD21low B-cell subset." Blood **117**(20): 5425-5437.

Chaturvedi, A., R. Martz, D. Dorward, M. Waisberg and S. K. Pierce (2011). "Endocytosed BCRs sequentially regulate MAPK and Akt signaling pathways from intracellular compartments." Nat Immunol **12**(11): 1119-1126.

Chen, C., M. Z. Radic, J. Erikson, S. A. Camper, S. Litwin, R. R. Hardy, et al. (1994). "Deletion and editing of B cells that express antibodies to DNA." J Immunol **152**(4): 1970-1982.

Chen, J., M. Trounstine, F. W. Alt, F. Young, C. Kurahara, J. F. Loring, et al. (1993). "Immunoglobulin gene rearrangement in B cell deficient mice generated by targeted deletion of the JH locus." Int Immunol **5**(6): 647-656.

Chiu, C. W., M. Dalton, M. Ishiai, T. Kurosaki and A. C. Chan (2002). "BLNK: molecular scaffolding through 'cis'-mediated organization of signaling proteins." Embo j **21**(23): 6461-6472.

Claes, L., S. Recknagel and A. Ignatius (2012). "Fracture healing under healthy and inflammatory conditions." Nat Rev Rheumatol **8**(3): 133-143.

Clayton, E., G. Bardi, S. E. Bell, D. Chantry, C. P. Downes, A. Gray, et al. (2002). "A crucial role for the p110delta subunit of phosphatidylinositol 3-kinase in B cell development and activation." J Exp Med **196**(6): 753-763.

Cohen, C. J., S. Q. Crome, K. G. MacDonald, E. L. Dai, D. L. Mager and M. K. Levings (2011). "Human Th1 and Th17 cells exhibit epigenetic stability at

signature cytokine and transcription factor loci." J Immunol **187**(11): 5615-5626.

Coughlin, C. M., B. A. Vance, S. A. Grupp and R. H. Vonderheide (2004). "RNA-transfected CD40-activated B cells induce functional T-cell responses against viral and tumor antigen targets: implications for pediatric immunotherapy." Blood **103**(6): 2046-2054.

Crawford, A., M. Macleod, T. Schumacher, L. Corlett and D. Gray (2006). "Primary T cell expansion and differentiation in vivo requires antigen presentation by B cells." J Immunol **176**(6): 3498-3506.

Cua, D. J., J. Sherlock, Y. Chen, C. A. Murphy, B. Joyce, B. Seymour, et al. (2003). "Interleukin-23 rather than interleukin-12 is the critical cytokine for autoimmune inflammation of the brain." Nature **421**(6924): 744-748.

Cyster, J. G. and C. C. Goodnow (1995). "Antigen-induced exclusion from follicles and anergy are separate and complementary processes that influence peripheral B cell fate." Immunity **3**(6): 691-701.

Cyster, J. G., S. B. Hartley and C. C. Goodnow (1994). "Competition for follicular niches excludes self-reactive cells from the recirculating B-cell repertoire." Nature **371**(6496): 389-395.

Dempsey, P. W., M. E. Allison, S. Akkaraju, C. C. Goodnow and D. T. Fearon (1996). "C3d of complement as a molecular adjuvant: bridging innate and acquired immunity." Science **271**(5247): 348-350.

Depoil, D., S. Fleire, B. L. Treanor, M. Weber, N. E. Harwood, K. L. Marchbank, et al. (2008). "CD19 is essential for B cell activation by promoting B cell receptor-antigen microcluster formation in response to membrane-bound ligand." Nat Immunol **9**(1): 63-72.

DiLillo, D. J., T. Matsushita and T. F. Tedder (2010). "B10 cells and regulatory B cells balance immune responses during inflammation, autoimmunity, and cancer." Ann N Y Acad Sci **1183**: 38-57.

Dolmetsch, R. E., R. S. Lewis, C. C. Goodnow and J. I. Healy (1997). "Differential activation of transcription factors induced by Ca2+ response amplitude and duration." Nature **386**(6627): 855-858.

Draube, A., N. Klein-Gonzalez, S. Mattheus, C. Brillant, M. Hellmich, A. Engert, et al. (2011). "Dendritic cell based tumor vaccination in prostate and renal cell cancer: a systematic review and meta-analysis." PLoS One **6**(4): e18801.

Duty, J. A., P. Szodoray, N. Y. Zheng, K. A. Koelsch, Q. Zhang, M. Swiatkowski, et al. (2009). "Functional anergy in a subpopulation of naive B cells from healthy humans that express autoreactive immunoglobulin receptors." J Exp Med **206**(1): 139-151.

Edwards, J. C., L. Szczepanski, J. Szechinski, A. Filipowicz-Sosnowska, P. Emery, D. R. Close, et al. (2004). "Efficacy of B-cell-targeted therapy with rituximab in patients with rheumatoid arthritis." N Engl J Med **350**(25): 2572-2581.

Engelke, M., N. Engels, K. Dittmann, B. Stork and J. Wienands (2007). "Ca(2+) signaling in antigen receptor-activated B lymphocytes." Immunol Rev **218**: 235-246.

Epstein, M. M., F. Di Rosa, D. Jankovic, A. Sher and P. Matzinger (1995). "Successful T cell priming in B cell-deficient mice." J Exp Med **182**(4): 915-922.

Erdei, A., A. Isaak, K. Torok, N. Sandor, M. Kremlitzka, J. Prechl, et al. (2009). "Expression and role of CR1 and CR2 on B and T lymphocytes under physiological and autoimmune conditions." Mol Immunol **46**(14): 2767-2773.

Erdei, A., A. Isaák, K. Török, N. Sándor, M. Kremlitzka, J. Prechl, et al. (2009). "Expression and role of CR1 and CR2 on B and T lymphocytes under physiological and autoimmune conditions." Molecular Immunology **46**(14): 2767-2773.

Erikson, J., M. Z. Radic, S. A. Camper, R. R. Hardy, C. Carmack and M. Weigert (1991). "Expression of anti-DNA immunoglobulin transgenes in non-autoimmune mice." Nature **349**(6307): 331-334.

Evans, D. E., M. W. Munks, J. M. Purkerson and D. C. Parker (2000). "Resting B lymphocytes as APC for naive T lymphocytes: dependence on CD40 ligand/CD40." J Immunol **164**(2): 688-697.

Faassen, A. E., D. P. Dalke, M. T. Berton, W. D. Warren and S. K. Pierce (1995). "CD40-CD40 ligand interactions stimulate B cell antigen processing." Eur J Immunol **25**(12): 3249-3255.

Fanslow, W. C., S. Srinivasan, R. Paxton, M. G. Gibson, M. K. Spriggs and R. J. Armitage (1994). "Structural characteristics of CD40 ligand that determine biological function." Semin Immunol **6**(5): 267-278.

Faris, M., F. Gaskin, J. T. Parsons and S. M. Fu (1994). "CD40 signaling pathway: anti-CD40 monoclonal antibody induces rapid dephosphorylation and phosphorylation of tyrosine-phosphorylated proteins including protein tyrosine kinase Lyn, Fyn, and Syk and the appearance of a 28-kD tyrosine phosphorylated protein." J Exp Med **179**(6): 1923-1931.

Fearon, D. T. and M. C. Carroll (2000). "Regulation of B lymphocyte responses to foreign and self-antigens by the CD19/CD21 complex." Annu Rev Immunol **18**: 393-422.

Fecteau, J. F. and S. Neron (2003). "CD40 stimulation of human peripheral B lymphocytes: distinct response from naive and memory cells." J Immunol **171**(9): 4621-4629.

Finnegan, A., S. Ashaye and K. M. Hamel (2012). "B effector cells in rheumatoid arthritis and experimental arthritis." Autoimmunity **45**(5): 353-363.

Fleire, S. J., J. P. Goldman, Y. R. Carrasco, M. Weber, D. Bray and F. D. Batista (2006). "B cell ligand discrimination through a spreading and contraction response." Science **312**(5774): 738-741.

Foerster, C., N. Voelxen, M. Rakhmanov, B. Keller, S. Gutenberger, S. Goldacker, et al. (2010). "B cell receptor-mediated calcium signaling is impaired in B lymphocytes of type Ia patients with common variable immunodeficiency." J Immunol **184**(12): 7305-7313.

Fu, C., C. W. Turck, T. Kurosaki and A. C. Chan (1998). "BLNK: a central linker protein in B cell activation." Immunity **9**(1): 93-103.

Fuertes, I., J. Luelmo, L. Leal, J. Romani, S. Sanchez and J. M. Mascaro, Jr. (2013). "Refractory childhood pemphigoid successfully treated with rituximab." Pediatr Dermatol **30**(5): e96-97.

Fujimoto, M., A. P. Bradney, J. C. Poe, D. A. Steeber and T. F. Tedder (1999). "Modulation of B lymphocyte antigen receptor signal transduction by a CD19/CD22 regulatory loop." Immunity **11**(2): 191-200.

Fujisaku, A., J. B. Harley, M. B. Frank, B. A. Gruner, B. Frazier and V. M. Holers (1989). "Genomic organization and polymorphisms of the human C3d/Epstein-Barr virus receptor." J Biol Chem **264**(4): 2118-2125.

Galibert, L., N. Burdin, C. Barthelemy, G. Meffre, I. Durand, E. Garcia, et al. (1996). "Negative selection of human germinal center B cells by prolonged BCR cross-linking." J Exp Med **183**(5): 2075-2085.

Garcia-Marquez, M. A., A. Shimabukuro-Vornhagen, S. Theurich, M. Kochanek, T. Weber, K. Wennhold, et al. (2014). "A multimerized form of recombinant human CD40 ligand supports long-term activation and proliferation of B cells." Cytotherapy **16**(11): 1537-1544.

Gathings, W. E., A. R. Lawton and M. D. Cooper (1977). "Immunofluorescent studies of the development of pre-B cells, B lymphocytes and immunoglobulin isotype diversity in humans." European Journal of Immunology **7**(11): 804-810.

Geisberger, R., M. Lamers and G. Achatz (2006). "The riddle of the dual expression of IgM and IgD." Immunology **118**(4): 429-437.

Ghosh, D. and G. C. Tsokos (2010). "Spleen tyrosine kinase: an Src family of non-receptor kinase has multiple functions and represents a valuable therapeutic target in the treatment of autoimmune and inflammatory diseases." Autoimmunity **43**(1): 48-55.

Good, K. L., D. T. Avery and S. G. Tangye (2009). "Resting human memory B cells are intrinsically programmed for enhanced survival and responsiveness to diverse stimuli compared to naive B cells." J Immunol **182**(2): 890-901.

Goodnow, C. C., J. Crosbie, S. Adelstein, T. B. Lavoie, S. J. Smith-Gill, R. A. Brink, et al. (2009). "Altered immunoglobulin expression and functional silencing of self-reactive B lymphocytes in transgenic mice." J Immunol **183**(9): 5442-5448.

Grattone, M. L., C. L. Villiers, M. B. Villiers, C. Drouet and P. N. Marche (1999). "Co-operation between human CR1 (CD35) and CR2 (CD21) in internalization of their C3b and iC3b ligands by murine-transfected fibroblasts." Immunology **98**(1): 152-157.

Griffin, D. O., N. E. Holodick and T. L. Rothstein (2011). "Human B1 cells in umbilical cord and adult peripheral blood express the novel phenotype CD20+ CD27+ CD43+ CD70." J Exp Med **208**(1): 67-80.

Gunn, M. D., S. Kyuwa, C. Tam, T. Kakiuchi, A. Matsuzawa, L. T. Williams, et al. (1999). "Mice lacking expression of secondary lymphoid organ chemokine have defects in lymphocyte homing and dendritic cell localization." J Exp Med **189**(3): 451-460.

Gururajan, M., C. D. Jennings and S. Bondada (2006). "Cutting edge: constitutive B cell receptor signaling is critical for basal growth of B lymphoma." J Immunol **176**(10): 5715-5719.

Guttormsen, H. K., A. H. Sharpe, A. K. Chandraker, A. K. Brigtsen, M. H. Sayegh and D. L. Kasper (1999). "Cognate stimulatory B-cell-T-cell interactions are critical for T-cell help recruited by glycoconjugate vaccines." Infect Immun **67**(12): 6375-6384.

Hackstein, H., A. E. Morelli and A. W. Thomson (2001). "Designer dendritic cells for tolerance induction: guided not misguided missiles." Trends Immunol **22**(8): 437-442.

Hanissian, S. H. and R. S. Geha (1997). "Jak3 is associated with CD40 and is critical for CD40 induction of gene expression in B cells." Immunity **6**(4): 379-387.

Harnett, M. M. (2004). "CD40: a growing cytoplasmic tale." Sci STKE **2004**(237): pe25.

Harrington, L. E., R. D. Hatton, P. R. Mangan, H. Turner, T. L. Murphy, K. M. Murphy, et al. (2005). "Interleukin 17-producing CD4+ effector T cells develop via a lineage distinct from the T helper type 1 and 2 lineages." Nat Immunol **6**(11): 1123-1132.

Harris, D. P., L. Haynes, P. C. Sayles, D. K. Duso, S. M. Eaton, N. M. Lepak, et al. (2000). "Reciprocal regulation of polarized cytokine production by effector B and T cells." Nat Immunol **1**(6): 475-482.

Hartley, S. B., M. P. Cooke, D. A. Fulcher, A. W. Harris, S. Cory, A. Basten, et al. (1993). "Elimination of self-reactive B lymphocytes proceeds in two stages: arrested development and cell death." Cell **72**(3): 325-335.

Haswell, L. E., M. J. Glennie and A. Al-Shamkhani (2001). "Analysis of the oligomeric requirement for signaling by CD40 using soluble multimeric forms of its ligand, CD154." Eur J Immunol **31**(10): 3094-3100.

Hauser, S. L., E. Waubant, D. L. Arnold, T. Vollmer, J. Antel, R. J. Fox, et al. (2008). "B-cell depletion with rituximab in relapsing-remitting multiple sclerosis." N Engl J Med **358**(7): 676-688.

Hausmann, M. J., B. Rogachev, M. Weiler, C. Chaimovitz and A. Douvdevani (2000). "Accessory role of human peritoneal mesothelial cells in antigen presentation and T-cell growth." Kidney Int **57**(2): 476-486.

Herrmann, P., M. H. Schreier, H. Bazin, R. M. Zinkernagel and A. Cerny (1988). "Delayed type hypersensitivity (DTH) in anti-IgM-treated B cell-depleted mice: analysis of induction and effector phase." Immunobiology **177**(4-5): 382-389.

Hiller, D. and Q. D. Chu (2011). "CXCR4 and Axillary Lymph Nodes: Review of a Potential Biomarker for Breast Cancer Metastasis." International Journal of Breast Cancer **2011**: 420981.

Hofer, M. F., O. Jirapongsananuruk, A. E. Trumble and D. Y. Leung (1998). "Upregulation of B7.2, but not B7.1, on B cells from patients with allergic asthma." J Allergy Clin Immunol **101**(1 Pt 1): 96-102.

Hogerkorp, C. M. and C. A. Borrebaeck (2006). "The human CD77- B cell population represents a heterogeneous subset of cells comprising centroblasts, centrocytes, and plasmablasts, prompting phenotypical revision." J Immunol **177**(7): 4341-4349.

Holodick, N. E., J. R. Tumang and T. L. Rothstein (2009). "Continual signaling is responsible for constitutive ERK phosphorylation in B-1a cells." Mol Immunol **46**(15): 3029-3036.

Ichii, M., K. Oritani and Y. Kanakura (2014). "Early B lymphocyte development: Similarities and differences in human and mouse." World J Stem Cells **6**(4): 421-431.

Imadome, K., M. Shirakata, N. Shimizu, S. Nonoyama and Y. Yamanashi (2003). "CD40 ligand is a critical effector of Epstein-Barr virus in host cell survival and transformation." Proc Natl Acad Sci U S A **100**(13): 7836-7840.

Irish, J. (2014). Fold Change and Basal.

Irish, J. M., D. K. Czerwinski, G. P. Nolan and R. Levy (2006). "Kinetics of B cell receptor signaling in human B cell subsets mapped by phosphospecific flow cytometry." J Immunol **177**(3): 1581-1589.

Isnardi, I., Y. S. Ng, L. Menard, G. Meyers, D. Saadoun, I. Srdanovic, et al. (2010). "Complement receptor 2/CD21- human naive B cells contain mostly autoreactive unresponsive clones." Blood **115**(24): 5026-5036.

Ivanov, R., T. Aarts, A. Hagenbeek, S. Hol and S. Ebeling (2005). "B-cell expansion in the presence of the novel 293-CD40L-sCD40L cell line allows the

generation of large numbers of efficient xenoantigen-free APC." Cytotherapy **7**(1): 62-73.

Jabara, H. H., R. H. Buckley, J. L. Roberts, G. Lefranc, J. Loiselet, G. Khalil, et al. (1998). "Role of JAK3 in CD40-mediated signaling." Blood **92**(7): 2435-2440.

Jackson, S. M., P. C. Wilson, J. A. James and J. D. Capra (2008). "Human B cell subsets." Adv Immunol **98**: 151-224.

Jacobson, A. C. and J. H. Weis (2008). "Comparative functional evolution of human and mouse CR1 and CR2." J Immunol **181**(5): 2953-2959.

Jahnmatz, M., S. Amu, M. Ljungman, L. Wehlin, F. Chiodi, N. Mielcarek, et al. (2014). "B-cell responses after intranasal vaccination with the novel attenuated Bordetella pertussis vaccine strain BPZE1 in a randomized phase I clinical trial." Vaccine **32**(27): 3350-3356.

Janeway, C. A., Jr., J. Ron and M. E. Katz (1987). "The B cell is the initiating antigen-presenting cell in peripheral lymph nodes." J Immunol **138**(4): 1051-1055.

Kaczmarek, E., K. Koziak, J. Sevigny, J. B. Siegel, J. Anrather, A. R. Beaudoin, et al. (1996). "Identification and characterization of CD39/vascular ATP diphosphohydrolase." J Biol Chem **271**(51): 33116-33122.

Karras, J. G., Z. Wang, L. Huo, D. A. Frank and T. L. Rothstein (1997). "Induction of STAT protein signaling through the CD40 receptor in B lymphocytes: distinct STAT activation following surface Ig and CD40 receptor engagement." J Immunol **159**(9): 4350-4355.

Kashiwada, M., Y. Kaneko, H. Yagita, K. Okumura and T. Takemori (1996). "Activation of mitogen-activated protein kinases via CD40 is distinct from that stimulated by surface IgM on B cells." Eur J Immunol **26**(7): 1451-1458.

Katkere, B., S. Rosa and J. R. Drake (2012). "The Syk-binding ubiquitin ligase c-Cbl mediates signaling-dependent B cell receptor ubiquitination and B cell receptor-mediated antigen processing and presentation." J Biol Chem **287**(20): 16636-16644.

Kawai, K., N. H. Tsuno, J. Kitayama, E. Sunami, K. Takahashi and H. Nagawa (2011). "Catechin inhibits adhesion and migration of peripheral blood B cells by blocking CD11b." Immunopharmacol Immunotoxicol **33**(2): 391-397.

Kennedy, M. K., K. M. Mohler, K. D. Shanebeck, P. R. Baum, K. S. Picha, C. A. Otten-Evans, et al. (1994). "Induction of B cell costimulatory function by recombinant murine CD40 ligand." Eur J Immunol **24**(1): 116-123.

King, L. B. and J. G. Monroe (2000). "Immunobiology of the immature B cell: plasticity in the B-cell antigen receptor-induced response fine tunes negative selection." Immunol Rev **176**: 86-104.

Kitamura, D., J. Roes, R. Kuhn and K. Rajewsky (1991). "A B cell-deficient mouse by targeted disruption of the membrane exon of the immunoglobulin mu chain gene." Nature **350**(6317): 423-426.

Klaus, G. G., M. Holman and J. Hasbold (1994). "Properties of mouse CD40: the role of homotypic adhesion in the activation of B cells via CD40." Eur J Immunol **24**(11): 2714-2719.

Klein-González, N., S. Balkow, E. Kondo, S. Grabbe, T. Liebig, A. Shimabukuro-Vornhagen, et al. (2010). CD40-Activated B Cells Migrate Towards Secondary Lymphoid Organs And Interact Dynamically With T Cells. Biology of Blood and Marrow Transplant, Elsevier. **16:** S173-S174.

Klein, J. and A. Sato (2000). "The HLA system. First of two parts." N Engl J Med **343**(10): 702-709.

Klein, U. and R. Dalla-Favera (2007). "Unexpected steps in plasma-cell differentiation." Immunity **26**(5): 543-544.

Klein, U., R. Kuppers and K. Rajewsky (1997). "Evidence for a large compartment of IgM-expressing memory B cells in humans." Blood **89**(4): 1288-1298.

Klein, U., K. Rajewsky and R. Kuppers (1998). "Human immunoglobulin (Ig)M+IgD+ peripheral blood B cells expressing the CD27 cell surface antigen carry somatically mutated variable region genes: CD27 as a general marker for somatically mutated (memory) B cells." J Exp Med **188**(9): 1679-1689.

Kondo, E., M. S. Topp, H. P. Kiem, Y. Obata, Y. Morishima, K. Kuzushima, et al. (2002). "Efficient generation of antigen-specific cytotoxic T cells using retrovirally transduced CD40-activated B cells." J Immunol **169**(4): 2164-2171.

Kurosaki, T. and M. Hikida (2009). "Tyrosine kinases and their substrates in B lymphocytes." Immunol Rev **228**(1): 132-148.

Kurosaki, T., S. A. Johnson, L. Pao, K. Sada, H. Yamamura and J. C. Cambier (1995). "Role of the Syk autophosphorylation site and SH2 domains in B cell antigen receptor signaling." J Exp Med **182**(6): 1815-1823.

Lam, K. P., R. Kuhn and K. Rajewsky (1997). "In vivo ablation of surface immunoglobulin on mature B cells by inducible gene targeting results in rapid cell death." Cell **90**(6): 1073-1083.

Lane, P. J., F. M. McConnell, G. L. Schieven, E. A. Clark and J. A. Ledbetter (1990). "The role of class II molecules in human B cell activation. Association with phosphatidyl inositol turnover, protein tyrosine phosphorylation, and proliferation." J Immunol **144**(10): 3684-3692.

Lanzavecchia, A. (1985). "Antigen-specific interaction between T and B cells." Nature **314**(6011): 537-539.

Lapointe, R., A. Bellemare-Pelletier, F. Housseau, J. Thibodeau and P. Hwu (2003). "CD40-stimulated B lymphocytes pulsed with tumor antigens are effective antigen-presenting cells that can generate specific T cells." Cancer Res **63**(11): 2836-2843.

Lapteva, N., M. R. Seethammagari, B. A. Hanks, J. Jiang, J. M. Levitt, K. M. Slawin, et al. (2007). "Enhanced activation of human dendritic cells by inducible CD40 and Toll-like receptor-4 ligation." Cancer Res **67**(21): 10528-10537.

LeBien, T. W. (2000). "Fates of human B-cell precursors." Blood **96**(1): 9-23.

LeBien, T. W. and T. F. Tedder (2008). "B lymphocytes: how they develop and function." Blood **112**(5): 1570-1580.

Lenschow, D. J., A. I. Sperling, M. P. Cooke, G. Freeman, L. Rhee, D. C. Decker, et al. (1994). "Differential up-regulation of the B7-1 and B7-2 costimulatory molecules after Ig receptor engagement by antigen." J Immunol **153**(5): 1990-1997.

Lesley, R., Y. Xu, S. L. Kalled, D. M. Hess, S. R. Schwab, H. B. Shu, et al. (2004). "Reduced competitiveness of autoantigen-engaged B cells due to increased dependence on BAFF." Immunity **20**(4): 441-453.

Liebig, T. M., A. Fiedler, S. Zoghi, A. Shimabukuro-Vornhagen and M. S. von Bergwelt-Baildon (2009). "Generation of Human CD40-activated B cells." J Vis Exp(32).

Lin, J. and A. Weiss (2001). "T cell receptor signalling." J Cell Sci **114**(Pt 2): 243-244.

Liu, Y., Y. Wu, L. Ramarathinam, Y. Guo, D. Huszar, M. Trounstine, et al. (1995). "Gene-targeted B-deficient mice reveal a critical role for B cells in the CD4 T cell response." Int Immunol **7**(8): 1353-1362.

Liu, Y. J. and C. Arpin (1997). "Germinal center development." Immunol Rev **156**: 111-126.

Looney, R. J., J. H. Anolik, D. Campbell, R. E. Felgar, F. Young, L. J. Arend, et al. (2004). "B cell depletion as a novel treatment for systemic lupus

erythematosus: a phase I/II dose-escalation trial of rituximab." Arthritis Rheum **50**(8): 2580-2589.

Lowell, C. A., L. B. Klickstein, R. H. Carter, J. A. Mitchell, D. T. Fearon and J. M. Ahearn (1989). "Mapping of the Epstein-Barr virus and C3dg binding sites to a common domain on complement receptor type 2." J Exp Med **170**(6): 1931-1946.

Lund, F. E. (2008). "Cytokine-producing B lymphocytes-key regulators of immunity." Curr Opin Immunol **20**(3): 332-338.

Lyubchenko, T., J. M. Dal Porto, V. M. Holers and J. C. Cambier (2007). "Cutting edge: Complement (C3d)-linked antigens break B cell anergy." J Immunol **179**(5): 2695-2699.

Macaulay, A. E., R. H. DeKruyff and D. T. Umetsu (1998). "Antigen-primed T cells from B cell-deficient JHD mice fail to provide B cell help." J Immunol **160**(4): 1694-1700.

Mackay, F., W. A. Figgett, D. Saulep, M. Lepage and M. L. Hibbs (2010). "B-cell stage and context-dependent requirements for survival signals from BAFF and the B-cell receptor." Immunol Rev **237**(1): 205-225.

Maliszewski, C. R., G. J. Delespesse, M. A. Schoenborn, R. J. Armitage, W. C. Fanslow, T. Nakajima, et al. (1994). "The CD39 lymphoid cell activation antigen. Molecular cloning and structural characterization." J Immunol **153**(8): 3574-3583.

Mauri, C. and A. Bosma (2012). "Immune regulatory function of B cells." Annu Rev Immunol **30**: 221-241.

Mazzei, G. J., M. D. Edgerton, C. Losberger, S. Lecoanet-Henchoz, P. Graber, A. Durandy, et al. (1995). "Recombinant soluble trimeric CD40 ligand is biologically active." J Biol Chem **270**(13): 7025-7028.

McGaha, T. L., B. Sorrentino and J. V. Ravetch (2005). "Restoration of tolerance in lupus by targeted inhibitory receptor expression." Science **307**(5709): 590-593.

McLaughlin, P., A. J. Grillo-Lopez, B. K. Link, R. Levy, M. S. Czuczman, M. E. Williams, et al. (1998). "Rituximab chimeric anti-CD20 monoclonal antibody therapy for relapsed indolent lymphoma: half of patients respond to a four-dose treatment program." J Clin Oncol **16**(8): 2825-2833.

Mei, H., S. Schmidt and T. Dorner (2012). "Rationale of anti-CD19 immunotherapy: an option to target autoreactive plasma cells in autoimmunity." Arthritis Research & Therapy **14**(Suppl 5): S1.

Melamed, D., R. J. Benschop, J. C. Cambier and D. Nemazee (1998). "Developmental Regulation of B Lymphocyte Immune Tolerance Compartmentalizes Clonal Selection from Receptor Selection." Cell **92**(2): 173-182.

Mizuno, T. and T. L. Rothstein (2005). "B cell receptor (BCR) cross-talk: CD40 engagement creates an alternate pathway for BCR signaling that activates I kappa B kinase/I kappa B alpha/NF-kappa B without the need for PI3K and phospholipase C gamma." J Immunol **174**(10): 6062-6070.

Moir, S. and A. S. Fauci (2009). "B cells in HIV infection and disease." Nat Rev Immunol **9**(4): 235-245.

Moir, S., J. Ho, A. Malaspina, W. Wang, A. C. DiPoto, M. A. O'Shea, et al. (2008). "Evidence for HIV-associated B cell exhaustion in a dysfunctional memory B cell compartment in HIV-infected viremic individuals." J Exp Med **205**(8): 1797-1805.

Morris, A. E., R. L. Remmele, Jr., R. Klinke, B. M. Macduff, W. C. Fanslow and R. J. Armitage (1999). "Incorporation of an isoleucine zipper motif enhances the biological activity of soluble CD40L (CD154)." J Biol Chem **274**(1): 418-423.

Morrison, V. L., T. A. Barr, S. Brown and D. Gray (2010). "TLR-mediated loss of CD62L focuses B cell traffic to the spleen during Salmonella typhimurium infection." J Immunol **185**(5): 2737-2746.

Mounho, B. J. and S. W. Burchiel (1998). "Alterations in human B cell calcium homeostasis by polycyclic aromatic hydrocarbons: possible associations with cytochrome P450 metabolism and increased protein tyrosine phosphorylation." Toxicol Appl Pharmacol **149**(1): 80-89.

Naito, M., U. Hainz, U. E. Burkhardt, B. Fu, D. Ahove, K. E. Stevenson, et al. (2013). "CD40L-Tri, a novel formulation of recombinant human CD40L that effectively activates B cells." Cancer Immunol Immunother **62**(2): 347-357.

Nakamura, A., T. Nukiwa and T. Takai (2003). "Deregulation of peripheral B-cell development in enhanced severity of collagen-induced arthritis in FcgammaRIIB-deficient mice." J Autoimmun **20**(3): 227-236.

Nemerow, G. R., C. Mold, V. K. Schwend, V. Tollefson and N. R. Cooper (1987). "Identification of gp350 as the viral glycoprotein mediating attachment of Epstein-Barr virus (EBV) to the EBV/C3d receptor of B cells: sequence homology of gp350 and C3 complement fragment C3d." J Virol **61**(5): 1416-1420.

Nguyen, K. A., L. Mandik, A. Bui, J. Kavaler, A. Norvell, J. G. Monroe, et al. (1997). "Characterization of anti-single-stranded DNA B cells in a non-autoimmune background." J Immunol **159**(6): 2633-2644.

Niiro, H. and E. A. Clark (2002). "Regulation of B-cell fate by antigen-receptor signals." Nat Rev Immunol **2**(12): 945-956.

Niiro, H., A. Maeda, T. Kurosaki and E. A. Clark (2002). "The B lymphocyte adaptor molecule of 32 kD (Bam32) regulates B cell antigen receptor signaling and cell survival." J Exp Med **195**(1): 143-149.

Nimmerjahn, F. and J. V. Ravetch (2008). "Fcgamma receptors as regulators of immune responses." Nat Rev Immunol **8**(1): 34-47.

Noorchashm, H., N. Noorchashm, J. Kern, S. Y. Rostami, C. F. Barker and A. Naji (1997). "B-cells are required for the initiation of insulitis and sialitis in nonobese diabetic mice." Diabetes **46**(6): 941-946.

Norman, D. J. (1995). "Mechanisms of action and overview of OKT3." Ther Drug Monit **17**(6): 615-620.

Novak, E. J. and P. S. Rabinovitch (1994). "Improved sensitivity in flow cytometric intracellular ionized calcium measurement using fluo-3/Fura Red fluorescence ratios." Cytometry **17**(2): 135-141.

O'Garra, A. (1998). "Cytokines induce the development of functionally heterogeneous T helper cell subsets." Immunity **8**(3): 275-283.

O'Neill, S. K., M. J. Shlomchik, T. T. Glant, Y. Cao, P. D. Doodes and A. Finnegan (2005). "Antigen-specific B cells are required as APCs and autoantibody-producing cells for induction of severe autoimmune arthritis." J Immunol **174**(6): 3781-3788.

Odegard, V. H. and D. G. Schatz (2006). "Targeting of somatic hypermutation." Nat Rev Immunol **6**(8): 573-583.

Ohman, L., A. C. Lindmark, S. Isaksson, I. Posserud, H. Strid, H. Sjovall, et al. (2009). "B-cell activation in patients with irritable bowel syndrome (IBS)." Neurogastroenterol Motil **21**(6): 644-650, e627.

Parkin, J. and B. Cohen (2001). "An overview of the immune system." Lancet **357**(9270): 1777-1789.

Pateinakis, P. and A. Pyrpasopoulou (2014). "CD20+ B cell depletion in systemic autoimmune diseases: common mechanism of inhibition or disease-specific effect on humoral immunity?" Biomed Res Int **2014**: 973609.

Perez-Andres, M., B. Paiva, W. G. Nieto, A. Caraux, A. Schmitz, J. Almeida, et al. (2010). "Human peripheral blood B-cell compartments: a crossroad in B-cell traffic." Cytometry B Clin Cytom **78 Suppl 1**: S47-60.

Peters, A. L., L. L. Stunz, D. K. Meyerholz, C. Mohan and G. A. Bishop (2010). "Latent membrane protein 1, the EBV-encoded oncogenic mimic of CD40, accelerates autoimmunity in B6.Sle1 mice." J Immunol **185**(7): 4053-4062.

Phillips, J. A., C. G. Romball, M. V. Hobbs, D. N. Ernst, L. Shultz and W. O. Weigle (1996). "CD4+ T cell activation and tolerance induction in B cell knockout mice." J Exp Med **183**(4): 1339-1344.

Polymenis, M. and E. V. Schmidt (1999). "Coordination of cell growth with cell division." Curr Opin Genet Dev **9**(1): 76-80.

Rakhmanov, M., B. Keller, S. Gutenberger, C. Foerster, M. Hoenig, G. Driessen, et al. (2009). "Circulating CD21low B cells in common variable immunodeficiency resemble tissue homing, innate-like B cells." Proc Natl Acad Sci U S A **106**(32): 13451-13456.

Ranheim, E. A. and T. J. Kipps (1993). "Activated T cells induce expression of B7/BB1 on normal or leukemic B cells through a CD40-dependent signal." J Exp Med **177**(4): 925-935.

Ray, A., S. Basu, C. B. Williams, N. H. Salzman and B. N. Dittel (2012). "A novel IL-10-independent regulatory role for B cells in suppressing autoimmunity by maintenance of regulatory T cells via GITR ligand." J Immunol **188**(7): 3188-3198.

Reth, M. and J. Wienands (1997). "Initiation and processing of signals from the B cell antigen receptor." Annu Rev Immunol **15**: 453-479.

Revy, P., C. Hivroz, G. Andreu, P. Graber, C. Martinache, A. Fischer, et al. (1999). "Activation of the Janus kinase 3-STAT5a pathway after CD40 triggering of human monocytes but not of resting B cells." J Immunol **163**(2): 787-793.

Rickert, R. C. (2005). "Regulation of B lymphocyte activation by complement C3 and the B cell coreceptor complex." Curr Opin Immunol **17**(3): 237-243.

Rivera, A., C.-C. Chen, N. Ron, J. P. Dougherty and Y. Ron (2001). "Role of B cells as antigen-presenting cells in vivo revisited: antigen-specific B cells are essential for T cell expansion in lymph nodes and for systemic T cell responses to low antigen concentrations." Int Immunol **13**(12): 1583-1593.

Rivera, A., C. C. Chen, N. Ron, J. P. Dougherty and Y. Ron (2001). "Role of B cells as antigen-presenting cells in vivo revisited: antigen-specific B cells are essential for T cell expansion in lymph nodes and for systemic T cell responses to low antigen concentrations." Int Immunol **13**(12): 1583-1593.

Roberts, M. L., A. T. Luxembourg and N. R. Cooper (1996). "Epstein-Barr virus binding to CD21, the virus receptor, activates resting B cells via an intracellular pathway that is linked to B cell infection." J Gen Virol **77 (Pt 12)**: 3077-3085.

Rodríguez-Pinto, D. (2005). "B cells as antigen presenting cells." Cellular Immunology **238**(2): 67-75.

Romagnani, S. (2008). "Human Th17 cells." Arthritis Res Ther **10**(2): 206.

Ron, Y., P. De Baetselier, J. Gordon, M. Feldman and S. Segal (1981). "Defective induction of antigen-reactive proliferating T cells in B cell-deprived mice." Eur J Immunol **11**(12): 964-968.

Ron, Y., P. De Baetselier, E. Tzehoval, J. Gordon, M. Feldman and S. Segal (1983). "Defective induction of antigen-reactive proliferating T cells in B cell-deprived mice. II. Anti-mu treatment affects the initiation and recruitment of T cells." Eur J Immunol **13**(2): 167-171.

Ron, Y. and J. Sprent (1987). "T cell priming in vivo: a major role for B cells in presenting antigen to T cells in lymph nodes." J Immunol **138**(9): 2848-2856.

Saemann, M. D., P. Kelemen, M. Zeyda, G. Bohmig, G. Staffler and G. J. Zlabinger (2002). "CD40 triggered human monocyte-derived dendritic cells convert to tolerogenic dendritic cells when JAK3 activity is inhibited." Transplant Proc **34**(5): 1407-1408.

Saijo, K., C. Schmedt, I. H. Su, H. Karasuyama, C. A. Lowell, M. Reth, et al. (2003). "Essential role of Src-family protein tyrosine kinases in NF-kappaB activation during B cell development." Nat Immunol **4**(3): 274-279.

Sakaguchi, S., N. Sakaguchi, M. Asano, M. Itoh and M. Toda (1995). "Immunologic self-tolerance maintained by activated T cells expressing IL-2 receptor alpha-chains (CD25). Breakdown of a single mechanism of self-tolerance causes various autoimmune diseases." J Immunol **155**(3): 1151-1164.

Salmi, M. and S. Jalkanen (2005). "Cell-surface enzymes in control of leukocyte trafficking." Nat Rev Immunol **5**(10): 760-771.

Samuels, J., Y. S. Ng, C. Coupillaud, D. Paget and E. Meffre (2005). "Impaired early B cell tolerance in patients with rheumatoid arthritis." J Exp Med **201**(10): 1659-1667.

Sanz, I., J. H. Anolik and R. J. Looney (2007). "B cell depletion therapy in autoimmune diseases." Front Biosci **12**: 2546-2567.

Sanz, I. and F. E.-H. Lee (2010). "B cells as therapeutic targets in SLE." Nat Rev Rheumatol **6**(6): 326-337.

Sarkar, S., M. C. Glassy, S. Ferrone and O. W. Jones (1980). "Cell cycle and the differential expression of HLA-A,B and HLA-DR antigens on human B lymphoid cells." Proc Natl Acad Sci U S A **77**(12): 7297-7301.

Sato, S., M. Fujimoto, M. Hasegawa and K. Takehara (2004). "Altered blood B lymphocyte homeostasis in systemic sclerosis: expanded naive B cells and diminished but activated memory B cells." Arthritis Rheum **50**(6): 1918-1927.

Scholzen, T. and J. Gerdes (2000). "The Ki-67 protein: from the known and the unknown." J Cell Physiol **182**(3): 311-322.

Schonbeck, U., F. Mach and P. Libby (2000). "CD154 (CD40 ligand)." Int J Biochem Cell Biol **32**(7): 687-693.

Schultze, J. L., A. A. Cardoso, G. J. Freeman, M. J. Seamon, J. Daley, G. S. Pinkus, et al. (1995). "Follicular lymphomas can be induced to present alloantigen efficiently: a conceptual model to improve their tumor immunogenicity." Proceedings of the National Academy of Sciences **92**(18): 8200-8204.

Schultze, J. L., S. Michalak, M. J. Seamon, G. Dranoff, K. Jung, J. Daley, et al. (1997). "CD40-activated human B cells: an alternative source of highly efficient antigen presenting cells to generate autologous antigen-specific T cells for adoptive immunotherapy." J Clin Invest **100**(11): 2757-2765.

Schwabe, R. F., B. Schnabl, Y. O. Kweon and D. A. Brenner (2001). "CD40 activates NF-kappa B and c-Jun N-terminal kinase and enhances chemokine secretion on activated human hepatic stellate cells." J Immunol **166**(11): 6812-6819.

Seifert, M. and R. Kuppers (2009). "Molecular footprints of a germinal center derivation of human IgM+(IgD+)CD27+ B cells and the dynamics of memory B cell generation." J Exp Med **206**(12): 2659-2669.

Shimabukuro-Vornhagen, A., M. A. García-Márquez, R. N. Fischer, J. Iltgen, A. Fiedler, K. Wennhold, et al. (in review). "The CD21low B cell population is composed of an anergic and an immunostimulatory germinal center-like B cell subset " J Exp Med.

Shimabukuro-Vornhagen, A., M. J. Hallek, R. F. Storb and M. S. von Bergwelt-Baildon (2009). "The role of B cells in the pathogenesis of graft-versus-host disease." Blood **114**(24): 4919-4927.

Shimabukuro-Vornhagen, A., H. A. Schlosser, L. Gryschok, J. Malcher, K. Wennhold, M. Garcia-Marquez, et al. (2014). "Characterization of tumor-associated B-cell subsets in patients with colorectal cancer." Oncotarget **5**(13): 4651-4664.

Shlomchik, M. J. (2008). "Sites and stages of autoreactive B cell activation and regulation." Immunity **28**(1): 18-28.

Siemasko, K., B. J. Eisfelder, E. Williamson, S. Kabak and M. R. Clark (1998). "Cutting edge: signals from the B lymphocyte antigen receptor regulate MHC class II containing late endosomes." J Immunol **160**(11): 5203-5208.

Smith, K. G. and M. R. Clatworthy (2010). "FcgammaRIIB in autoimmunity and infection: evolutionary and therapeutic implications." Nat Rev Immunol **10**(5): 328-343.

Solvason, N. and J. F. Kearney (1992). "The human fetal omentum: a site of B cell generation." J Exp Med **175**(2): 397-404.

Stoddart, A., M. L. Dykstra, B. K. Brown, W. Song, S. K. Pierce and F. M. Brodsky (2002). "Lipid rafts unite signaling cascades with clathrin to regulate BCR internalization." Immunity **17**(4): 451-462.

Stone, G. W., S. Barzee, V. Snarsky, K. Kee, C. A. Spina, X. F. Yu, et al. (2006). "Multimeric soluble CD40 ligand and GITR ligand as adjuvants for human immunodeficiency virus DNA vaccines." J Virol **80**(4): 1762-1772.

Szakonyi, G., J. M. Guthridge, D. Li, K. Young, V. M. Holers and X. S. Chen (2001). "Structure of complement receptor 2 in complex with its C3d ligand." Science **292**(5522): 1725-1728.

Tangye, S. G., Y. J. Liu, G. Aversa, J. H. Phillips and J. E. de Vries (1998). "Identification of functional human splenic memory B cells by expression of CD148 and CD27." J Exp Med **188**(9): 1691-1703.

Tangye, S. G. and D. M. Tarlinton (2009). "Memory B cells: effectors of long-lived immune responses." Eur J Immunol **39**(8): 2065-2075.

Taylor, J. J., K. A. Pape and M. K. Jenkins (2012). "A germinal center-independent pathway generates unswitched memory B cells early in the primary response." J Exp Med **209**(3): 597-606.

Tedder, T. F., J. Tuscano, S. Sato and J. H. Kehrl (1997). "CD22, a B lymphocyte-specific adhesion molecule that regulates antigen receptor signaling." Annu Rev Immunol **15**: 481-504.

Ten Boekel, E., C. E. Siegert, G. J. Vrielink, V. C. Van Dam, A. Ceelen and W. De Kieviet (2007). "Analyses of CD27++ plasma cells in peripheral blood from patients with bacterial infections and patients with serum antinuclear antibodies." J Clin Immunol **27**(5): 467-476.

Teshima, R., H. Ikebuchi, M. Nakanishi and J. Sawada (1994). "Stimulatory effect of pervanadate on calcium signals and histamine secretion of RBL-2H3 cells." Biochemical Journal **302**(Pt 3): 867-874.

Thiel, J., L. Kimmig, U. Salzer, M. Grudzien, D. Lebrecht, T. Hagena, et al. (2012). "Genetic CD21 deficiency is associated with hypogammaglobulinemia." Journal of Allergy and Clinical Immunology **129**(3): 801-810.e806.

Thorley-Lawson, D. A. (2005). "EBV the prototypical human tumor virus—just how bad is it?" Journal of Allergy and Clinical Immunology **116**(2): 251-261.

Toba, K., H. Hanawa, I. Fuse, M. Sakaue, K. Watanabe, Y. Uesugi, et al. (2002). "Difference in CD22 molecules in human B cells and basophils." Exp Hematol **30**(3): 205-211.

Treanor, B. (2012). "B-cell receptor: from resting state to activate." Immunology **136**(1): 21-27.

Trudel, S., M. R. Pâquet and S. Grinstein (1991). "Mechanism of vanadate-induced activation of tyrosine phosphorylation and of the respiratory burst in HL60 cells. Role of reduced oxygen metabolites." Biochemical Journal **276**(Pt 3): 611-619.

Tuveson, D. A., J. M. Ahearn, A. K. Matsumoto and D. T. Fearon (1991). "Molecular interactions of complement receptors on B lymphocytes: a CR1/CR2 complex distinct from the CR2/CD19 complex." J Exp Med **173**(5): 1083-1089.

Uchida, J., Y. Hamaguchi, J. A. Oliver, J. V. Ravetch, J. C. Poe, K. M. Haas, et al. (2004). "The innate mononuclear phagocyte network depletes B lymphocytes through Fc receptor-dependent mechanisms during anti-CD20 antibody immunotherapy." J Exp Med **199**(12): 1659-1669.

Uchida, J., T. Yasui, Y. Takaoka-Shichijo, M. Muraoka, W. Kulwichit, N. Raab-Traub, et al. (1999). "Mimicry of CD40 signals by Epstein-Barr virus LMP1 in B lymphocyte responses." Science **286**(5438): 300-303.

Uckun, F. M., G. L. Schieven, I. Dibirdik, M. Chandan-Langlie, L. Tuel-Ahlgren and J. A. Ledbetter (1991). "Stimulation of protein tyrosine phosphorylation, phosphoinositide turnover, and multiple previously unidentified serine/threonine-specific protein kinases by the Pan-B-cell receptor

CD40/Bp50 at discrete developmental stages of human B-cell ontogeny." J Biol Chem **266**(26): 17478-17485.

van Kooten, C. and J. Banchereau (2000). "CD40-CD40 ligand." J Leukoc Biol **67**(1): 2-17.

van Zelm, M. C., T. Szczepanski, M. van der Burg and J. J. van Dongen (2007). "Replication history of B lymphocytes reveals homeostatic proliferation and extensive antigen-induced B cell expansion." J Exp Med **204**(3): 645-655.

Visentini, M., M. Cagliuso, V. Conti, M. Carbonari, M. Cibati, G. Siciliano, et al. (2012). "Clonal B cells of HCV-associated mixed cryoglobulinemia patients contain exhausted marginal zone-like and CD21 low cells overexpressing Stra13." Eur J Immunol **42**(6): 1468-1476.

von Andrian, U. H. and T. R. Mempel (2003). "Homing and cellular traffic in lymph nodes." Nat Rev Immunol **3**(11): 867-878.

von Andrian, U. H. and T. R. Mempel (2003). "Homing and cellular traffic in lymph nodes." Nat Rev Immunol **3**(11): 867-878.

von Bergwelt-Baildon, M., A. Shimabukuro-Vornhagen, A. Popov, N. Klein-Gonzalez, F. Fiore, S. Debey, et al. (2006). "CD40-activated B cells express full lymph node homing triad and induce T-cell chemotaxis: potential as cellular adjuvants." Blood **107**(7): 2786-2789.

von Bergwelt-Baildon, M. S., R. H. Vonderheide, B. Maecker, N. Hirano, K. S. Anderson, M. O. Butler, et al. (2002). "Human primary and memory cytotoxic T lymphocyte responses are efficiently induced by means of CD40-activated B

cells as antigen-presenting cells: potential for clinical application." Blood **99**(9): 3319-3325.

Wang, L. D. and M. R. Clark (2003). "B-cell antigen-receptor signalling in lymphocyte development." Immunology **110**(4): 411-420.

Warnatz, K., C. Wehr, R. Drager, S. Schmidt, H. Eibel, M. Schlesier, et al. (2002). "Expansion of CD19(hi)CD21(lo/neg) B cells in common variable immunodeficiency (CVID) patients with autoimmune cytopenia." Immunobiology **206**(5): 502-513.

Wehr, C., H. Eibel, M. Masilamani, H. Illges, M. Schlesier, H. Peter, et al. (2004). "A new CD21low B cell population in the peripheral blood of patients with SLE." Clin Immunol **113**: 161 - 171.

Wehr, C., H. Eibel, M. Masilamani, H. Illges, M. Schlesier, H. H. Peter, et al. (2004). "A new CD21low B cell population in the peripheral blood of patients with SLE." Clin Immunol **113**(2): 161-171.

Weller, S., M. C. Braun, B. K. Tan, A. Rosenwald, C. Cordier, M. E. Conley, et al. (2004). "Human blood IgM "memory" B cells are circulating splenic marginal zone B cells harboring a prediversified immunoglobulin repertoire." Blood **104**(12): 3647-3654.

Weninger, W., N. Manjunath and U. H. von Andrian (2002). "Migration and differentiation of CD8+ T cells." Immunol Rev **186**: 221-233.

Wennhold, K., A. Shimabukuro-Vornhagen, S. Theurich and M. von Bergwelt-Baildon (2013). "CD40-activated B cells as antigen-presenting cells: the final sprint toward clinical application." Expert Rev Vaccines **12**(6): 631-637.

Wiede, F., P. D. Fromm, I. Comerford, E. Kara, J. Bannan, W. Schuh, et al. (2013). "CCR6 is transiently upregulated on B cells after activation and modulates the germinal center reaction in the mouse." Immunol Cell Biol **91**(5): 335-339.

Wienands, J., O. Larbolette and M. Reth (1996). "Evidence for a preformed transducer complex organized by the B cell antigen receptor." Proc Natl Acad Sci U S A **93**(15): 7865-7870.

Winer, D. A., S. Winer, L. Shen, P. P. Wadia, J. Yantha, G. Paltser, et al. (2011). "B cells promote insulin resistance through modulation of T cells and production of pathogenic IgG antibodies." Nat Med **17**(5): 610-617.

Wing, K. and S. Sakaguchi (2010). "Regulatory T cells exert checks and balances on self tolerance and autoimmunity." Nat Immunol **11**(1): 7-13.

Wykes, M. (2003). "Why do B cells produce CD40 ligand?" Immunol Cell Biol **81**(4): 328-331.

Xiu, Y., C. P. Wong, J. D. Bouaziz, Y. Hamaguchi, Y. Wang, S. M. Pop, et al. (2008). "B lymphocyte depletion by CD20 monoclonal antibody prevents diabetes in nonobese diabetic mice despite isotype-specific differences in Fc gamma R effector functions." J Immunol **180**(5): 2863-2875.

Yanaba, K., J. D. Bouaziz, K. M. Haas, J. C. Poe, M. Fujimoto and T. F. Tedder (2008). "A regulatory B cell subset with a unique CD1dhiCD5+ phenotype controls T cell-dependent inflammatory responses." Immunity **28**(5): 639-650.

Yellin, M. J., J. Sinning, L. R. Covey, W. Sherman, J. J. Lee, E. Glickman-Nir, et al. (1994). "T lymphocyte T cell-B cell-activating molecule/CD40-L molecules induce normal B cells or chronic lymphocytic leukemia B cells to express CD80 (B7/BB-1) and enhance their costimulatory activity." J Immunol **153**(2): 666-674.

Yoon, S. H., H. I. Cho and T. G. Kim (2005). "Activation of B cells using Schneider 2 cells expressing CD40 ligand for the enhancement of antigen presentation in vitro." Exp Mol Med **37**(6): 567-574.

Youinou, P. (2007). "B cell conducts the lymphocyte orchestra." J Autoimmun **28**(2-3): 143-151.

Yuseff, M.-I., P. Pierobon, A. Reversat and A.-M. Lennon-Dumenil (2013). "How B cells capture, process and present antigens: a crucial role for cell polarity." Nat Rev Immunol **13**(7): 475-486.

Yuseff, M. I., A. Reversat, D. Lankar, J. Diaz, I. Fanget, P. Pierobon, et al. (2011). "Polarized secretion of lysosomes at the B cell synapse couples antigen extraction to processing and presentation." Immunity **35**(3): 361-374.

Zarnegar, B., J. Q. He, G. Oganesyan, A. Hoffmann, D. Baltimore and G. Cheng (2004). "Unique CD40-mediated biological program in B cell activation requires both type 1 and type 2 NF-kappaB activation pathways." Proc Natl Acad Sci U S A **101**(21): 8108-8113.

Zimmermann, V. S., P. Rovere, J. Trucy, K. Serre, P. Machy, F. Forquet, et al. (1999). "Engagement of B cell receptor regulates the invariant chain-dependent MHC class II presentation pathway." J Immunol **162**(5): 2495-2502.

Attachments

5 ATTACHMENTS

5.1 Erklärung § 4 Abs. 1 Nr. 9

Ich versichere, dass ich die von mir vorgelegte Dissertation selbstständig angefertigt, die benutzen Quellen und Hilfsmittel vollständig angegeben und die Stellen der Arbeit – einschließlich Tabellen, Karten, Abbildungen -, die anderen Werken im Wortlaut oder dem Sinn nach entnommen sind, in jedem Einzelfall als Entlehnung kenntlich gemacht habe; dass diese Dissertation noch keiner anderen Fakultät oder Universität zur Prüfung vorgelegen hat; dass sie – abgesehen von unten angegebenen Teilpublikationen – noch nicht veröffentlicht worden ist sowie, dass ich eine solche Veröffentlichung vor Abschluss des Promotionsverfahrens nicht vornehmen werde. Die Bestimmungen der Promotionsordnung sind mir bekannt. Die von mir vorgelegte Dissertation ist von PD Dr. Thomas Wunderlich und Prof. Dr. Dr. Michael von Bergwelt-Baildon betreut worden.

Köln, den 20.04.2015

Maria Alejandra García Márquez

5.2 Teilpublikationen

Shimabukuro-Vornhagen*, A., **M. A. García-Márquez***, R. N. Fischer*, J. Iltgen, A. Fiedler, K. Wennhold, G. Rappl, H. Abken, P. Hartmann, C. Lehmann, M. Herling, D. Wolf, G. Fätkenheuer, A. Rubbert, M. Hallek, S. Theurich and M. S. von Bergwelt-Baildon. " The homeostasis of the $CD21^{low}$ B cell compartment is perturbed in patients with inflammatory conditions " Manuscript in preparation for submission to Immunity. * Contributed equally

Garcia-Marquez, M. A., A. Shimabukuro-Vornhagen, S. Theurich, M. Kochanek, T. Weber, K. Wennhold, A. Dauben, A. Dzionek, C. Reinhard and M. von Bergwelt-Baildon (2014). "A multimerized form of recombinant human CD40 ligand supports long-term activation and proliferation of B cells." Cytotherapy 16(11): 1537-1544.

Shimabukuro-Vornhagen, A., H. A. Schlosser, L. Gryschok, J. Malcher, K. Wennhold, **M. Garcia-Marquez**, T. Herbold, L. S. Neuhaus, H. J. Becker, A. Fiedler, P. Scherwitz, T. Koslowsky, R. Hake, D. L. Stippel, A. H. Holscher, S. Eidt, M. Hallek, S. Theurich and M. S. von Bergwelt-Baildon (2014). "Characterization of tumor-associated B-cell subsets in patients with colorectal cancer." Oncotarget 5(13): 4651-4664.

5.3 Lebenslauf

María Alejandra García Márquez

MSc in Cancer Immunology and

Biotechnology

_____

Dürener Str.396-398

50935 Köln

PERSÖNLICHE DATEN

Geburtsdatum	04. Januar 1986
Geburtsort	Maracay, Venezuela
Nationalität	Venezuelanisch - Spanisch

BERUFLICHER WERDEGANG UND AUSBILDUNG

10/2011 – heute	Interventionelle Immunologie Köln, Uniklinikum Köln, Doktorandin
02/2011 – 07/2011	Masterarbeit an der Queens Medical Centre, Nottingham, UK., Division of pre-clinical oncology
09/2010 – 09/2011	Master in Cancer Immunology and Biotechnology Masterstudium 'Cancer Immunology and Biotechnology' an der University of Nottingham, UK
12/2007 - 07/2010	Biologin bei IVIC (venezolanisches Institut für wissenschaftliche Forschung)
03/2006 – 12/2007	Bachelorarbeit an der Instituto venezolano de investigaciones cientificas (venezolanischen Institut für wissenschaftliche Forschung)
09/2002 – 12/2007	Bachelor of Science in Cellular Biology (Regelstudienzeit 5 Jahre)

	Bachelorstudium 'Cellular Biology' an der Universidad Central de Venezuela	
1998 – 2002	U.E.N 'Elizabeth von Keller', Venezuela Abschluss: Äquivalent zu Abitur	Colonia Tovar,
1992 – 1997	U.E.N 'San Martin de Tours', Venezuela	Colonia Tovar,

Köln, den 20.04.2015

5.4 Publikationen

2015 Shimabukuro-Vornhagen*, A., **M. A. García-Márquez***, R. N. Fischer*, J. Iltgen, A. Fiedler, K. Wennhold, G. Rappl, H. Abken, P. Hartmann, C. Lehmann, M. Herling, D. Wolf, G. Fätkenheuer, A. Rubbert, M. Hallek, S. Theurich and M. S. von Bergwelt- Baildon. "The CD21low B cell population is composed of an anergic and an immunostimulatory germinal center-like B cell subset" The Journal of Experimental Medicine. in review. * Contributed equally

Kerstin Wennhold, Martin Thelen, **Maria Garcia-Marquez**, Alexander Shimabukuro-Vornhagen, Michael von Bergwelt-Baildon. "Tumorantigen-specific CD40B cells: Combining enhanced antigen presentation and antibody-secretion for tumor targeting". Manuscript in preparation for submission to Nature Biotech.

G Chakupurakal*, **M Garcia-Marquez*,** A Shimabukuro- Vornhagen, S Theurich, M Hallek, C Scheid, U Holtick, M von Bergwelt-Baildon. "Regulatory B-cells can be identified early post-transplant independent of acute Graft versus Host disease" Haematologica. in revision. * Contributed equally

Nela Klein Gonzalez*, Kerstin Wennhold*, Sandra Balkow, Eisei Kondo, Birgit Bölck, Tanja Weber, **Maria Garcia-Marquez**, Stephan Grabbe, Wilhelm Bloch, Michael von Bergwelt-Baildon & Alexander Shimabukuro-Vornhagen (2015). "In vitro and in vivo imaging of initial B-T-cell interactions in the setting of B-cell based cancer immunotherapy" *Oncoimmunology*. * Contributed equally.

2014 Garcia-Marquez, M. A., A. Shimabukuro-Vornhagen, S. Theurich, M. Kochanek, T. Weber, K. Wennhold, A. Dauben, A. Dzionek, C. Reinhard and M. von Bergwelt-Baildon (2014). "A multimerized form of recombinant human CD40 ligand supports long-term activation and proliferation of B cells" Cytotherapy 16(11): 1537-1544.

Shimabukuro-Vornhagen, A., H. A. Schlosser, L. Gryschok, J. Malcher, K. Wennhold, **M. Garcia-Marquez**, T. Herbold, L. S. Neuhaus, H. J. Becker, A. Fiedler, P. Scherwitz, T. Koslowsky, R. Hake, D. L. Stippel, A. H. Holscher, S. Eidt, M. Hallek, S. Theurich and M. S. von Bergwelt-Baildon (2014). "Characterization of tumor-associated B-cell subsets in patients with colorectal cancer" Oncotarget 5(13): 4651-4664.

2013 **Garcia-Marquez, M., A.** Shimabukuro-Vornhagen and M. von Bergwelt-Baildon (2013). "Complex interactions between B cells and dendritic cells" Blood 121(12): 2367-2368.

Garcia-Marquez, M. A., A. Shimabukuro-Vornhagen, S. Theurich and M. von Bergwelt-Baildon (2013). "Vaccination with dendritic cell-tumor fusion cells in multiple myeloma patients: a promising strategy?" Immunotherapy 5(10): 1039-1042.

2012 **Garcia-Marquez, M. A.,** K. Wennhold, A. Draube and M. von Bergwelt-Baildon (2012). "Results of a Phase II clinical trial with Id-protein-loaded dendritic cell vaccine in multiple myeloma: encouraging or discouraging?" Immunotherapy 4(10): 991-994.